

CATALOGED BY SEPIR

TI-85,137

FDL-TDR-64-26

AD 0681611

DO NOT DESTROY
RETURN TO
TECHNICAL INFORMATION LIBRARY
SEPIR

ANALYTICAL AND EXPERIMENTAL INVESTIGATION OF THE ACOUSTIC ENVIRONMENT OF THE RTD SONIC FATIGUE MAIN TEST CHAMBER

TECHNICAL DOCUMENTARY REPORT FDL-TDR-64-26

APRIL 1964

AF FLIGHT DYNAMICS LABORATORY
RESEARCH AND TECHNOLOGY DIVISION
AIR FORCE SYSTEMS COMMAND
WRIGHT-PATTERSON AIR FORCE BASE, OHIO

Project No. 4437, Task No. 443701

(Prepared under Contract No. AF 33(657)-10927 by
IIT Research Institute, Chicago, Illinois
Franklin G. Tyzzer and David F. Pernet, Authors)

20080818 030

NOTICES

When Government drawings, specifications, or other data are used for any purpose other than in connection with a definitely related Government procurement operation, the United States Government thereby incurs no responsibility nor any obligation whatsoever; and the fact that the Government may have formulated, furnished, or in any way supplied the said drawings, specifications, or other data, is not to be regarded by implication or otherwise as in any manner licensing the holder or any other person or corporation, or conveying any rights or permission to manufacture, use, or sell any patented invention that may in any way be related thereto.

Qualified requesters may obtain copies of this report from the Defense Documentation Center (DDC), (formerly ASTIA), Cameron Station, Bldg. 5, 5010 Duke Street, Alexandria, Virginia, 22314.

This report has been released to the Office of Technical Services, U.S. Department of Commerce, Washington 25, D. C., in stock quantities for sale to the general public.

Copies of this report should not be returned to the Research and Technology Division, Wright-Patterson Air Force Base, Ohio, unless return is required by security considerations, contractual obligations, or notice on a specific document.

AD601611

FOREWORD

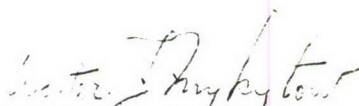
The research in this report was performed by IIT Research Institute, Chicago, Illinois, for the Aero-Acoustics Branch, Vehicle Dynamics Division, AF Flight Dynamics Laboratory, Wright-Patterson AFB, Ohio, under Contract AF33(657)-10927 "Investigation of the Acoustic Environment of the RTD Sonic Fatigue Facility." This research is part of a continuing effort to provide reliable simulation of aero-acoustic sources for establishing design criteria in the specific area of sonic fatigue and is part of the Research and Technology Division, Air Force Systems Command's exploratory development program. This work was performed under Project 4437, "High Intensity Sound Environment Simulation" and Task 443701 "Sonic Facility Development." Mr. Axel W. Kolb and later Mr. Davey L. Smith of the Aero-Acoustics Branch, AF Flight Dynamics Laboratory were Project Engineers.

The research was conducted from 6 March 1963 to 15 February 1964 by the Acoustics Section of the Fluid Dynamics Division of IIT Research Institute. W. C. Sperry was manager of the section and advised in the direction of this program. F. G. Tyzzer was project leader, responsible for the general direction of the work. He performed the diffuse field analysis and was joint author of this report with D. F. Pernet, who aided in the direction of the work and performed the majority of the experimental model study and theoretical study of the far-field distribution. V. J. Raelson contributed to a portion of the theoretical study of the field produced by the sirens, and G. Hruska performed some of the calculations of these fields.

ABSTRACT

The extreme versatility of the RTD Sonic Fatigue Facility creates problems in analysis and control of attainable environments. Acoustic environments have been analyzed using both theoretical and experimental modeling techniques, with regard to spatial distribution and correlation of sound pressures. A diffuse field study has enabled predictions of sound fields to be made for many cases of source and test structure parameters. Progressive-wave operation of the facility for small groups of sources was analyzed and some typical pressure field distributions were evaluated. The modifying effect on the progressive wave pressure fields, caused by locating test structures in these fields, was studied with respect to the size, location, and orientation of test-structures, the operational frequency of the source system and the relationship between the individual sources forming the overall system. Conditions were established for obtaining uniform, gradual, or rapid variations, and alternate maxima and minima in sound pressure level on the exposed surfaces of structures. In addition, conditions were established for operation of the facility in order to produce on structures areas of phase coherence having both large and small extent as well as narrow elongated extent.

This technical documentary report has been reviewed and is approved.



WALTER J. MYKYTOW
Asst. for Research & Technology
Vehicle Dynamics Division

TABLE OF CONTENTS

<u>Section</u>		<u>Page</u>
I	Introduction and Summary	1
II	Calculation of Characteristics of the Diffuse Field	3
	Sound Pressure Level in the Diffuse Field	4
	Sound Pressure Level Near Sound Sources	8
	Sound Pressure Level Near Room Boundaries	9
	Sound Pressure Level at Test Structures	10
III	Progressive-Type Sound Fields Calculated for One to Three Non-Directional Sources	12
IV	Experimental Model Study	20
	Experimental Facility	20
	Panel Orientations	22
	Single Source in Anechoic Condition	22
	Double Coherent Sources in Anechoic Condition	25
	Triple Coherent Sources in Anechoic Condition	26
	Double Incoherent Sources in Anechoic Condition	26
	Single Sources in Semi-Anechoic Condition	27
	Triple Coherent Sources in Semi-Anechoic Condition	29
	Semi-Anechoic Study with Degree of Acoustic Treatment	30
V	Types of Attainable Sound Fields	32
	Diffuse Field Operation of the Facility	32
	Progressive Wave Operation of the Facility	33
	Modifying Effects of Structures on Progressive-Wave Fields	33

TABLE OF CONTENTS (Continued)

<u>Section</u>		<u>Page</u>
VI	Conclusions and Recommendations	35
	Conclusions	35
	Recommendations	35
	List of References	37
	Figures	39
	Appendix A--Summation of Coherent and Incoherent Signals	88
	Appendix B--Acoustic Environments in the ASD Sonic Fatigue Facility	90

LIST OF ILLUSTRATIONS

<u>Figure No.</u>		<u>Page</u>
1	Location of Point P in the Far-Field with Respect to Three Sources A, B, C; Showing Differences in Path-Lengths PA, PB, and PC	39
2	Far-Field Pressure Distribution in Plane 50 ft. from 3-Source System, $f = 110$ cps	40
3	Far-Field Pressure Distribution in Plane 50 ft. from 3-Source System, $f = 220$ cps	41
4	Far-Field Pressure Distribution in Plane 50 ft. from 3-Source System, $f = 440$ cps	42
5	Far-Field Pressure Distribution in Plane 50 ft. from 2-Source System, $f = 110$ cps	43
6	Far-Field Pressure Distribution in Plane 50 ft. from 2-Source System, $f = 220$ cps	44
7	Far-Field Pressure Distribution in Plane 50 ft. from 2-Source System, $f = 440$ cps	45
8	Far-Field Pressure Distribution in Plane 50 ft. from Single Source	46
9	Anechoic Chamber Used in Model Study. Test Panel Arranged at 45° to Speaker System (Dashed Test Panel Outline Corresponds to Normal Incidence Orientation). Speaker System Composed of 8 ins. Speakers with 10 ins. Center Spacing.	47
10	Pressure and Phase Distribution on Test Panel Under Anechoic Conditions, Tone Source 600 c/s, $\alpha = 30^\circ$, $\beta = 0^\circ$ and $\alpha = 0^\circ$, $\beta = 0^\circ$	48
11	Pressure and Phase Distribution on Test Panel Under Anechoic Conditions, Tone Source 600 c/s, $\alpha = 90^\circ$, $\beta = 0^\circ$ and $\alpha = 60^\circ$, $\beta = 0^\circ$	49
12	Pressure and Phase Distribution on Test Panel Under Anechoic Conditions, Tone Source 200 c/s, $\alpha = 90^\circ$, $\beta = 0^\circ$ and $\alpha = 60^\circ$, $\beta = 0^\circ$	50
13	Pressure and Phase Distribution on Test Panel Under Anechoic Conditions, Tone Source 200 c/s, $\alpha = 30^\circ$, $\beta = 0^\circ$	51

LIST OF ILLUSTRATIONS (Continued)

<u>Figure No.</u>		<u>Page</u>
14	Pressure and Phase Distribution on Test Panel Under Anechoic Conditions, 1/3 Octave-Band Noise Source with Center Frequency 630 c/s, $\alpha = 30^\circ$, $\beta = 0^\circ$	52
15	Pressure and Phase Distribution on Test Panel Under Anechoic Conditions, 1/3 Octave-Band Noise Source with Center Frequency 630 c/s and 200 c/s, $\alpha = 45^\circ$, $\beta = 0^\circ$	53
16	Pressure and Phase Distribution on Test Panel Under Anechoic Conditions, 1/3 Octave-Band Noise Source with Center Frequency 630 c/s, $\alpha = 90^\circ$, $\beta = 0^\circ$	54
17	Pressure and Phase Distribution on Test Panel Under Anechoic Conditions, 1/3 Octave-Band Noise Source with Center Frequency 1600 c/s, $\alpha = 90^\circ$, $\beta = 0^\circ$	55
18	Pressure and Phase Distribution on Test Panel Under Anechoic Conditions, 1/3 Octave-Band Noise Source with Center Frequency 630 c/s, $\alpha = 45^\circ$, $\beta = 0^\circ$	56
19	Pressure and Phase Distribution on Test Panel Under Anechoic Conditions, 1/3 Octave-Band Noise Source with Center Frequency 1600 c/s, $\alpha = 45^\circ$, $\beta = 0^\circ$	57
20	Pressure and Phase Distribution on Test Panel Under Anechoic Conditions, 1/3 Octave-Band Noise Source with Center Frequency 630 c/s, $\alpha = 0^\circ$, $\beta = 0^\circ$	58
21	Pressure and Phase Distribution on Test Panel Under Anechoic Conditions, 1/3 Octave-Band Noise Source with Center Frequency 1600 c/s, $\alpha = 0^\circ$, $\beta = 0^\circ$	59
22	Absolute Pressure Increase Across ZZ' and YY' Axes of Panels, $\alpha = 90^\circ$, $\beta = 0^\circ$	60
23	Absolute Pressure Increase Across ZZ' and YY' Axes of Panels, $\alpha = 45^\circ$, $\beta = 0^\circ$	61
24	Pressure and Phase Distribution on Test Panel Under Anechoic Conditions, Coherent 1/3 Octave-Band Noise Sources S_2 , S_3 with Center Frequency 630 c/s, $\alpha = 90^\circ$, $\beta = 0^\circ$	62

LIST OF ILLUSTRATIONS (Continued)

<u>Figure No.</u>		<u>Page</u>
25	Pressure and Phase Distribution on Test Panel Under Anechoic Conditions, Coherent 1/3 Octave-Band Noise Sources S_2, S_3 with Center Frequency 630 c/s, $\alpha = 45^\circ, \beta = 0^\circ$	63
26	Pressure and Phase Distribution on Test Panel Under Anechoic Conditions, Coherent 1/3 Octave Band Noise Sources S_1, S_2 with Center Frequency 200 c/s, $\alpha = 45^\circ, \beta = 0^\circ$	64
27	Pressure and Phase Distribution on Test Panel Under Anechoic Conditions, Coherent 1/3 Octave-Band Noise Sources S_1, S_2 with Center Frequency 630 c/s, $\alpha = 45^\circ, \beta = 0^\circ$	65
28	Pressure and Phase Distribution on Test Panel Under Anechoic Conditions, Coherent 1/3 Octave-Band Noise Sources S_1, S_2 with Center Frequency 1600 c/s, $\alpha = 45^\circ, \beta = 0^\circ$	66
29	Pressure and Phase Distribution on Test Panel Under Anechoic Conditions, Coherent 1/3 Octave-Band Noise Sources S_1, S_2, S_3 with Center Frequency 630 c/s, $\alpha = 90^\circ, \beta = 0^\circ$	67
30	Pressure and Phase Distribution on Test Panel Under Anechoic Conditions, Coherent 1/3 Octave-Band Noise Sources S_1, S_2, S_3 with Center Frequency 630 c/s, $\alpha = 45^\circ, \beta = 0^\circ$	68
31	Pressure and Phase Distribution on Test Panel Under Anechoic Conditions, Incoherent 1/3 Octave-Band Noise Sources S_1, S_2 with Center Frequency 630 c/s, $\alpha = 45^\circ, \beta = 0^\circ$	69
32	Pressure Distribution on Test Panel Under Anechoic Conditions. A Single 1/3 Octave-Band Noise Source, $\alpha = +45^\circ$. B Single 1/3 Octave-Band Noise Source, $\alpha = -45^\circ$. C Superimposed Combination of A and B. D Two Incoherent 1/3 Octave-Band Noise Sources, $\alpha = +45^\circ$ and -45° . Center Frequency = 630 cps.	70
33	Pressure and Phase Distribution on Test Panel Under Semi-Anechoic Condition, 1/3 Octave-Band Noise Source with Center Frequency 630 c/s, $\alpha = 90^\circ, \beta = 0^\circ$, and $\alpha = 0^\circ, \beta = 0^\circ$, D = 3 ft.	71

LIST OF ILLUSTRATIONS (Continued)

<u>Figure No.</u>		<u>Page</u>
34	Pressure and Phase Distribution on Test Panel Under Semi-Anechoic Condition, 1/3 Octave-Band Noise Source with Center Frequency 630 c/s, $\alpha = 45^\circ$, $\beta = 0^\circ$, and $\alpha = 45^\circ$, $\beta = 45^\circ$, $D = 3$ ft.	72
35	Pressure and Phase Distribution on Test Panel Under Semi-Anechoic Condition, 1/3 Octave-Band Noise Source with Center Frequency 630 c/s, $\alpha = 90^\circ$, $\beta = 0^\circ$, $D = 3$ ft.	73
36	Pressure and Phase Distribution on Test Panel Under Semi-Anechoic Condition, 1/3 Octave-Band Noise Source with Center Frequency 630 c/s, $\alpha = 45^\circ$, $\beta = 0^\circ$, $D = 3$ ft.	74
37	Pressure and Phase Distribution on Test Panel Under Semi-Anechoic Condition, 1/3 Octave-Band Noise Source with Center Frequency 630 c/s, $\alpha = 0^\circ$, $\beta = 0^\circ$, $D = 3$ ft.	75
38	Pressure and Phase Distribution on Test Panel Under Semi-Anechoic Condition, 1/3 Octave-Band Noise Source with Center Frequency 1600 c/s, $\alpha = 45^\circ$, $\beta = 0^\circ$, $D = 3$ ft.	76
39	Pressure and Phase Distribution on Test Panel Under Semi-Anechoic Condition, 1/3 Octave-Band Noise Source with Center Frequency 630 c/s, $\alpha = 90^\circ$, $\beta = 0^\circ$, $D = 9$ ins.	77
40	Pressure and Phase Distribution on Test Panel Under Semi-Anechoic Condition, 1/3 Octave-Band Noise Source with Center Frequency 630 c/s, $\alpha = 90^\circ$, $\beta = 0^\circ$, $D = 9$ ins.	78
41	Pressure and Phase Distribution on Test Panel Under Semi-Anechoic Condition, 1/3 Octave-Band Noise Source with Center Frequency 630 c/s, $\alpha = 45^\circ$, $\beta = 0^\circ$, $D = 9$ ins.	79
42	Pressure and Phase Distribution on Test Panel Under Semi-Anechoic Condition, 1/3 Octave-Band Noise Source with Center Frequency 1600 c/s, $\alpha = 45^\circ$, $\beta = 0^\circ$, $D = 9$ ins.	80

LIST OF ILLUSTRATIONS (Continued)

<u>Figure No.</u>		<u>Page</u>
43	Pressure and Phase Distribution on Test Panel Under Semi-Anechoic Condition, Coherent 1/3 Octave-Band Noise Sources S_1 , S_2 , S_3 with Center Frequency 630 c/s, $\alpha = 45^\circ$, $\beta = 0^\circ$, $D = 3$ ft.	81
44	Pressure and Phase Distribution on Test Panel Under Semi-Anechoic Condition, Coherent 1/3 Octave-Band Noise Sources S_1 , S_2 , S_3 with Center Frequency 630 c/s, $\alpha = 90^\circ$, $\beta = 0^\circ$, $D = 9$ ins.	82
45	Pressure and Phase Distribution on Test Panel Under Semi-Anechoic Condition, Coherent 1/3 Octave-Band Noise Sources S_1 , S_2 , S_3 with Center Frequency 630 c/s, $\alpha = 45^\circ$, $\beta = 0^\circ$, $D = 9$ ins.	83
46	Pressure and Phase Distribution on Test Panel Under Semi-Anechoic Condition, 1/3 Octave-Band Noise Source with Center Frequency 630 c/s, $\alpha = 45^\circ$, $\beta = 0^\circ$, One and Two Layers Absorbent, $D = 3$ ft.	84
47	Pressure and Phase Distribution on Test Panel Under Semi-Anechoic Condition, 1/3 Octave-Band Noise Source with Center Frequency 630 c/s, $\alpha = 45^\circ$, $\beta = 0^\circ$, One Layer Absorbent, $D = 3$ ft.	85
48	Pressure and Phase Distribution on Test Panel Under Semi-Anechoic Condition, 1/3 Octave-Band Noise Source with Center Frequency 630 c/s, $\alpha = 45^\circ$, $\beta = 0^\circ$, Two Layers Absorbent, $D = 3$ ft.	86
49	Pressure and Phase Distribution on Test Panel Under Semi-Anechoic Condition, 1/3 Octave-Band Noise Source with Center Frequency 630 c/s, $\alpha = 45^\circ$, $\beta = 0^\circ$, Three Layers Absorbent, $D = 3$ ft.	87

LIST OF IMPORTANT SYMBOLS

<u>Symbol</u>	<u>Definition</u>
2a	minor dimension of test panel; diameter of source
2b	major dimension of test panel
c	velocity of sound
D	energy density, energy per unit volume; separation of source from reflecting surface
f	frequency
G(t)	time dependent signal
k	wave number = $\omega/c = 2\pi/\lambda$
L	sound pressure level re. a reference RMS pressure of $0.0002 \text{ dynes cm}^{-2}$
L_D	sound pressure level in the diffuse field of a reverberation room
ΔL	sound pressure level increase at center of test panel
ΔL_1	sound pressure level at point P in a plane in the far-field relative to the maximum sound pressure level in that plane
m	energy attenuation constant in air
P (x, y, z)	general point in space
p_o	sound pressure amplitude unit distance from sound source; reference sound pressure of $0.0002 \text{ dynes/cm}^2$

LIST OF IMPORTANT SYMBOLS (Continued)

<u>Symbol</u>	<u>Definition</u>
p_i	sound pressure amplitude at point P due to i'th source (i = A, B, C)
P_i	root mean square sound pressure at P due to i'th source (i = A, B, C)
p_r	generalized root mean square sound pressure
Q_θ	directivity factor, ratio of intensity at a point in the far-field of a sound source to the intensity at this point from a non-directional source of equal power
R	generalized distance to point P from source system = $(x^2 + y^2 + z^2)^{1/2}$
R_i	distance to point P from i'th source (i = A, B, C)
r	distance
S	area
s	distance between source centers
u	directivity index of source in normal direction
V	volume
v	directivity index of source in given direction
W	source power (acoustic)
X	$\sum_i (\cos kR_i/R_i)$

LIST OF IMPORTANT SYMBOLS (Continued)

<u>Symbol</u>	<u>Definition</u>
Y	$\sum_i (\sin kR_i / R_i)$
YY'	minor axis of test panel
ZZ'	major axis of test panel
α	angle between normal to test panel and source plane; absorption coefficient
$\bar{\alpha}$	absorption coefficient averaged over the surface of an enclosure
$\bar{\alpha}_T$	total average absorption coefficient including surface absorption and air absorption
β	angle between normal to test panel and room surface containing reflecting surface; room constant, $\bar{\alpha}s/(1 - \bar{\alpha})$
γ	angle defining point P in far-field of sound source
θ	angle defining point P in far-field of sound source
λ	wavelength = c/f
ρ	density, mass per unit volume
Φ	$\tan^{-1} (Y/X)$
ω	angular frequency

SECTION I

INTRODUCTION AND SUMMARY

The RTD Sonic Fatigue Facility, currently under construction at Wright-Patterson Air Force Base, Ohio, will serve a dual purpose. It will provide information on the fragility levels of structures and will also make possible the proof-testing of final design structures. The facility, which has been described in detail by Kolb and Rogers (Ref. 1), was designed as a tool for investigating the effects of acoustic excitation on structures of flight vehicles and of electronic and power equipment. It consists of a test chamber 70 x 56 x 42 ft in size, with a volume of approximately 165,000 ft³. Low frequency acoustic power in the range 50 cps to 2400 cps is provided by a bank of twenty-five sirens located in one corner of the facility. This bank produces approximately 10⁶ watts of acoustical power and an additional 90,000 watts are produced from nine high frequency sirens in the range 500 cps to 9600 cps. By means of an acoustical lining treatment (Ref. 2) with removable and collapsible elements, the facility is capable of being operated under either progressive wave or diffuse field conditions. These two extreme methods of operation are particularly significant with respect to service environments. Fields of interest which are classified under the progressive type would include the fields on the exterior surfaces of planes, missiles, rockets or other flight vehicles. These fields result from combinations of the following sources which produce pressure fluctuations: jet or rocket engine sources, and aerodynamic noise sources in all their various forms. Diffuse-type fields would include those encountered in the interior spaces of flight vehicles or in missile silos. The pressure fluctuations which result from either jet or rocket engine noise and several of the various aerodynamic noise sources are very similar. Characteristically, both types possess broad-band spectral distribution and may be of very intense level. However, there are other parameters of sound fields whose values are characteristic of the type of source producing the sound field. This raises the question as to which are the most important parameters which must be reproduced in any service field simulation. Ideally any fatigue facility should reproduce all of the characteristic parameters of a service field. To attain such a goal is beyond the present state of the art and consequently it is not expected that the facility can reproduce all the parameters of a service field but only that it will be able to simulate the most important of these. The most significant parameters would certainly appear to include the spatial power spectral distribution as well as the temporal and spatial correlation of the field. Thus, if a service field can be specified in terms of its most important parameters, such as those mentioned above, the objective in the service field simulation would be that of producing a field possessing as good a reproduction of those

Manuscript released February 1964 for publication as an FDL Technical Documentary Report.

parameters as possible. This still might appear a formidable task, but one must recognize that it is not necessary to simulate a service field over a complete volume in space so long as the simulation occurs adjacent to the surface of the test structure. It is, of course, necessary to know whether the sound field parameters are to be simulated in the presence or absence of the test structure. In most cases, a service field will be specified at the surface of a test structure, but there may be other instances in which the characteristics of the field are known in the absence of the test structure, for example, the predicted or measured environment in a space vehicle in which a structure is to be located.

Assuming that service fields can be specified in terms of their most important parameters, it is necessary to simulate these fields in the RTD facility. In order to achieve this with the minimum of operational effort and in the most economical manner, it has been the aim of this study to investigate the potentialities of the facility. This study has not been directed toward simulating specific service fields, one reason for this being that insufficient data exists on anticipated service fields of the future (Ref. 3). This study has been concerned with obtaining generalized information on attainable environments. This approach to the problem has one important advantage over that of attempting service field simulation. This generalized study will enable such non-service fields as may be required for specific fatigue testing studies, such as accelerated life tests, to be more readily simulated. Our approach has been to investigate attainable fields in terms of the spatial power spectral level and correlation. Thus the investigation of fields is in terms of RMS pressure levels and phase relationship in the fields. The study consists of:

1. A theoretical study of the characteristics of the diffuse field operation, examining the anticipated sound pressure level in the field and defining the extent of the diffuse field as influenced by anticipated siren directivity as well as the effect of test structures on the sound field.
2. A theoretical study of the characteristics of the progressive wave operation of the facility as influenced by the manner in which sirens are grouped in order to enable broad-band noise simulation to occur. Selected far-field distributions are presented which have been calculated for some simple siren groupings.
3. An experimental study to determine how the size and orientation of simple test structures influence the field at the structure's surface when exposed to simple sound fields such as may be produced by one or a small number of sources operating simultaneously in the same frequency range.

SECTION II

CALCULATION OF CHARACTERISTICS OF THE DIFFUSE FIELD

In a diffuse sound field, sound waves can be considered to arrive at a point with equal probability from any direction and are equal in amplitude and random in phase. If a sound source with a very narrow band of frequencies is used, there will be fluctuations in sound pressure level as a microphone is moved through the field but, for a source with a wider band width, such as a one-third octave, the fluctuations with microphone position are small and a space average of sound pressure level is easily obtained. The requirements for a diffuse (random or reverberant) sound field have been studied in connection with architectural acoustics and the measurement of sound absorption coefficients and there is much published material on the subject. For instance, Morse and Bolt (Ref. 4) have analyzed sound waves in rooms in terms of room modes and, more recently, space correlation of sound pressure in diffuse fields has been discussed by Cook, et al (Ref. 5), Balachandran (Ref. 6), Dämmig (Ref. 7), and by Richardson and Meyer (Ref. 8) who also discuss its effect on structure vibration.

A diffuse field in the RTD facility has the following advantages for sonic fatigue testing.

1. High sound pressure levels can be attained since the absorption coefficient of the room surfaces is small.
2. The sound pressure level is relatively independent of position over the greater part of the room volume and is not affected by the distance from the sound sources.
3. The field is easily defined and can be specified both in terms of the magnitude of the sound pressure level in bands of frequency and in terms of the theoretical spatial correlation.
4. Large test structures can be exposed to a relatively uniform and well defined field as a consequence of 2 and 3 without the necessity of monitoring the sound field at many points.

Limitations in the use of a diffuse field environment are concerned with its lack of flexibility. Variation of sound pressure level along the surface of a test structure cannot be obtained except close to the sound source and the spatial correlation of sound pressure cannot be materially changed.

SOUND PRESSURE LEVEL IN THE DIFFUSE FIELD

The sound pressure level in a diffuse field can be calculated quite simply provided that the source sound power and the total absorption in the room are known. Close to a sound source the level from the direct sound is higher than the level for the diffuse sound. Hopkins and Stryker (Ref. 9) have shown curves relating sound pressure level at a distance r from a source of directivity factor Q_0

$$|p_r|^2 = W_p c \left(\frac{Q_0}{4\pi r^2} + \frac{4}{\beta} \right) \quad (1)$$

where the first term corresponds to the direct sound from the source and the second term to the sound in the diffuse field. The room constant β is determined by the average absorption of the room. When only the room boundaries determine the absorption

$$\beta = S\bar{a}/(1 - \bar{a}) \quad (2)$$

and

$$\bar{a} = \sum a_1 S_1 + a_2 S_2 + \dots \quad (3)$$

When there is additional absorption in the air, it is customary to use the energy attenuation constant m defined by an energy density relation,

$$D_1 = D_2 e^{-m(x_2 - x_1)} \quad (4)$$

The air absorption can be combined with the surface absorption by assuming a mean free path to obtain a total average room absorption \bar{a}_T (see, for example, Beranek, Ref. 10)

$$\bar{a}_T = \bar{a} + 4 \text{ mV/S} \quad (5)$$

When the air absorption term is significant compared to \bar{a} , Eq (2) should be modified to get

$$\beta = S\bar{a}_T / (1 - \bar{a}_T) \quad (6)$$

The second term in Eq (5) is important at high frequencies and in large rooms. Curves of m in terms of relative humidity at normal pressures and temperatures are given in many acoustical textbooks and a recent discussion is contained in an article by Harris (Ref. 11).

At high sound intensities there will also be absorption associated with nonlinear propagation of finite amplitude sound and this will increase the effective room absorption over the value calculated for small amplitude conditions. This could be added to the usual attenuation coefficient in air, if the attenuation due to finite amplitudes were small and could be approximated in terms of db/per unit distance. At high sound pressure levels, however, the losses in propagation are not easily determined and may be more significant in the case of a diffuse field with a long mean-free path than in the usual case of a progressive wave with spherical spreading.

Ignoring the effect of finite amplitudes, the sound pressure level in the diffuse field L_D can be calculated from the second term in Eq (1)

$$L_D = 10 \log \left(\frac{p_r}{p_o} \right)^2 = 10 \log \left(\frac{4W\rho c}{p_o^2 \beta} \right) \quad (7)$$

For a reference sound pressure p_o of $0.0002 \text{ dynes/cm}^2$, W in acoustic watts, and β in square foot units

$$L_D = 10 \log W - 10 \log \beta + 136.5 \quad (8)$$

which allows a calculation of L_D . The source sound power for the fixed sirens is 10^6 watts and the room constant β can be estimated from the absorption in the room. A rough estimate of the room constant was given in Table XI page 138 of Reference 2 as $3,940 \text{ ft}^2$ for the collapsed wall treatment with ceiling treatment removed.

A recalculation of the room volume and surface areas based on the blueprints now available, instead of a rectangular room assumption used previously, has resulted in the following values

Volume	$160,000 \text{ ft}^3$
Total Surface Area	$17,600 \text{ ft}^2$
Collapsed Treatment Area	$4,060 \text{ ft}^2$
Untreated Surface Area	$13,500 \text{ ft}^2$

The area of the collapsed treatment was estimated by determining the exposed area of bands of material of rectangular cross section at the edges of the ceiling. The horizontal dimension of a band was taken as six feet and the vertical dimension as one third the wall height (assuming that each polyurethane wall layer is raised with two folds and has three verticle portions). This estimated area of collapsed treatment, 4060 sq ft , is larger than that used in previous calculations, 3216 sq ft , based on a ten foot height of collapsed treatment. The total absorption of the walls and collapsed treatment and the average absorption coefficient are given below.

Untreated surface area x 0.02	=	270 sabins
Collapsed treatment area x 0.90	=	$\frac{3654}{3924}$
Average absorption coefficient	=	$\frac{3924}{17,600} = 0.22$

This value of $\bar{\alpha}$ is not greatly different from the previous estimate of 0.20. Since both are based on a rather doubtful estimate of 90 per cent absorption coefficient for the collapsed treatment, predictions of reverberation time and sound pressure level have a considerable margin of error.

The second term 4 mV/S from Eq (5) is negligible at frequencies below about 2000 cps compared to the uncertainty in the first term, $\bar{\alpha}$. From

Ref. 11, m is less than 0.001 ft^{-1} at 2000 cps for relative humidities of 40 per cent or greater and for normal atmospheric pressure and temperature of 20°C , and is considerably smaller at lower frequencies. The corresponding values of 4 mV/S at 2000 cps is 0.037 which should be added to 0.022 to get 0.026 for \bar{a}_T .

It is noted that, while air absorption is not important below about 2000 cps in the RTD room with the collapsed wall treatment, it is significant at much lower frequencies in the room without treatment. For the bare room the average absorption coefficient for the surface was taken as 0.02 and, using the previously estimated value of 4 mV/S of 0.037, at 40 per cent RH, \bar{a}_T would be 0.057. This is in fairly good agreement with measured values of reverberation time reported for the bare room. Thus at 300 cps the measured reverberation time was 21.2 sec and at 2000 cps and 9.2 sec at 4000 cps giving an approximate ratio of \bar{a}_{T2000} to \bar{a}_{300} of 2.3 compared to the estimated ratio of 2.85. The room constant β at frequencies below about 2000 cps is given by substituting values of \bar{a}_T equal to 0.22 and $S\bar{a}_T$ equal to 3920 ft^2 in Eq (6)

$$\beta = \frac{3920}{1 - 0.22} = 5030 \text{ ft}^2 \quad (9)$$

Substituting in Eq (8) to obtain the sound pressure level in the diffuse field for 10^6 watts acoustical power from all the fixed sirens

$$\begin{aligned} L_D &= 10 \log (10^6) - 10 \log 5030 + 136.5 \\ &= 160 \text{ db re } 0.0002 \text{ dynes cm}^{-2} \end{aligned} \quad (10)$$

This value is approximate because of uncertainty in the value of 0.90 for the absorption coefficient of the collapsed treatment and because no allowance has been made for absorption due to finite amplitude effects at high sound levels. Measurements made when the room is completed can be made to provide information on the accuracy of various estimated values. Thus decay curves from initial levels of 140 db or less will determine the total surface absorption and decay curves from high levels may have higher initial slopes indicating that finite amplitude effects are significant. The steady state level in the diffuse field may then be used to determine the total power of the sources since the absorption will be known from the decay curve measurements.

No consideration has yet been given to the effect on radiated source power of the location of the source with respect to reflecting surfaces. Reflecting surfaces near a source change the acoustical impedance reflected

into the source and thus may change its power output. For many sources such as loudspeakers, transformers, appliances, etc., it can be assumed that the vibration amplitude is independent of the medium. The internal impedance is much higher than the radiation impedance and the acoustic power output is proportional to the radiation resistance. Waterhouse (Ref. 12) has shown the variation of output from simple sources as a function of the distance from reflecting planes, edges, and corners based on interference patterns between the source and its images. He also gives experimental confirmation and discusses the effect of source bandwidth. For this type of sound source, the power varies with distance from the reflector in wavelength and reaches maximum values of 2, 4, and 8 times its free field power for one plane, two plane and three plane reflectors at right angles.

It is not known whether a siren noise source can be considered as a source of constant volume velocity independent of radiation impedance. It is expected that this condition is at least partially fulfilled and that the output will be increased by adjacent reflecting surfaces. Thus sirens near the floor will probably have greater power outputs than sirens near the middle of the array.

SOUND PRESSURE LEVEL NEAR SOUND SOURCES

The sound field near the source or sources is determined by the first term of Eq (1), $Q/4\pi r^2$, corresponding to the direct sound field from the source. When the sound pressure level corresponding to $|p_r|^2$ is plotted against $\log r$, it decreases as a straight line until the level approaches that of the diffuse field (see Ref. 9) and then becomes constant for large values of r . It is convenient to designate the extent of the direct field by the value of r when the direct field energy equals the diffuse field energy.

$$r' = (Q_0 \beta / 16\pi)^{1/2} \quad (11)$$

At this point, the sound pressure level is 3 db above the level in the diffuse field.

Using the previously estimated value of β , 5030 ft²,

$$r' = (100 Q_0)^{1/2} \quad (12)$$

For a nondirectional source, Q_0 is unity and r' is ten feet.

Of interest is the directivity factor Q_0 for one siren or a group of sirens. A single siren might be considered similar in directionality pattern to a plane circular source. Graphical representations of the directionality patterns of such sources are given by Olson (Ref. 13), Fig. 2.10, pp. 39 and by Beranek (Ref. 10) who gives patterns of a piston in an infinite baffle, Fig. 4.10, pp. 102, and in the end of a long rigid tube, Fig. 4.12, pp. 104. Much of this material is based on Jones (Ref. 14) who gives extensive tables of directionality patterns. The directionality pattern is essentially that of a simple source $Q_0 = 1$, when ka is much less than unity (a is the radius of the circular source, 1 ft for the fixed sirens). A single siren located away from the edges of the fixed siren array can be considered, at least qualitatively as similar to a circular piston at the end of a long tube. From Fig. 4.12 of Ref. 10, the maximum directivity factor Q_{\max} for $ka = 0.5$ is about 1.29 corresponding to a frequency of 90 cps, for $ka = 1.0$, Q_{\max} is about 1.9 corresponding to 180 cps and for $ka = 2.0$, Q_{\max} is about 4.6 corresponding to 360 cps. From Eq (12), r'_{\max} defining the extent of the direct field opposite the siren would be multiplied by the square root of Q_{\max} . Thus r'_{\max} would be 10 ft at low frequencies, 11.3 ft at 90 cps, 13.8 ft at 180 cps, and 21.5 ft at 360 cps.

Two or more sirens operated in phase will have sharper directional patterns than a single source and will be characterized by ks (s is the center spacing of the sources, 2.5 ft for adjacent fixed sirens). Olson (Ref. 13) Fig. 2.3 gives curves of directional patterns of two separated small sources and these exhibit rather complicated patterns with secondary lobes for large values of ks . Reflecting room surfaces near a source will produce image effects and thus will affect the directionality as well as the sound power, discussed previously. Thus Beranek (Ref. 10), Table 10.2, pp. 319, gives values of Q_{\max} for a small nondirectional source as 1 near the center of a room, 2 at the center of a wall, 4 at a dihedral corner and 8 at a trihedral corner.

Source directionality effects thus may increase considerably the extent of the direct field and this may be detrimental in some fatigue tests. Portions of large test objects to be tested in a diffuse field may extend into the direct or non-diffuse field. This can be prevented by using one or more reflecting baffles in front of the source area to reflect sound energy toward adjacent room surfaces.

Source directionality effects may be advantageous, however, since there will be a portion of the room where sound pressure levels are higher than the level in the diffuse field. A desirable sound field on a test object may be one which has progressive wave characteristics close to the source and diffuse field characteristics at greater distances from the source.

SOUND PRESSURE LEVEL NEAR ROOM BOUNDARIES

Although the sound pressure level in a diffuse field is essentially independent of position at measuring points away from room surfaces, this is not true for positions close to these surfaces. Waterhouse (Ref. 15) discusses

this effect and gives theoretical and experimental results for sound pressure level variations in a rectangular room close to large plane surfaces and close to dihedral and trihedral corners. The interference effects resemble those for the effect of reflecting surfaces on source output (Ref. 12). At a reflecting plane the sound pressure level is 3 db higher than the level far from the plane, at a dihedral angle it is 6 db higher, and at a trihedral angle, 9 db higher. The distance from the reflector at which the sound pressure level closely approaches the diffuse field value is proportional to the wavelength and the effect of the reflector is small at distances greater than about one wavelength.

SOUND PRESSURE LEVEL AT TEST STRUCTURES

When a test structure is located in a diffuse field, the sound pressure level at its surfaces will be affected (1) by its location with respect to the sound source (direct sound field), (2) by its size and shape, and (3) by its surface impedance. The most simple case is that of a test structure with dimensions small compared with a wavelength. The sound pressure level at its surface will be that of the sound field existing at that point without the presence of the object.

If the test structure dimensions are large compared to a wavelength and its surface impedance is large, the pressure level at its surface will be similar to that of a reflecting room surface discussed previously under Sound Pressure Level Near Room Boundaries. Thus a large flat test structure will have a sound pressure level at its surface about 3 db higher than the level in the diffuse field. Near the edges of such a large surface, interference or diffraction effects will occur and the sound pressure level will vary in a manner not easily predictable. Large pressure level variations are not to be expected, however. The same can be said for a test structure with dimensions comparable with a wavelength.

If a large test structure is located close to the room boundaries the sound pressure level at its surfaces will be affected. Thus a flat structure may be located parallel to the floor and with its lower surface within a wavelength of the floor. The sound pressure level on the lower surface will not be the same as on its upper surface and the pressure level distribution is again not easily predictable. Large variations from the diffuse pressure level can be expected for some surface to floor spacings. If a test structure is located so as to partially enclose a portion of the room, the pressure level in this portion may be different from the level in the remainder of the room. This condition is similar to coupled spaces such as balcony recesses in architectural acoustics and estimation of the level in the enclosed space can be made from the size of the connecting openings and the absorption in the coupled space.

If the surface impedance of a test object is low compared to the impedance of the medium, approximately 4 pc in a diffuse field, partial reflection or absorption will occur. Because of the high surface density of most

materials, this acoustic impedance matching will occur at non-porous surfaces only when resonant vibration occurs in narrow frequency regions or at particular angles of sound incidence when the sound pressure along a surface is in phase with transverse vibration of the surface material. Wave coincidence effects are discussed in connection with sound transmission through walls by Cremer (Ref. 16) and Watters (Ref. 17). For porous material, the surface impedance may be such that much of the sound energy is absorbed. It would be expected that the sound pressure levels at highly absorptive surfaces would be the same as in the diffuse field or less than this because of diffraction effects. Experimental confirmation of this is not available nor of effect on the sound field of surfaces which are caused to vibrate by the sound field.

SECTION III

PROGRESSIVE-TYPE SOUND FIELDS CALCULATED FOR ONE TO THREE NON-DIRECTIONAL SOURCES

In order that the facility can be operated with a broad-band noise simulation such as may be desired for many service fields, it will be necessary to distribute the sirens' outputs over wide frequency ranges. One practical way is to allow either one or a small number of sirens to supply energy to a narrow segment of the frequency band of interest. Several such groupings of sirens could be used, each covering different segments of the frequency range, and in this manner a broad-band source system would be achieved. The aim of this analysis was to consider what acoustic fields could be produced when small numbers of sirens were operated at a given frequency. We considered only three simple groupings of sources, a single source, two adjacent sources, and three adjacent sources, arranged on three corners of a square. These groupings of sources will allow twenty-five, twelve or eight sets of sources to be obtained in the cases of one, two, and three sirens per group respectively. These simple source groupings are only a few of many possible siren groupings which could be employed in the facility, but they allow some representative progressive wave field distributions to be determined.

In common with sound radiation from any source array, the sound field may be classified as either the near- or the far-field. The far-field may be defined as the field in which the sound pressure is decreasing linearly with distance along a radius from the source array. Accepted criteria which must be adhered to are that if R is the distance of any point in the far-field from the source array then $R > \lambda/6$ and $R > 2s^2/\lambda$ where s is the extent of the source array (Ref. 10, page 100). For the previously mentioned arrays in the facility, s is 2.5 ft and consequently it is this second condition which is most important in determining the extent of the far-field. If we assume a velocity of sound of approximately 1000 ft/sec, then at typical operational frequencies 50, 100, 200, 500, 1000, and 2000 c/s, the corresponding wavelengths will be 20, 10, 5, 2, 1, and 0.5 ft. Thus, at these frequencies, the far-field will extend to within the following distances of the source array, 0.6, 1.2, 2.5, 6.2, 12.5, and 25 ft correspondingly. Thus for all practical purposes one can assume that the far-field extends over nearly the whole volume of the facility at low frequencies. Consequently, although we have developed expressions for both the near and the far-field in the facility, we have given more attention to the far-field and have evaluated these expressions for some operating conditions. The assumptions we made about the operating conditions in the facility were that all the siren sources in a group are sinusoidally operated in phase and that all sirens are identical omnidirectional sources. In addition, completely progressive wave operation of the facility was assumed, i.e. no sound is reflected from the boundaries of the facility.

Figure 1 shows a typical three-source figuration. The sources are represented by the points A, B, and C, and $P(x, y, z)$ represents any point

in the field at distances R_A , R_B , and R_C from the three points A, B, and C. Then the sound pressure at the field point P produced by each source can be represented by

$$p_i = \frac{p_o}{R_i} (\cos \omega t - kR_i) \quad (i = A, B, C) \quad (13)$$

where p_o represents the pressure amplitude at unit distance from a single source.

Then the total sound pressure at P produced by the group is given by

$$\begin{aligned} p &= \sum_i p_i = \sum_i \frac{p_o}{R_i} \cos (\omega t - kR_i) \\ &= p_o \sum_i \frac{(\cos \omega t \cos kR_i + \sin \omega t \sin kR_i)}{R_i} \end{aligned} \quad (14)$$

$$p = p_o \left[\cos \omega t \sum_i \frac{(\cos kR_i)}{R_i} + \sin \omega t \sum_i \frac{(\sin kR_i)}{R_i} \right] \quad (15)$$

$$\begin{aligned} p &= p_o (\cos \omega t \cdot X + \sin \omega t \cdot Y) = p_o (X^2 + Y^2)^{1/2} \left[\cos \omega t \cdot \frac{X}{(X^2 + Y^2)^{1/2}} \right. \\ &\quad \left. + \sin \omega t \cdot \frac{Y}{(X^2 + Y^2)^{1/2}} \right] \end{aligned} \quad (16)$$

$$p = p_o (X^2 + Y^2)^{1/2} \cos (\omega t - \Phi) \quad (17)$$

where

$$\Phi = \tan^{-1} \left(\frac{Y}{X} \right) \quad (18)$$

$$X = \sum_i \frac{(\cos kR_i)}{R_i} \quad (19)$$

$$Y = \sum_i \frac{(\sin kR_i)}{R_i} \quad (20)$$

The evaluation of this expression in the near-field demands the use of a computer program. This evaluation has not been attempted because of the limited extent of the near-field in the facility. However, a slide-rule evaluation of the far-field has been performed for this three-source system as well as for the two-source and the single-source systems.

With reference to Fig. 1, if we designate PA (= R_A) by R, and if P is in the far-field, we may assume that $p_o/R_i \simeq p_o/R$ and Eq (14) reduces to

$$p = \frac{p_o}{R} \sum_i \cos (\omega t - kR_i) \quad (21)$$

Thus,

$$p = \frac{p_o}{R} \left[\left(\sum \cos kR_i \right)^2 + \left(\sum \sin kR_i \right)^2 \right]^{1/2} \cos (\omega t - \Phi) \quad (22)$$

where Φ is now reduced to

$$\tan^{-1} \left(\frac{\sum \sin kR_i}{\sum \cos kR_i} \right) \quad (23)$$

We have designated $PA (= R_A)$ by R and from Fig. 1 it follows that

$$PB = R_B = PA + DB = R + s \sin \theta = R + s \cdot z/R \quad (24)$$

Similarly

$$\begin{aligned} PC = R_C = PA + EC = R + DB + FC = R + s \cdot z/R \\ + s \cos \gamma = R + s \cdot z/R + s \cdot y/R \end{aligned} \quad (25)$$

Thus

$$\begin{aligned} \left(\sum \cos kR_i \right)^2 = (\cos kR_A + \cos kR_B + \cos kR_C)^2 = \left[\cos kR \right. \\ \left. + \cos k(R + s \cdot z/R) + \cos k(R + sz/R + sy/R) \right]^2 \end{aligned} \quad (26)$$

and similarly

$$\begin{aligned} \left(\sum \sin kR_i \right)^2 = \left[\sin kR + \sin k(R + s \cdot z/R) + \sin k(R + sz/R \right. \\ \left. + sy/R) \right]^2 \end{aligned} \quad (27)$$

Thus the amplitude of the pressure at P which follows from Eq (22), is

$$\frac{p_o}{R} \left[\left(\sum \cos kR_i \right)^2 + \left(\sum \sin kR_i \right)^2 \right]^{1/2} = \frac{p_o}{R} \left[3 + 2 \left(\cos \frac{ksy}{R} + \cos \frac{ksz}{R} + \cos \frac{ks(y+z)}{R} \right) \right]^{1/2} \quad (28)$$

It is this expression which enables the far-field distribution to be calculated for this three-source system. In particular we used it to determine the pressure amplitude distribution in a plane parallel to the source plane and containing the point P. We have calculated pressures in such a plane and express the result in decibels relative to the pressure at the point on the plane having maximum pressure level. Although this point will lie on the circumcenter of the image of triangle ABC in the plane under consideration, we may assume this point lies on the intersection of the X axis with the plane. The pressure amplitude at this point is simply $3p_o/x$, so that the pressure level, ΔL_1 , at P relative to this point is

$$\Delta L_1 = -20 \log_{10} \left(\frac{x}{3} \cdot \frac{1}{R} \left[3 + 2 \left(\cos \frac{ksy}{R} + \cos \frac{ksz}{R} + \cos \frac{ks(y+z)}{R} \right) \right]^{1/2} \right) \text{db} \quad (29)$$

where

$$R = (x^2 + y^2 + z^2)^{1/2} \quad (30)$$

This expression was computed for three values of the siren spacing parameter s . These were $\lambda/4$, $\lambda/2$, and λ . This corresponds to frequencies of 110, 200, and 440 c/s, assuming the velocity of sound is 1100 ft/sec. The planes in which the distribution was computed were chosen to be respectively 5λ , 10λ , and 20λ from the source system. Thus, in all three frequency cases, the plane was situated 50 ft from the source system. This plane represents an approximation to a vertical diagonal plane in the RTD

facility. The evaluation of Eq (29) for the three frequencies 110, 220, and 440 c/s is shown in Figs. 2, 3, and 4.

If we consider only a two-source operation, e.g. sources A and B, only the following modifications to Eqs (26) and (27) result,

$$(\sum \cos kR_i)^2 = \left(\cos kR + \cos k \left(R + \frac{sz}{R} \right) \right) \quad (31)$$

$$(\sum \sin kR_i)^2 = \left(\sin kR + \sin k \left(R + \frac{sz}{R} \right) \right) \quad (32)$$

Similarly Eq (29) reduces to

$$\Delta L_1 = -20 \log_{10} \left[\frac{x}{2R} \left(2 + 2 \cos \frac{ksz}{R} \right)^{1/2} \right] \text{db} \quad (33)$$

This further reduces to

$$\Delta L_1 = -20 \log_{10} \left[\frac{x}{R} \cos \frac{ksz}{2R} \right] \text{db} \quad (34)$$

This expression was evaluated for the plane identical to that used in the three-source case and the results are shown in Figs. 5, 6, and 7 for the three frequencies 110, 220, 440. Figure 8 shows the distribution in the same plane for a single-source case. The distribution in this case is independent of frequency.

We have thus established pressure amplitude distributions in a fixed plane for a single-, a two- and a three-source system as a function of frequency. The assumption has been made that the sirens are omnidirectional. If, in practice, this condition is not fulfilled, adjustments to the pressure distribution in the given plane can be made if the directivity pattern of a siren is known. For example, if the directivity index of a siren is +u db in the normal radiating direction, i.e. along the x-axis, and is -v db in some other radiating direction, then a correction of (-u + v) db must be made to the pressure contour on the fixed plane at the intersection of this latter radiating direction and the fixed plane.

From the distribution in a plane it is possible to establish the pressure at any other point in the facility. For example, if the distribution in plane 1 is known, then the distribution on any other plane 2 may be determined. If the point $P_1 (x_1, y_1, z_1)$ lies on a contour $-\Delta L_1$ db relative to the maximum pressure in plane 1, then a point $P_2 (x_2, y_2, z_2)$ will also lie on a contour $-\Delta L_1$ db relative to the maximum pressure in the plane 2, if the following condition is satisfied:

$$\frac{z_1}{z_2} = \frac{y_1}{y_2} = \frac{x_1}{x_2} \quad \left(= \frac{R_1}{R_2} \right)$$

This follows from inspection of Eq (29).

Thus any contour in plane 2 will be identical to the equal-valued contour in plane 1, except that the representative dimensions of the contour will be enlarged in the ratio x_2/x_1 . However, the pressure level in the center of plane 2 will be $-20 \log (x_2/x_1)$ db relative to the pressure in the center of plane 1. Utilizing these two facts, the far-field distribution throughout the whole extent of the facility can be determined, once the distribution in a single plane parallel to the source plane is known.

Again it must be noted that these pressure amplitude distributions shown in Figs. 2 through 8 represent the field distributions in the facility operated under completely anechoic conditions and that the sources are identical, omnidirectional and are operated in phase at a single frequency. Any variation in any of these conditions may modify these distributions. However, these distributions serve as a basis for establishing attainable fields in the facility. The value of knowing these distributions in the far-field is two-fold. Firstly, it enables those regions to be defined in which the spatial distribution of pressure amplitude is (a) changing only gradually or not at all, and (b) changing rapidly. When a test structure is located in a region of the RTD facility where there is an even distribution of pressure, the distribution existing on the surface of the structure can be predicted approximately by methods outlined in a later section of the report. One may assume in such cases that the source system, comprising a number of sirens, can be regarded as acting as a single source with regard to the particular region of interest in the far-field. In regions in which rapid changes in spatial distribution occur in the field in the absence of the test structure, it may be anticipated that this will produce more complexity in distribution on a test structure placed in this field. These complex distributions, however, can certainly be expected to be of interest in producing service field simulation.

It is of interest to consider operations of the sirens other than the discrete frequency case. If the sirens are operated, identically, in a frequency modulated manner to simulate a narrow frequency band, for example, then the far-field distributions for each of the band's frequencies components will be almost identical and equal to the distribution when the system is

operated at a discrete frequency. However, sufficiently different far-field distributions may be produced for each of the component frequencies that a 'smoothing-out' of the overall field may occur if, for example, it is analyzed with a one-third octave band filter. However, the complexities will be observed if a sufficiently narrow band filter is used so that only the field of one of the modulation frequencies is analyzed at a time. Further simplification of the field will occur if the sirens are not operated coherently when this frequency modulation is applied. The field will be the result of the superimposition of the fields produced from numbers of incoherent sources. For the closely situated sirens cited in our analysis the field will degenerate into one closely approximating that from a single source. Some of these hypotheses are confirmed by the results of the experimental program in which pressure distributions measured on the surface of a test panel are of a complex nature when obtained by operating numbers of sirens coherently and are simplified by operating them incoherently.

SECTION IV

EXPERIMENTAL MODEL STUDY

The aim of this experimental model study was to obtain generalized information on the types of sound fields which may exist at the surface of simulated test structures exposed to progressive sound waves. The fields were studied as functions of the sizes of the test structures, their location and orientation with respect to the sound source system, as well as the number, distribution, and operating frequency of the individual sources comprising the system and the degree of coherence existing between them. In addition to this wholly progressive wave study, a semi-anechoic investigation was conducted. For this experimental study the IITRI anechoic chamber was used as a model of the RTD sonic fatigue facility operating in the progressive wave condition.

EXPERIMENTAL FACILITY

The IITRI anechoic chamber has a working volume of size 17 x 12 x 8 ft compared to the dimensions of the RTD facility of approximately 70 x 56 x 42 ft. Because of the difference in sizes between the two facilities, a modeling technique was adopted for the experimental study for which a scaling factor of $1/4$ was used. Thus all dimensions of the source system, test structures and distances in the RTD facility were scaled down by this factor in the IITRI anechoic chamber. To preserve scaling similarity, all frequencies of interest were scaled up by a factor of 4.

Because large test structures may be placed in the RTD facility, it may not be possible or practical to line the floor with absorbent treatment. As a result, the assumption of a completely anechoic operating condition will be invalid. Consequently, for the purpose of a semi-anechoic study, one wall of the IITRI anechoic chamber was faced with a $1/2$ inch thick plywood surface 24 x 6 ft. The reason for covering a wall rather than a floor was simply one of experimental convenience. Figure 9 illustrates the experimental facility. The source system initially used in the study consisted of a single horn-driver coupled to a resonance tube. Three resonance tubes were designed for frequencies of 200, 600, and 1800 cps. When one of these tubes was coupled to a horn-driver, a good simulation of a spherically radiating, omnidirectional point source was achieved. These single source systems were replaced by a multiple loudspeaker system when the study incorporated the use of one-third octave band noise rather than a pure tone. Four 8 inch cone loudspeakers were mounted in individual enclosures and arranged in a square array with speaker center spacings of 10 inches, as shown in Fig. 9. This represented a good approximation to four adjacent sirens arranged in a square array in the RTD facility. It was considered necessary to choose simple structures for this study which might be representative of anticipated test structures. It was decided that plane panels of either square or rectangular

shape would adequately meet these requirements. Consequently two plane test panels were adopted for the study. These were formed of 1/2 inch thick plywood and had dimensions of 5 x 4 ft and 2 x 2 ft respectively. These represented plane test panels of 20 x 16 ft and 8 x 8 ft in the RTD facility. These panels were capable of being mounted in a stand which enabled the panels to assume any orientation with respect to the source system. For these studies the center of a particular panel under test was always maintained 6 ft from the source system, which would represent structures located 24 ft from the source system in the RTD facility.

The sound pressure level on the surface of the panels was measured initially with a 1/2 inch diameter condenser microphone mounted on a framework attached to the panel. This framework permitted the levels to be taken at points on an orthogonal grid system marked on the surface of the panel. Interpolation between this pattern of sound pressure levels enabled equal pressure contours to be obtained. These contours were referred to the sound pressure level at the center of the panel. This technique was used with pure tone sound fields but when experiments were conducted with one-third octave band noise fields, a hand-held microphone enabled more rapid exploration to be made of pressure distributions on panels. The output from the microphone, first filtered using a Brüel and Kjaer 1/3 octave filter, was displayed on a Brüel and Kjaer voltmeter using the slow RMS scale. The locus of constant sound pressure level contours was obtained by moving the microphone along the panel surface so as to maintain a constant reading on the voltmeter.

Relative phase distributions of the acoustic field at the surface of the panels was obtained in the following manner. A second fixed microphone was located in a convenient position at the surface of the test panel. The output from this microphone formed a reference signal to which the output from the exploring microphone could be compared. The phase comparison between the outputs of the fixed reference microphone and the exploring microphone was achieved by displaying the two outputs on the X and Y plates of an oscilloscope. In this manner a Lissajou figure was formed. For tone signals this figure was an ellipse which degenerated into a straight line when the two outputs were $+n\pi$ out of phase with each other ($n = 0, 1, 2, 3$, etc.). The exploring and reference microphones were located on the panel so as to produce a straight-line Lissajou figure. The exploring microphone was then scanned across the panel surface so as to maintain this straight line display. The path of the microphone had then traced out the locus of an equal phase contour. This was repeated with the exploring microphone displaced to a position on another equal phase contour, so as to again produce a straight line oscilloscope display. In this manner a series of equal phase contours was produced, each being separated by a phase angle π from the preceding one. Intermediate phase contours could also be obtained when the Lissajou figure degenerated to a circle. This method of phase determinations gave a qualitative indication of the degree of correlation between two signals. This technique was also applied to phase contour determinations when the tone source was replaced by a one-third octave band noise source. It was still possible to recognize the degenerated line trace. However, when the microphones were separated by distances greater than the order of the wavelength of the center frequency of interest, the two microphone outputs were uncorrelatable and consequently phase determinations were not possible. This was in contrast to the method

as applied to pure tones, where phase determinations could still be produced when the microphones were separated by several wavelengths. In the absence of any test panel it was decided to determine what amount of separation could be tolerated between the two microphones before relative phase information, as determined by this Lissajou figure method, could no longer be obtained. Tests were carried out for a one-third octave band noise source at the following three center frequencies: 200, 630, and 1600 c/s. These tests showed that when two microphones were placed in a progressive wave field, no phase determinations were possible when their separations, along the direction of propagation, were greater than distances of the order $\lambda/2$, λ , and $3\lambda/2$ for these three frequencies respectively. It is not known why different maximum separations in wavelengths were obtained for the three one-third octave band signals. Inspection of the auto-correlation function for one-third octave band noise signals suggests that the maximum microphone separation at any frequency should be a fixed number of wavelengths. It is possible that the filtering systems for the microphones were imperfect, having differences with respect to bandwidth and phase.

PANEL ORIENTATIONS

It has been previously stated in this report that one of the parameters of interest for this study was that of test panel orientation with respect to the source system. In addition, the orientation of the panel with respect to the reflecting surface in the case of the semi-anechoic study will be another significant parameter in determining the pressure distribution on the test panel. Consequently, the orientation of panels is given in terms of angles α and β . Angle α represents the angle between a normal to the test panel plane and the source plane, and angle β represents the angle between a normal to the test panel plane and the plane of the reflecting surface. Thus, in Fig. 9, the panel orientation would be $\alpha = 45^\circ$, $\beta = 0^\circ$. The dashed panel's orientation would be $\alpha = 90^\circ$, $\beta = 0^\circ$.

SINGLE SOURCE IN ANECHOIC CONDITION

Initial studies were conducted on the smaller test panel with dimensions 2 x 2 ft, using a pure tone source. Figures 10 and 11 show the pressure and phase distributions on this panel when subjected to a 600 c/s tone at four inclinations to the fixed single source ranging from normal incidence to grazing incidence. For this panel and frequency, the ka value was 3.3, where $2a$ is the dimension of the panel. This corresponds to orientation angles ranging from $\alpha = 90^\circ$, $\beta = 0^\circ$ to $\alpha = 0^\circ$, $\beta = 0^\circ$. α represents the angle between a normal to the test panel plane and the source plane, and β represents the angle between a normal to the test panel plane and the room surface which in later studies will contain the reflecting surface. The equal pressure contours are relative to the sound pressure level at the center of the panel, and similarly, the phase contours are also relative to the center of the panel. In addition, the sound pressure level at the position of the panel center was determined both with the panel in position and with the panel removed from

this location. The difference between these levels gave a measure of the reflecting, or more strictly the diffracting, effect of the panel. It may be seen that significantly large pressure increases of the order 10 db occur in cases of normal and near normal incidence. In the case of grazing incidence the pressure increases were insignificant and the magnitude of the pressure contours suggested that no diffraction effects were occurring. The decreasing magnitudes with distance from the source were due to inverse square law pressure drop. Consequently, less attention has been devoted to grazing incidence in the following studies.

Figures 12 and 13 show the result for a similar study with a 200 c/s frequency source. At this frequency corresponding to a ka value of 1.1, the pressure increases were smaller than in the previous study. In addition, no phase contour determinations relative to the center of the panel were possible, because phase differences would be less than $\pi/2$ over the panel at this longer wavelength.

An attempt was made next to continue the study using a pure tone source at 1800 c/s. However, it was not possible to complete the contours with the sound pressure level determinations obtained at points on the orthogonal grid marked on the panel, because the grid was not sufficiently fine for the detail at this higher frequency. Making the grid finer would have made the determinations very tedious. Consequently, it was decided to replace the pure tone source with a one-third octave band noise source. This method had the following advantages:

1. Experimentally, the test procedure was made easier and less time-consuming, because it enabled an observer to stand fairly close to the test panel and explore the pressure levels with a hand-held microphone without materially affecting the pressure contours on the panel. Experiment showed that it was impossible to use this technique with a pure tone signal, because the observer's presence had a significant disturbing effect on the pressure distribution.
2. Since anticipated service fields can be expected to be of broadband noise nature rather than pure tone, it was more meaningful to continue the study using a noise source.

Consequently, the horndriver sources were replaced by the cone-loudspeaker sources driven by approximately octave band noise at center frequencies 200, 630, and 1600 c/s. The exploring microphone output was filtered using a one-third octave filter at the corresponding center frequencies. Thus pressure distributions were obtained for an equivalent one-third octave band noise source.

A test was performed using a noise source with center frequency 630 c/s (corresponding to $ka = 3.5$) on the panel with orientation $\alpha = 30^\circ$, $\beta = 0^\circ$. The results are shown in Fig. 14. This may be compared to the pure tone source case as shown in Fig. 10. The agreement between the two tests conducted with a one-third octave band of noise and a pure tone signal is remarkably good. Consequently, this technique for determining pressure

distributions on panels exposed to one-third octave bands of noise was judged to produce equally good results as the method used for pure tone sources, and was adopted for all the following studies. It was also decided to change from contouring pressure in 1 db units to 2 db units as it was considered unnecessary to obtain such detail in pressure distributions. In addition, it was decided to further reduce the number of orientations used in the study. The cases of $\alpha = 30^\circ$, $\beta = 0^\circ$ and $\alpha = 60^\circ$, $\beta = 0^\circ$ representing angles of incidence of 60° and 30° , were replaced by a single orientation $\alpha = 45^\circ$, $\beta = 0^\circ$, so that generally three cases with different angles of incidence were studied: normal, 45° , and grazing incidence.

Figure 15 shows the distribution on the 2 x 2 ft panel at $\alpha = 45^\circ$, $\beta = 0^\circ$ at one-third octave band center frequencies of 630 and 200 c/s (corresponding to $ka = 3.5$ and 1.1). The 630 c/s case distribution is quite similar to both 60° and 30° incidence distributions for pure tone as shown in Figs. 10 and 11. Likewise, the 200 c/s distribution is noted to be similar to both 60° and 30° incidence distributions for pure tones as shown in Figs. 12 and 13.

The 2 x 2 ft panel was replaced by the 5 x 4 ft panel and pressure distributions at normal incidence ($\alpha = 90^\circ$, $\beta = 0^\circ$), 45° incidence ($\alpha = 45^\circ$, $\beta = 0^\circ$) and grazing incidence ($\alpha = 0^\circ$, $\beta = 0^\circ$) were obtained at frequencies of 630 c/s and 1600 c/s, using one-third octave bands of noise. For this panel size and these frequencies, the two mean ka values were approximately 8 and 20 (if we denote this rectangular panel dimension by $2a$, $2b$ then $ka = 7.0$, $kb = 8.8$, and $ka = 17.8$, $kb = 22.2$ for these two frequencies). In the two cases of normal incidence, Figs. 16 and 17, it is noted that the pressure distribution is uniform over the panel, or at least the variations are less than 2 db. This implies that at these high ka values, the test panels acted as infinite extent reflectors. Under such conditions pressure doubling occurred, which is equivalent to a 6 db pressure level increase on the surface of the panel. The experimentally measured levels are observed to be of this order. In the cases of grazing incidence, Figs. 20 and 21, the pressure distributions are again attributable to inverse square law rather than to diffraction effects. In cases of 45° incidence, Figs. 18 and 19, the diffraction effects are more noticeable in the lower frequency case ($ka = 7.0$, $kb = 8.8$) while in the higher frequency case ($ka = 17.8$, $kb = 22.2$) the distribution is again attributable to the inverse square law effect.

As a means of relating some of the results of this study, Fig. 22 shows the absolute pressure increase effect, due to the presence of the test panel along the two major axes of the panel in the case of normal incidence ($\alpha = 90^\circ$, $\beta = 0^\circ$). These axes are referred to in Fig. 9 as YY' and ZZ' . The pressure levels are obtained from knowledge of the relative distribution of the pressure contours on the panel's surface and the value of the pressure increase at the panel's center obtained from Figs. 11, 12, 16 and 17. Figure 23 shows the results for 45° incidence ($\alpha = 45^\circ$, $\beta = 0^\circ$). These levels have been obtained from distributions shown in Figs. 15, 18, and 19, but they have been corrected to conform to plane wave incidence. In practice, the panels were placed in a spherically radiating field and consequently pressure levels on various areas of the panels were influenced by the proximity of the area of interest to the source. The correction was simple and utilized the inverse

square law relationship. These corrected distributions were compared to distributions obtained by Wiener (Ref. 18) for square panels in the case of normal incidence, and circular discs in the case of 45° incidence, exposed to pure tone plane wave signals for appropriate values of the parameter ' ka '. The agreement between the experimental results and those of Wiener (Ref. 18) is good, and both indicate how the pressure distribution on panels exposed to a single source sound field is influenced by both the ka parameter and the angle of incidence. In addition, as previously stated equal phase contours existing over the test panel surface are produced in accordance with anticipated distribution, i.e. contours of approximately circular arcs with the source as the center.

DOUBLE COHERENT SOURCES IN ANECHOIC CONDITION

In the experimental system shown in Fig. 9, the individual sources are labelled 1, 2, and 3. To study the effects of exposing test panels to two sources operated coherently, the sources were arranged so that either 1 and 2 or 2 and 3 could be driven in phase from a single one-third octave band noise source.

Firstly, the 5 x 4 ft panel was exposed to the sources 2 and 3 operated at 630 c/s, (corresponding to $ka = 7.0$, $kb = 8.8$) at normal incidence ($\alpha = 90^\circ$, $\beta = 0^\circ$) and 45° incidence ($\alpha = 45^\circ$, $\beta = 0^\circ$). The pressure distributions are shown in Figs. 24 and 25. The contour distributions are not unlike those for a single source (Figs. 16 and 18) except that the absolute pressure increase levels are much greater.

The sources were then replaced by 1 and 2 and the distribution on the panel at 45° incidence ($\alpha = 45^\circ$, $\beta = 0^\circ$) was determined at 200, 630, and 1600 c/s, Figs. 26, 27, and 28. In the first case ($ka = 2.2$, $kb = 2.8$) the distribution appears as being due to an inverse square law decrease. In the two higher frequency cases ($ka = 7.0$, $kb = 8.8$ and $ka = 17.8$, $kb = 22.2$), the distributions become very complex. Rapid variations in pressure level across the ZZ' axis of the panel occur, resulting in both maximum and minimum values, while the pressure remains relatively constant across the opposite axis, YY'. These distributions may be attributed to interference effects between the two sources 1 and 2 predominating over diffraction effects. The source combination 1, 2 could be expected to produce interference effects more readily than the combination 2, 3, because the orientation of the sources 1, 2 with respect to the panel surface allows greater variations between the path lengths of each source to any point on the panel than does the combination 2, 3.

The result of this double coherent source study indicates that the pressure distributions can be expected to be more complex than those for single sources. Interference effects between sources rather than diffraction is responsible for this and, in contrast to diffraction, the distributions over a panel become more complex with increasing ka value.

TRIPLE COHERENT SOURCES IN ANECHOIC CONDITION

The three sources 1, 2, and 3, where operated together coherently, and the pressure distributions on the 5 x 4 ft panel were obtained at 630 c/s for cases of normal incidence ($\alpha = 90^\circ$, $\beta = 0^\circ$) and 45° incidence ($\alpha = 45^\circ$, $\beta = 0^\circ$), and are presented in Figs. 29 and 30. Figure 30 may be compared to Fig. 27, where the distribution for sources 1, 2 is shown. Although both source systems contain the complex producing combination of sources 1, 2 for this particular panel orientation, the addition of the third source, 3 (Fig. 30) reduces the complexity. This suggests that large numbers of sources may produce more simple distributions on panels such as those produced by a single source, if the sources are arranged randomly in the source plane so as to reduce the extent of interference effects. If, however, they were arranged in a linear array, interference effects would still occur.

DOUBLE INCOHERENT SOURCES IN ANECHOIC CONDITION

The result of tests using small numbers of coherent sources show that the pressure distributions on panels may be complex in certain cases, due to interference effects between sources. There appears to be no simple means by which the diffraction-governed pressure distributions on panels produced by numbers of coherently operated sources can be predicted from knowledge of the distribution produced by a single source. The approximate calculation method of Wiener (Ref. 18) might be extended to cover multiple sources, but evaluation for all possible numbers and configurations of sources would be a formidable task. However, it may be necessary in the RTD facility to operate several sirens simultaneously in the same frequency range to obtain sufficiently intense sound pressure levels. It is then of considerable importance to be able to predict the fields existing on panels exposed to numbers of sirens operating at the same frequency. To this end, some selected experiments with two sources were repeated. The case of the 5 x 4 ft panel at 45° incidence ($\alpha = 45^\circ$, $\beta = 0^\circ$) exposed to sources 1, 2 at 630 c/s was chosen to be repeated because of the complex interference-type pressure distribution. However, in this case, the two sources were operated from two independent noise generating systems at the same one-third octave band center frequency 630 c/s, and the electrical inputs to the speakers were arranged so that each source produced equal acoustic power. In this case, we have a panel exposed to a sound field produced from two incoherently operated sources. Figure 31 shows the pressure distribution on the panel. This is noted to be remarkably similar to that obtained using a single source (Fig. 18) and shows no resemblance to that obtained in the case of sources 1, 2 operated coherently (Fig. 27). However, one difference existed between the single-source case and the incoherently operated two-source case. In the latter case no continuous phase contours could be determined.

The interpretation of these results is that when two noise sources are incoherently operated, the RMS sound pressure level at any point in the field produced by the two sources is not affected by the randomly varying phase relationship between the two sources (See Appendix A). Consequently, the RMS pressure distribution on a panel is equal to the result of superimposing the

pressure distribution that would be produced from a single source onto that from the other source. In this case, where the two sources assume approximately equal angles of incidence to the panel, the two distributions are essentially identical and consequently their superimposition is also nearly identical to either of the single-source distributions.

The correctness of this hypothesis relating the pressure distribution on a panel exposed to two incoherent sources to the distribution produced by each source individually operated was demonstrated in the following experiment.

The 2 x 2 ft panel was exposed to two incoherently operated sources at 630 c/s. However, the sources were widely separated so that the respective angles of incidence were $+45^\circ$ and -45° , i.e. the angle between the incident beams was 90° . The distribution on the panel was determined as shown in Fig. 32. Figure 32 also shows the distribution for a single source at 45° incidence and the calculated distribution for two incoherent sources at $+45^\circ$ and -45° incidence. This is obtained by rotating the distribution pattern from the 45° incidence through 180° , which would then represent the distribution for -45° incidence, and superimposing both distributions by the method of Appendix A. The result of this superimposed distribution is then the predicted distribution for two sources operated incoherently and beamed at angles of 45° and -45° incidence. Comparison to the experimentally determined curve shows remarkably good agreement and demonstrates the correctness of the hypothesis for obtaining the distribution on panels exposed to a number of incoherently operated sources. It must be noted that operating sources incoherently precludes the use of single frequency sources. Sources could only be operated incoherently in the RTD facility if (a) the individual sources in a group had slightly different frequencies, or (b) the sources were amplitude or frequency modulated sources with separate modulating controls.

SINGLE SOURCE IN SEMI-ANECHOIC CONDITION

The RTD Sonic Fatigue Facility will most certainly include a semi-anechoic operation. Because of the difficulties in covering the floor of the facility with an acoustic treatment, which must be removable in order that large structures can be placed in position or that the facility can be operated in a reverberant condition, the floor may remain acoustically untreated. Consequently, the behavior of the facility operating in such a semi-anechoic condition must be examined.

The presence of this untreated floor will produce an acoustic image source in the same manner as an optical mirror produces an image of an object. This acoustic image source will cause interference effects to occur in the field in the facility. To perform an experimental study in the IITRI anechoic chamber simulating these conditions, one wall of the room was lined with a 24 x 6 ft section of 1/2 inch plywood. The distance between the source and the reflecting surface can certainly be expected to influence the sound field produced by the source and its image. For this study, two values for this distance separating the source and the simulated reflecting floor were used.

These values were 9 inches and 3 feet, representing scaled distances of 3 and 12 ft, approximately the minimum and maximum separation of the sirens from the floor, in the RTD facility.

No studies were carried out at 200 c/s because it was considered that the wavelength at this frequency was too long for the reflecting surface, of width 6 ft, to act as a simulation of the RTD floor. Ideally the 70 x 40 ft floor should have been scaled down to approximately 17 1/2 x 10 ft. However, it was not possible to exceed a width of 6 ft for the particular arrangement of floor simulation that was used in this model study. At the frequencies of 630 and 1600 c/s, where wavelengths are considerably shorter, the width of the undersized simulated floor will not be expected to effect its reflecting properties significantly. Consequently, the majority of the studies were performed at the middle frequency, 630 c/s, and a few at 1600 c/s.

Figure 33 shows the distribution on the 2 x 2 ft panel at normal incidence ($\alpha = 90^\circ$, $\beta = 0^\circ$) and grazing incidence ($\alpha = 0^\circ$, $\beta = 0^\circ$) with a source-reflecting surface separation of 3 ft. The normal distribution is very similar to that obtained under fully anechoic conditions (Fig. 11), but the grazing incidence case for fully anechoic conditions (Fig. 10) does not exhibit the interference effects shown in Fig. 33 for the semi-anechoic condition. It is noted that in the latter case no continuous equal phase contours were obtained. This is noted in all the following experiments when the source to reflecting surface distance was 3 ft. Figure 34 shows the distribution in two cases of 45° incidence, the first $\alpha = 45^\circ$, $\beta = 0^\circ$ and the second $\alpha = 45^\circ$, $\beta = 45^\circ$. The latter case ($\beta = 45^\circ$) represents a case of the plane being inclined to the reflecting surfaces as opposed to being perpendicular to the surface ($\beta = 0^\circ$) which is representative of the majority of the cases in this study. Phase information, in the form of continuous equal phase contours, was difficult to obtain, and contours shown in the case of $\alpha = 45^\circ$, $\beta = 0^\circ$ indicate only the possibility of the existence of continuous phase contours in this particular case.

Figures 35, 36, and 37 show the distribution on the 5 x 4 ft panel with the 630 c/s source maintained 3 ft from the reflecting surface for cases of normal ($\alpha = 90^\circ$, $\beta = 0^\circ$), 45° ($\alpha = 45^\circ$, $\beta = 0^\circ$), and grazing ($\alpha = 0^\circ$, $\beta = 0^\circ$) incidence. Figure 37 again shows the interference effect resulting from the source and its image. The normal and 45° incidence cases also show an interference type of distribution over their surface which appears to be superimposed upon the pressure-doubling effect resulting from reflection. This is demonstrated by the approximate 6 db level in the region over the center of the panels.

Figure 38 shows the distribution at 45° incidence at a frequency of 1600 c/s. Again the 6 db pressure level exists in the central region of the panel and on the side of the panel most distant from the reflecting surface. Interference effects predominate in the region nearest the wall. From the geometry of the situation (see Fig. 9) it is seen that the path difference between the sound reaching the panel directly from the source and that reaching it upon reflection from the reflecting surface is a function of the position on the panel. Portions of the panel close to the reflecting surface produce path differences from almost zero to a few wavelengths, and in these areas interference effects occur. Portions of the panel far from the reflecting surface

produce path differences much greater than a few wavelengths. Consequently, when the two wave trains recombine in these regions, they do so as if they originated from two incoherent sources due to the loss of correlation between them.

Experiments were then conducted with a source-reflecting surface spacing of 9 ins. Figure 39 shows the distribution on the 2 x 2 ft panel at 630 c/s at normal incidence ($\alpha = 90^\circ$, $\beta = 0^\circ$). Comparison with Fig. 33, in which the separation is 3 ft, shows that in the case of the smaller separation interference effects occur apparently superimposed upon the pressure reflection (or diffraction) effect.

Figures 40 and 41 show the distribution on the 5 x 4 ft panel at normal ($\alpha = 90^\circ$, $\beta = 0^\circ$) and 45° ($\alpha = 45^\circ$, $\beta = 0^\circ$) incidence. Both are similar to their corresponding cases for the source-reflecting surface separation of 3 ft (Figs. 35 and 36), but in addition, phase contour determination was possible in the case of the 45° incidence. While phase contours did not extend over the complete panel surface, several contours were determined forming a narrow elongated correlation area. Only one such area is shown in Fig. 41 for the fixed position of the reference microphone. However, similar areas exist over the whole area of the panel and were determined by relocating the reference microphone in other positions.

The 45° incidence test with a source-reflecting surface separation of 9 inches was repeated at 1600 c/s, Fig. 42. The interference effect now extended over the whole of the panel because with this smaller separation between the source and its image, the path difference to any area of the panel was less than a few wavelengths. Again the narrow elongated correlation area was observed on the panel. It should be noted that the major axis of this area passes through the mid-point of a line joining the source to its image.

The results of this single-source, semi-anechoic study are that the presence of the reflecting floor leads to complex interference effects between the real and the image source. If the source-reflecting floor separation is large, then the complex distribution will occur only in areas of the panel in which the difference in path length between the direct and the reflected sound incident on the panel is small. When this path difference exceeds the order of several wavelengths, the lack of coherence between signals prohibits interference effects and more simplified distributions result. These conclusions do not apply to a pure tone signal for which this incoherent condition cannot arise. In addition, continuous contour phase determinations can only be made in the case of small source-reflecting floor separations. The extent of each of these phase contours is short and gives rise to narrow elongated correlation areas.

TRIPLE COHERENT SOURCE IN SEMI-ANECCHOIC CONDITION

Figure 43 illustrates the distribution on a panel exposed to three coherent sources at 630 c/s with a mean separation from the reflecting surface of 3 ft. Comparison with a single source under identical conditions (Fig. 36)

shows a reasonable degree of similarity. Figures 44 and 45 show the distribution at normal ($\alpha = 90^\circ$, $\beta = 0^\circ$) and 45° ($\alpha = 45^\circ$, $\beta = 0^\circ$) incidence with a mean source separation from the reflecting surface of 9 inches. In these two cases there is no similarity to the equivalent single-source cases, Figs. 40 and 41. However, interference effects are apparent though more complex than in the single-source case.

The conclusion that may be drawn from these experiments is that a group of sources operated coherently in a semi-anechoic condition may be represented as a single source if the mean separation of the group from the reflecting surface is much greater than the inter-source separations. Interference effects are then more easily predicted. However, when the group-reflecting surface separation is of the order the inter-source separation, the interference effects become most complex because of effective doubling of the total number of individual sources. However, in the latter case, the phase contour determinations are again possible leading to elongated correlation areas.

SEMI-ANEOCHOIC STUDY WITH DEGREE OF ACOUSTIC TREATMENT

A short study was made to determine the degree of acoustic treatment which needed to be applied to the reflecting surface before pressure distributions on panels exposed to a sound field appeared to have reverted to their distribution under anechoic conditions.

The 2 x 2 ft panel at 45° incidence ($\alpha = 45^\circ$, $\beta = 0^\circ$) was exposed to a 630 c/s noise source with a source-reflecting surface separation of 3 ft. The distribution under these conditions is shown in Fig. 34. Then the distribution was redetermined when a single layer of absorbing material and then a double layer was applied to the reflecting surface. These distributions are shown in Fig. 46 and may be compared to the fully anechoic distribution shown in Fig. 15. Because of the relative similarity between distribution in the anechoic and the semi-anechoic conditions, no absolute conclusions are drawn. However, it was observed that as the absorption was increased so the degree of similarity increased. A more appropriate test was applied. The 5 x 6 ft panel at 45° incidence ($\alpha = 45^\circ$, $\beta = 0^\circ$) exposed to 630 c/s noise with a source-reflecting floor separation of 3 ft was chosen, since the distributions in the anechoic condition (Fig. 18) and the semi-anechoic conditions (Fig. 36) were vastly different. The distributions were obtained for cases of a single, double, and treble layer of absorption. It is noted that phase determinations are only restored in the cases of two and three layers of treatment and only in the latter case is the pressure distribution very similar to that for the anechoic case. The absorbing material used to cover the reflecting floor was: (1) one inch thick Johns-Manville Ductliner for tests shown in Figs. 46A and 47, (2) a single layer of ductliner covered by one layer of 1 1/2 inch Fiberglass for the tests of Figs. 46B and 48, 2 lb density, and (3) a single layer of ductliner covered by two layers of Fiberglass for the tests of Fig. 49. The normal incidence absorption coefficients measured in an impedance tube at 500 and 1000 cps were

	<u>500 cps</u>	<u>1000 cps</u>
Ductliner	.21	.42
Ductliner plus 1 layer Fiberglas	.61	.97
Ductliner plus 2 layers Fiberglas	.95	.96

On the basis of these limited tests, a material to nearly eliminate the reflection effects of the floor on the sound field should have a normal incidence absorption coefficient greater than 0.80 to 0.90. To obtain absorption coefficients in this range at low frequencies without using very thick panels, it will be necessary to use a layer or layers of material with air space backing.

SECTION V

TYPES OF ATTAINABLE SOUND FIELDS

In order to apply the results of this study to the problem of service or non-service field simulation in the RTD facility, it is necessary to generalize the results of the findings. No attempt has been made, however, to lay down a procedure for the operation of the facility that will enable specific service fields to be simulated. The study has shown that many fields with widely differing characteristics, and which can be expected to be of significant value in field simulation, can be attained by quite elementary operation of the facility. It is the aim of this section of the report to illustrate how various classes of fields may be produced by appropriate operation of the facility. It is necessary to classify fields in terms of the ranges of variations in the significant parameters. The parameters to which attention has been paid in this study are the spatial pressure and phase distribution. Some possible variations of interest of spatial pressure distribution include one or possible combinations of the following: a uniform sound pressure level; gradual or rapid sound pressure level changes in a specific direction; and alternate sound pressure level maxima and minima in a specific direction. Variations in phase would include well-defined progressive type phase-coherent areas extending over a wide area in a direction normal to propagation, progressive-type phase-coherent areas extending over a narrow area in a direction normal to propagation, and minimal or zero extent of phase-coherent areas.

It is necessary to consider these generalizations as they apply in the following three areas of interest:

1. Diffuse field operation of the facility,
2. Progressive wave operation of the facility, and
3. Modifying effects of structures on progressive wave fields.

DIFFUSE FIELD OPERATION OF THE FACILITY

In the diffuse field environment, test structures located at a distance from the sound sources and from room boundaries will be exposed to relatively predictable sound fields with sound levels closely related to the diffuse field sound level which is constant throughout most of the room volume. Test structures with dimensions small compared to a wavelength will be exposed to surface sound pressures equal to the diffuse field pressure. Test structures with dimensions much larger than a wavelength will be exposed to sound pressure levels about 3 db higher than the diffuse field level except near their edges. For test structures with dimensions comparable with a wavelength, there will be variations in surface sound pressures but these variations will not be as great as those caused by interference effects in progressive fields.

Although the principal use of the diffuse field environment will probably be to expose structures to high intensity sound with known spatial correlation properties and little variation in pressure level with location, advantage can be taken for special purposes by using locations where sizable spatial variations in sound pressure will occur. These are locations in the direct sound field (near the sources) and locations near a room boundary.

PROGRESSIVE WAVE OPERATION OF THE FACILITY

Our approach to the progressive wave operation of the facility, that of grouping a small number of sirens together to provide acoustic energy at a discrete frequency or in a narrow frequency band, enables expedient evaluation of attainable fields in the facility. Single-source operation under discrete frequency conditions yields a simple inverse square law field which will mean that the pressure distribution will remain approximately uniform and independent of frequency, over regions in the facility in which structures might be placed. Two- and three-source configurations, which enable interference effects to occur, produce fewer smaller regions of uniform pressure in the facility, the extent of any one of those regions decreasing with increasing frequency. In addition, regions exist in which very rapid pressure level changes occur. These regions and the rate of pressure level change can be determined only when the operating conditions, such as operating frequency and siren source configurations, are specified. Coherent frequency modulation of the sources will not significantly alter the pressure distribution if measured with a narrow band filter, but a general "smoothing-out" will occur if analyzed with a one-third octave band filter. Further simplification of the pressure distribution will occur if the frequency-modulated sources are not operated coherently and the field will reduce to that resulting from the superimposition of the fields produced from a number of incoherent sources.

MODIFYING EFFECTS OF STRUCTURES ON PROGRESSIVE WAVE FIELDS

Of major importance are the modifying effects of structures upon fields in which they are placed, since in the majority of anticipated operations, one will attempt to simulate a field on a structure rather than simply simulate a field in the facility. To achieve a uniform pressure level over a structure, it was necessary first that the structure be located in a field produced from a single source or in a region of that field produced by several sources in which a uniform pressure level exists. If the structure has dimensions either very much smaller or very much greater than the wavelength of interest, then a uniform pressure level will be experienced over the whole of the structure exposed to the sound field. In the latter condition, a higher pressure level will occur than that existing in the absence of the structure, due to the reflection phenomenon. For intermediate sizes of structure, depending on the sound incidence angle, more complex pressure level distributions will occur. These complexities could be reduced by either arranging the structure at grazing incidence so that diffracting or reflecting effects do not occur, or by surrounding the structure with a baffle which would be flush with the surface

of the structure, but mechanically and physically isolated from the structure. The composite structure, having larger dimensions than the original structure, will enable a more uniform pressure to occur over the region of the structure of interest. Alternative solutions would include the use of either reflecting structures located so as to increase the low pressure level areas, or acoustic shielding baffles to reduce the high pressure level areas.

Phase requirements will also govern the orientation of the structure. If a uniform coherent phase area over the entire surface of a structure is required, then it will be necessary to place the surface normal to the direction of propagation. If regularly progressive phase coherent areas over the surface are required, then it will be necessary to correctly incline the structure to obtain these phase conditions.

Uniform pressure over the surface of a structure may also be obtained when several sources, which would otherwise produce a complex distribution, are operated incoherently, assuming that the condition is met that the structure dimensions are either very much smaller or very much larger than the wavelength of interest. In these cases, phase coherent areas have a minimal extent. A single or a closely situated group of sources, when operated in a semi-anechoic condition, may also produce uniform pressure distributions, if the differences in direct and reflected sound paths incident on the structure differ considerably, so that effective incoherence exists between the sound source and its image. Narrow elongated progressive phase coherent areas may exist on the structure if the source-image separation is small.

Pressure distributions which vary either slowly or rapidly with distance over a structure may be obtained in cases in which structure dimensions are of the order the wavelength of interest.

Variation up to 10 db over the extent of a structure can be obtained by exposure to a single sound source by suitable adjustment of the incidence angle and the combined size of the test structure and any possible surrounding baffle structure. More rapid pressure level variations with distance across the structure are possible when numbers of sources are operated coherently or when a single source or group of sources are operated in the semi-anechoic condition when the rapid pressure variations occur in the region of the structure in which the direct and reflected sound paths to the structure are almost equal. For example, double sources have produced variations up to 20 db and sources in the semi-anechoic study have produced variations up to 10 db using one-third octave bands of noise. However, it is difficult to be more specific in describing these pressure level variations without citing complete individual operating conditions.

SECTION VI

CONCLUSIONS AND RECOMMENDATIONS

As a result of the research concerning utilization of the RTD Sonic Fatigue Facility for the production of acoustic environments, the following conclusions and recommendations are made.

CONCLUSIONS

1. Calculation of sound fields from a small number of sources in the progressive wave environment has shown that simple and complex field distributions can be determined but the effects of larger number of sources and of diffraction at test structures is very difficult to calculate or estimate.
2. Prediction of sound fields for the reverberant environment is much less difficult than for the progressive wave environment and prediction can be made for many cases of source and test structure parameters.
3. The model studies on a small number of sources in progressive wave fields has shown that simulation of source and acoustic conditions is satisfactory and that varied types of sound fields resembling certain service fields can be obtained by changing source system and test structure location and the size and orientation of test structures.
4. Because of the convenience in varying sound fields on test structures in a small scale model and because of the useful results obtained in the limited model study, it is very desirable to determine in a more potentially realistic model, the effects of source operation and location and of diffraction and reflection from test structures as an aid in simulating service fields. A small scale model can be operated and various parameters can be changed much more rapidly and at much less cost than would be the case for the full scale facility.

RECOMMENDATIONS

1. We recommend a continuation of the investigation along the lines of an acoustical modelling study with emphasis on the realistic operation of the facility which more closely resembles semi-reverberant or semi-anechoic operations than a completely reverberant or anechoic operation.

2. Effort should be devoted towards obtaining more extensive data on various anticipated service fields, enabling expected variations in the significant parameters to be established. This information will provide a target which will be invaluable in deciding which are the most significant modes of operating the facility.
3. In addition, the effects of various field-shaping devices, such as reflectors, etc., upon the field distribution should be investigated since such elements increase the versatility of the facility.

LIST OF REFERENCES

1. Kolb, A.W., Rogers, O.R., "The ASD Sonic Fatigue Facility," 30th Symposium on Shock and Vibration, Detroit, 10-12 October 1961.
2. Tyzzer, F.G., "Development of a Suitable Anechoic Treatment for the ASD Sonic Fatigue Facility," Technical Documentary Report ASD-TDR-62-985, November 1962, Contract No. AF 33(657)-7434.
3. Plumblee, H.E., Bartel, H.W., Ballentine, J.R., Carroll, J.R., Gibson, J.S., Cohen, B., "Development of Expected Noise Spectra, Siren Programming Techniques, and Experimental Plans for the ASD Sonic Fatigue Facility," Technical Documentary Report ASD-TDR-63-674, August 1963, Contract No. AF 33(657)-8327.
4. Morse, P.M., Bolt, R.H., "Sound Waves in Rooms," Rev. Mod. Physics, Vol. 16, April 1944, pp. 69-150.
5. Cook, R.K., Waterhouse, R.D., Berendt, R.D., Edelman, S., and Thompson, M.C. Jr., "Measurement of Correlation Coefficients in Reverberant Sound Fields," J. Acoust. Soc. Am., Vol. 27, November 1955, pp. 1072-1077.
6. Balachandran, C.G., "Random Sound Fields in Reverberation Chambers," J. Acoust. Soc. Am., Vol. 31, October 1959, pp. 1319-1321.
7. Dämmig, P., "Zur Messung der Diffusität von Schallfeldern durch Korrelation," Acustica, Vol. 7, No. 6, 1957, pp. 387-398.
8. Richardson, E.G., and Meyer, E., Technical Aspects of Sound, Vol. III, Chapter 4, Elsevier Publishing Company, New York, 1962.
9. Hopkins, H.F., Stryker, N.R., "A Proposed Loudness-Efficiency Rating for Loudspeakers and the Determination of System Power Requirements for Loudspeakers," Proc. Inst. Radio Engrs., Vol. 36, March 1948, pp. 315-335.
10. Beranek, L.L., Acoustics, McGraw-Hill Book Company, New York, 1954, pp. 313-314.
11. Harris, C.M., "Absorption of Sound in Air in the Audio-Frequency Range," J. Acoust. Soc. Am., Vol. 35, January 1963, pp. 11-17.
12. Waterhouse, R.V., "Output of a Sound Source in a Reverberation Chamber and Other Reflecting Environments," J. Acoust. Soc. Am., Vol. 30, January 1958, pp. 4-13.

LIST OF REFERENCES (Continued)

13. Olson, H.F., Elements of Acoustical Engineering, D. Van Nostrand Company, New York, 2nd Edition, 1947.
14. Jones, R.C., "On the Theory of the Directional Patterns of Continuous Source Distributions on a Plane Surface," J. Acoust. Soc. Am., Vol. 16, January 1945, pp. 147-171.
15. Waterhouse, R.V., "Interference Effects in Reverberant Sound Fields," J. Acoust. Soc. Am., Vol. 27, March 1955, pp. 247-258.
16. Cremer, L., "Theory of Sound-Damping of a Thin Wall at Oblique Incidence," Akust. Zeit., Vol. 7, 1942, pp. 81-104.
17. Watters, B.G., "Transmission Loss of Some Masonry Walls," J. Acoust. Soc. Am., Vol. 31, July 1959, pp. 898-911.
18. Wiener, F.M., "The Diffraction of Sound by Rigid Discs and Rigid Square Plates," J. Acoust. Soc. Am., Vol. 21, No. 4, July 1949, p. 334.
19. Goldman, S., Information Theory, Prentice-Hall, Inc., New York, 1953.

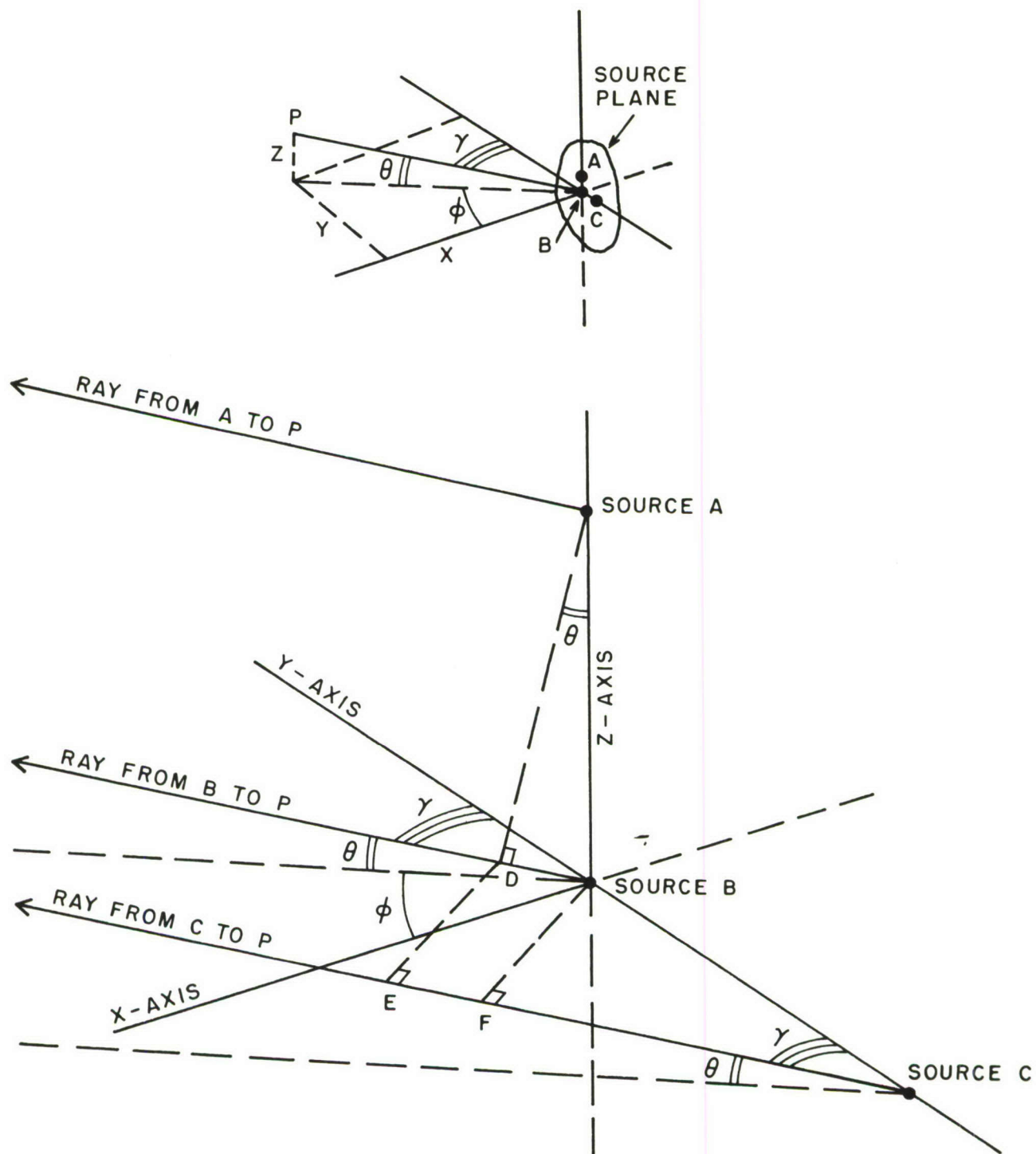


Figure 1. Location of Point P in the Far-Field with Respect to Three Sources A, B, C; Showing Differences in Path-Lengths PA, PB, and PC.

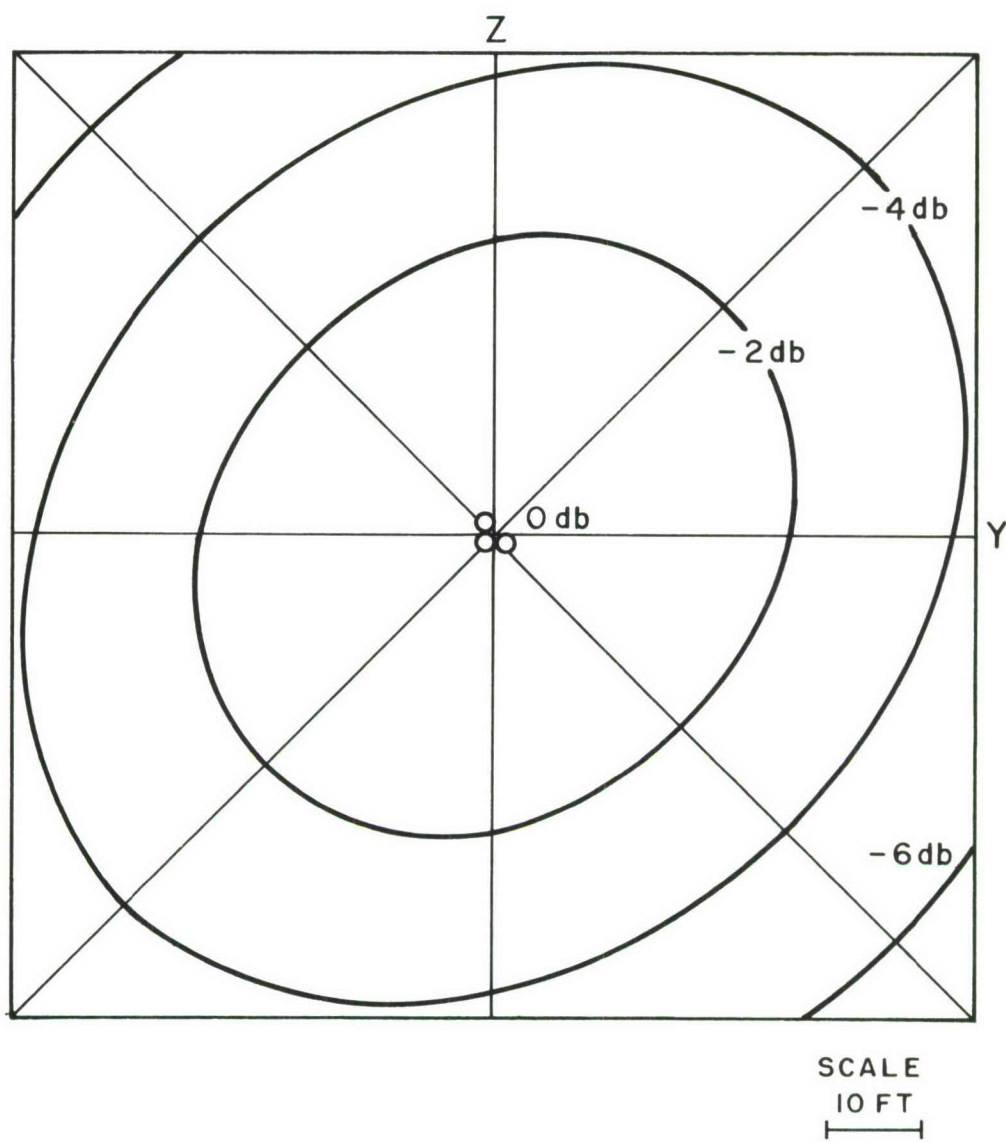


Figure 2. Far-Field Pressure Distribution in Plane 50 ft. from 3-Source System, $f = 110$ cps.

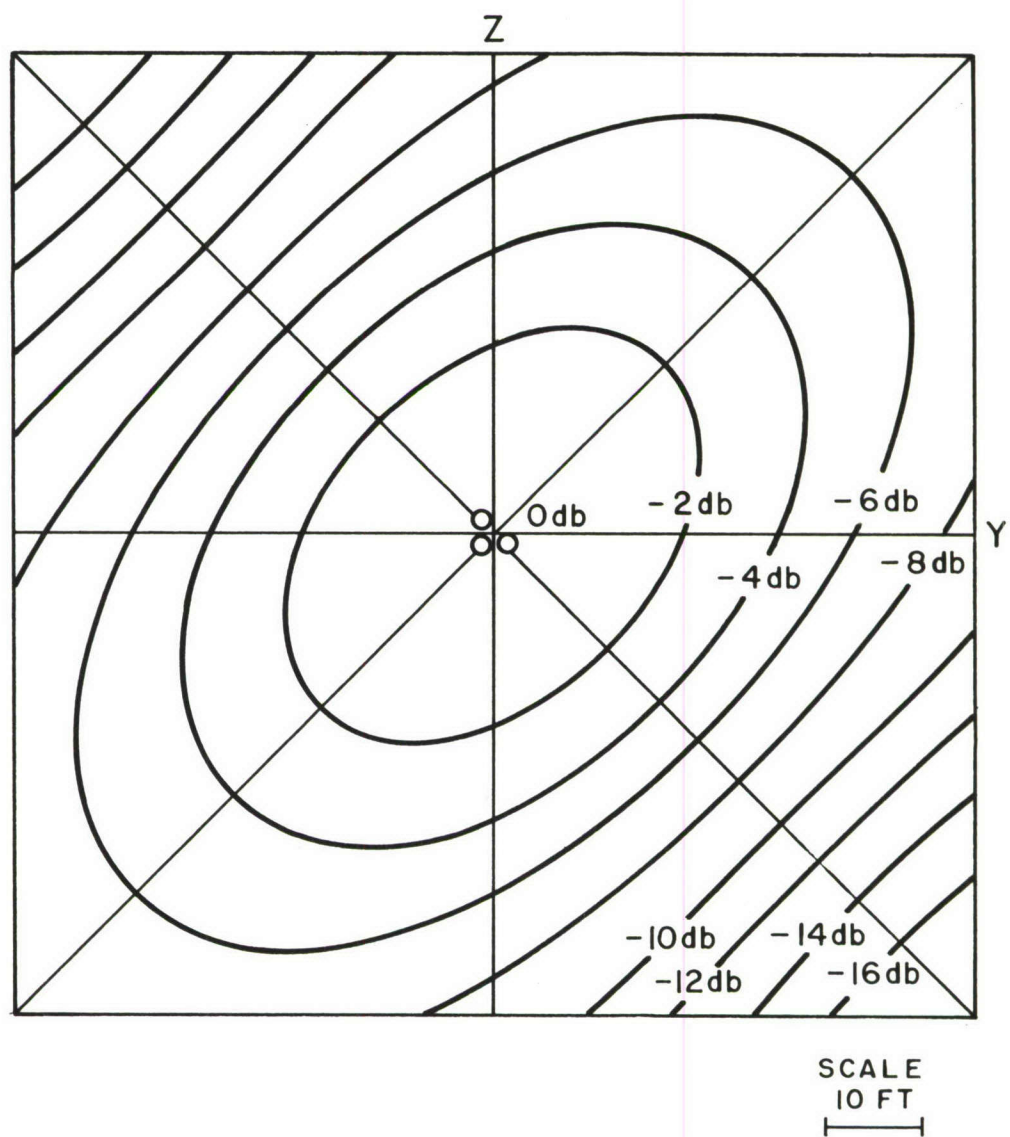


Figure 3. Far-Field Pressure Distribution in Plane 50 ft. from 3-Source System, $f = 220$ cps.

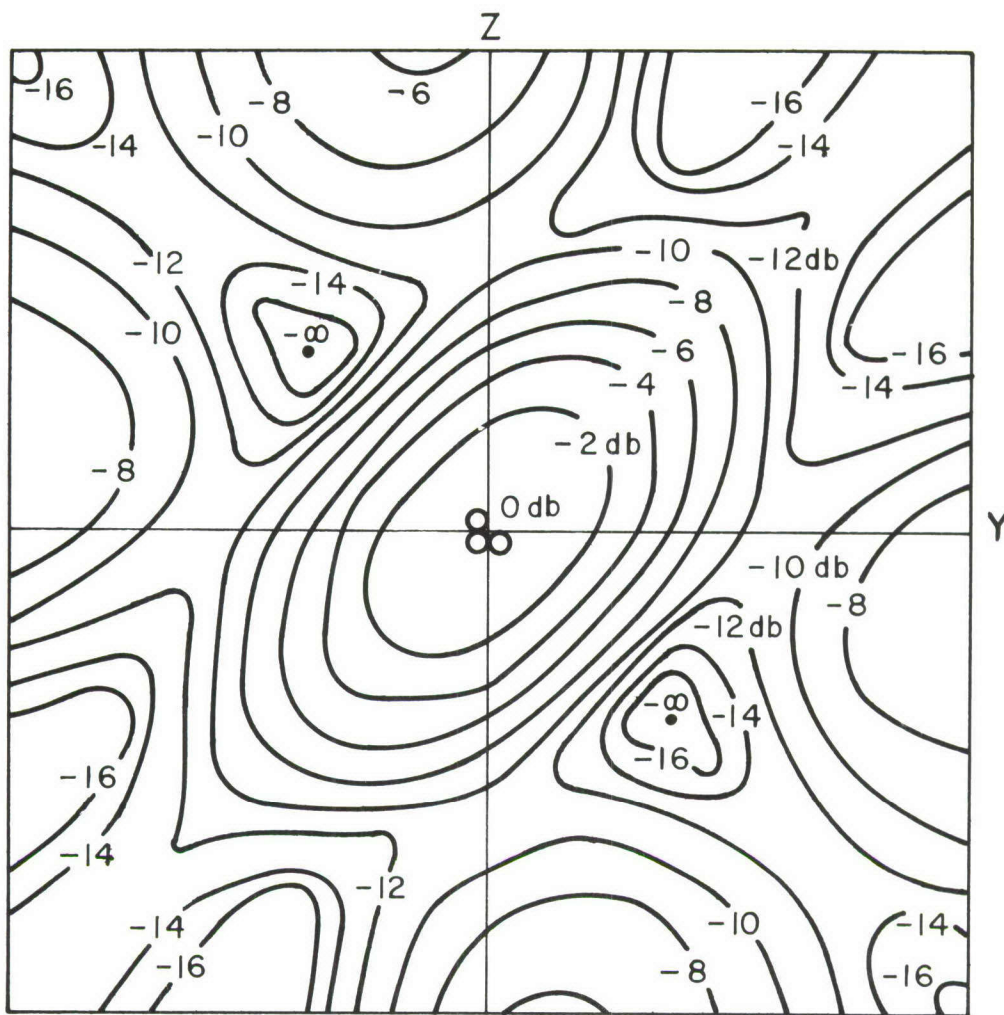
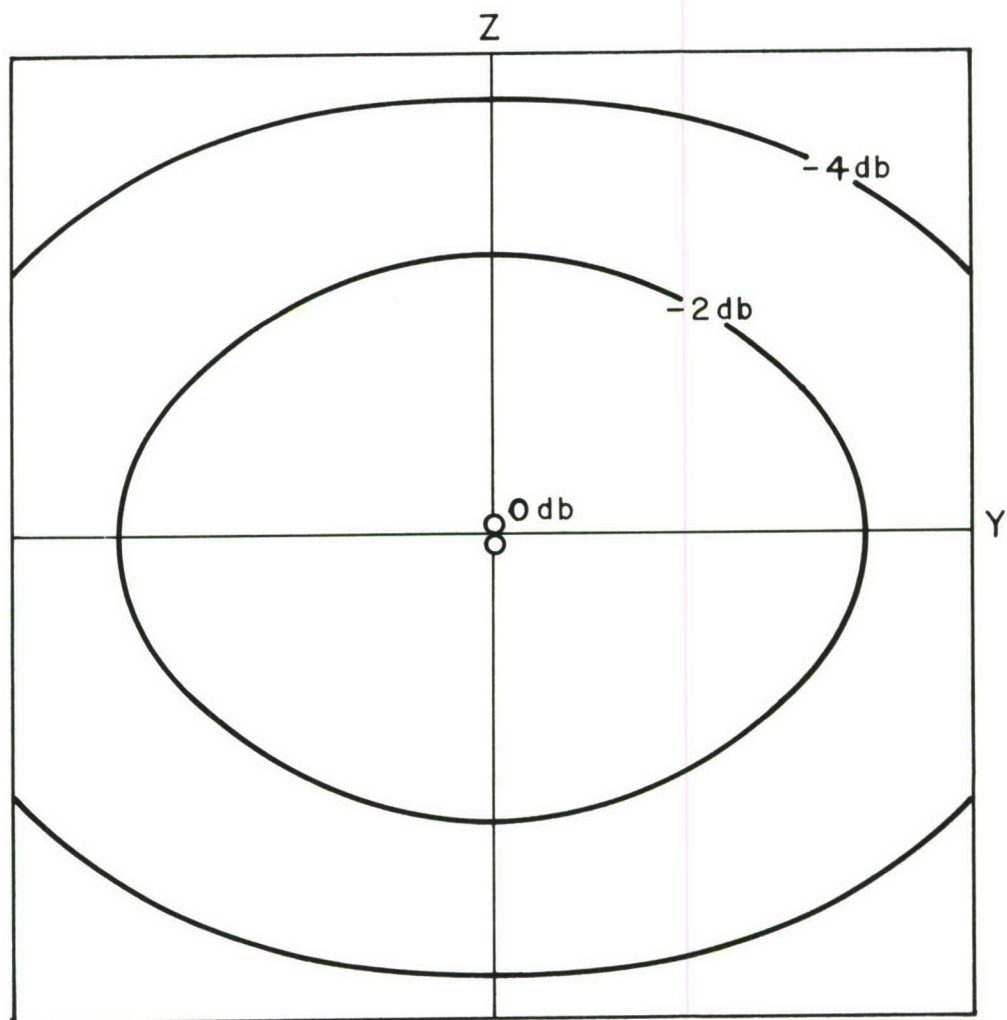


Figure 4. Far-Field Pressure Distribution in Plane 50 ft. from 3-Source System, $f = 440$ cps.



SCALE
10 FT
└───┘

Figure 5. Far-Field Pressure Distribution in Plane 50 ft. from 2-Source System, $f = 110$ cps.

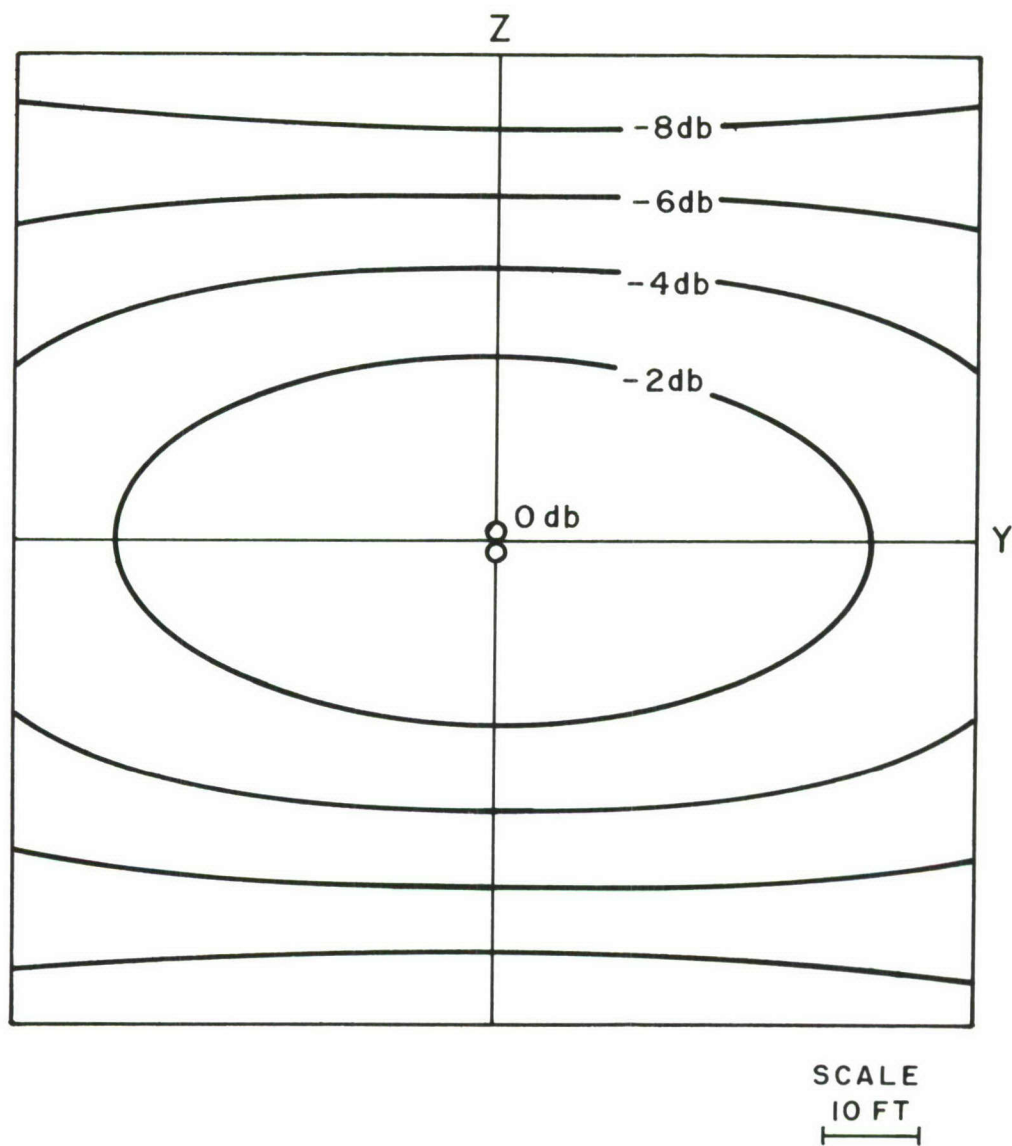


Figure 6. Far-Field Pressure Distribution in Plane 50 ft. from 2-Source System, $f = 220$ cps.

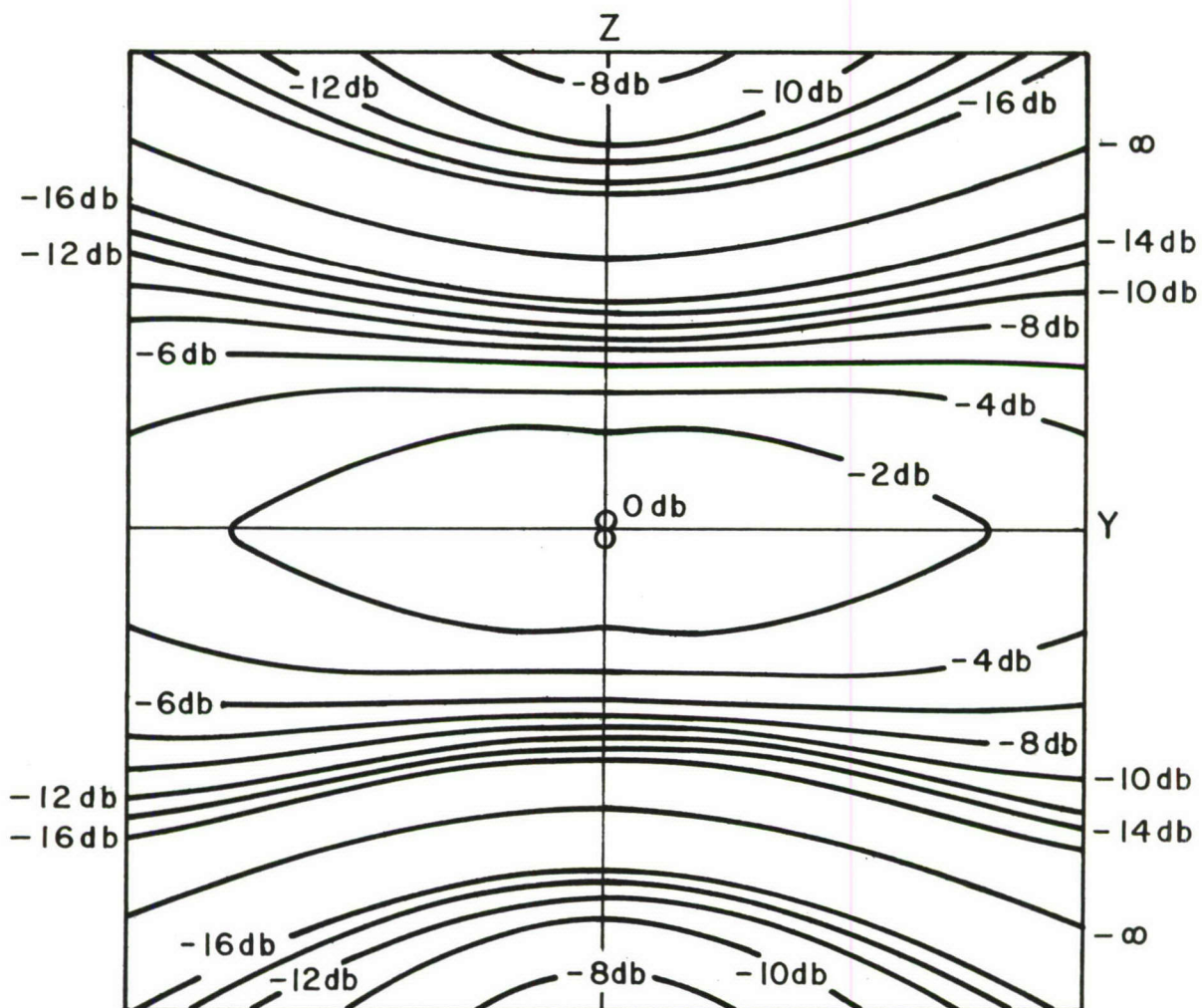


Figure 7. Far-Field Pressure Distribution in Plane 50 ft. from 2-Source System, $f = 440$ cps.

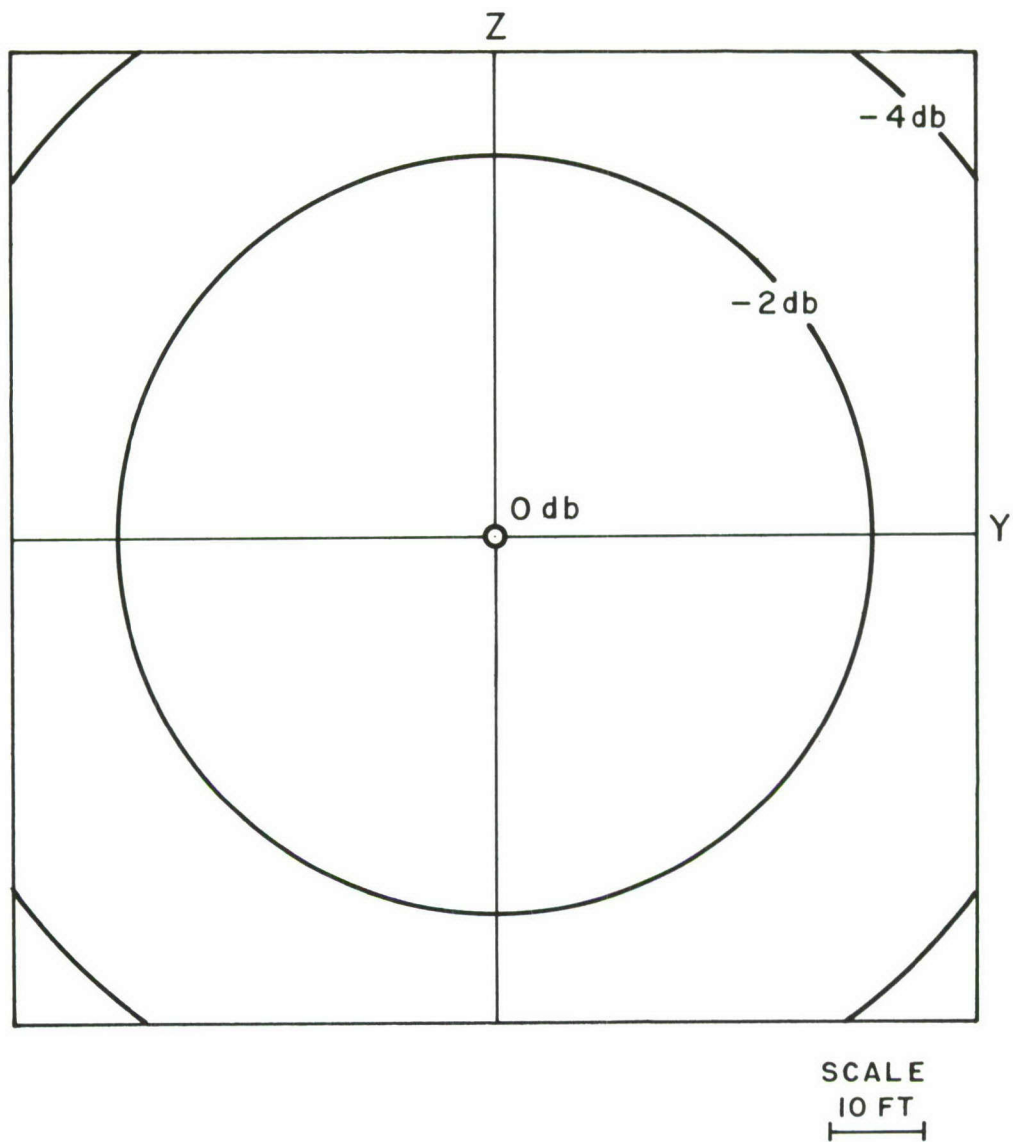


Figure 8. Far-Field Pressure Distribution in Plane 50 ft. from Single Source.

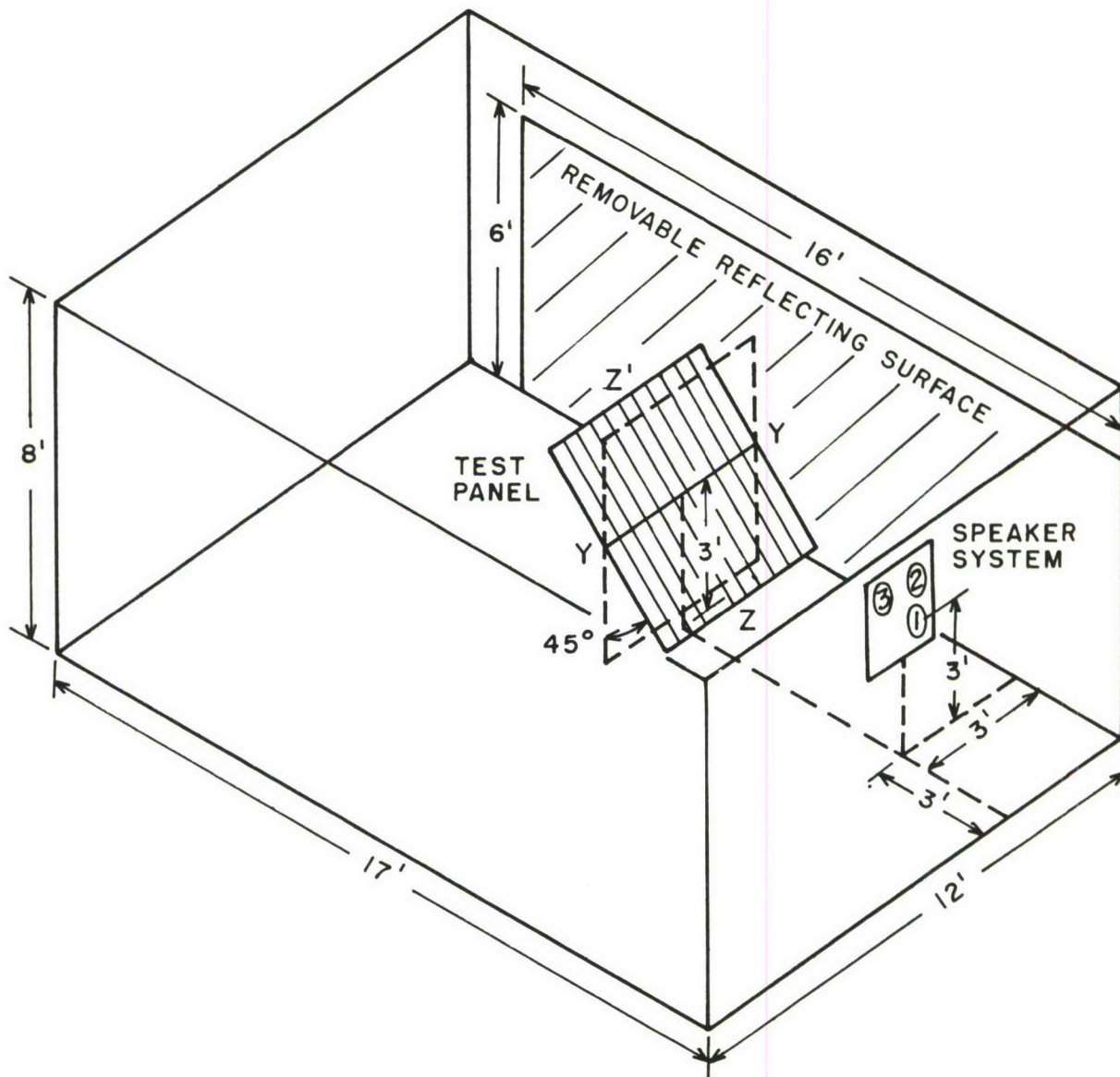
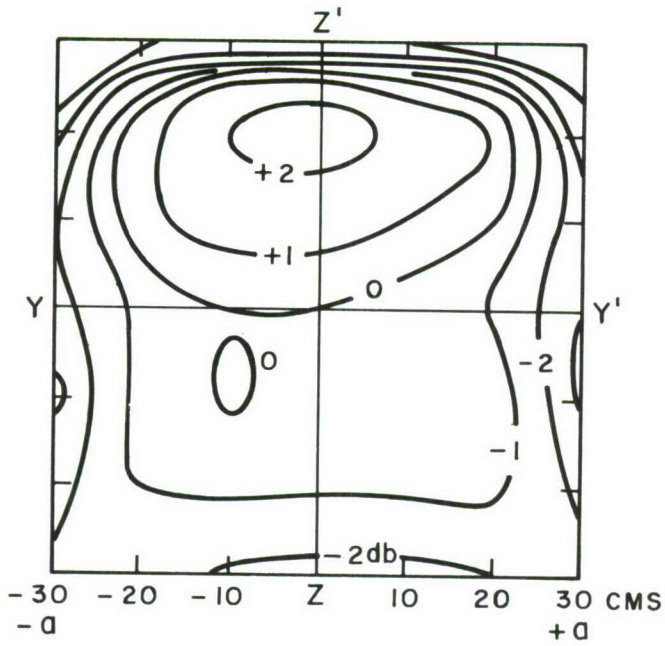
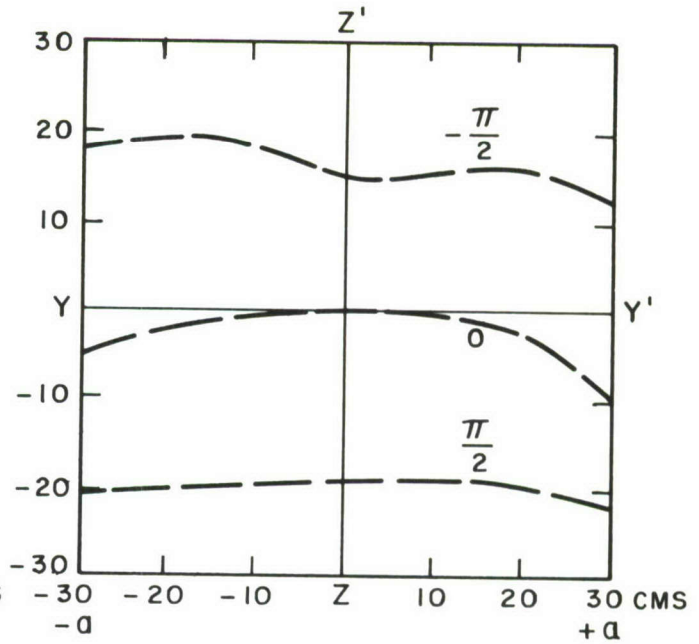


Figure 9. Anechoic Chamber Used in Model Study. Test Panel Arranged at 45° to Speaker System (Dashed Test Panel Outline Corresponds to Normal Incidence Orientation). Speaker System Composed of 8 ins. Speakers with 10 ins. Center Spacing.

$\alpha = 30^\circ$, $\beta = 0^\circ$, $\Delta L = 5.1 \text{ db}$, 600 C/S, $Ka = 3.3$



SOUND PRESSURE LEVEL



RELATIVE PHASE

$\alpha = 0^\circ$, $\beta = 0^\circ$, $\Delta L = 1.2 \text{ db}$, 600 C/S, $Ka = 3.3$

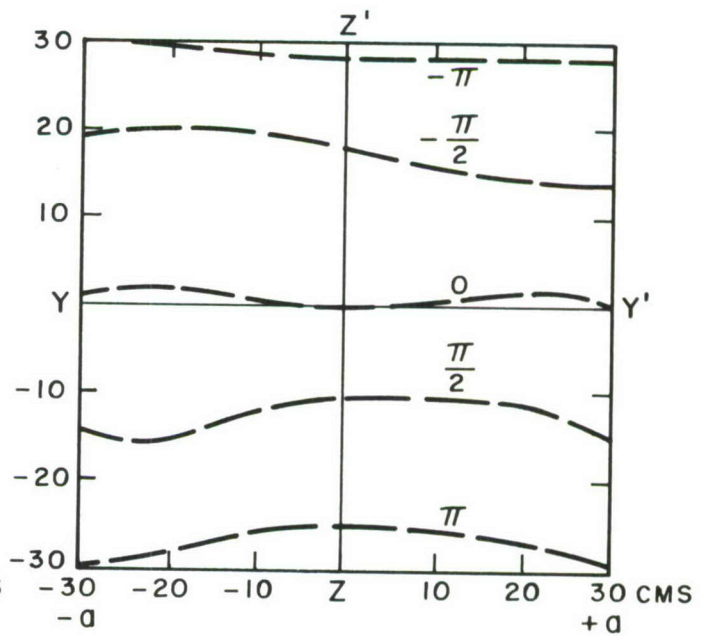
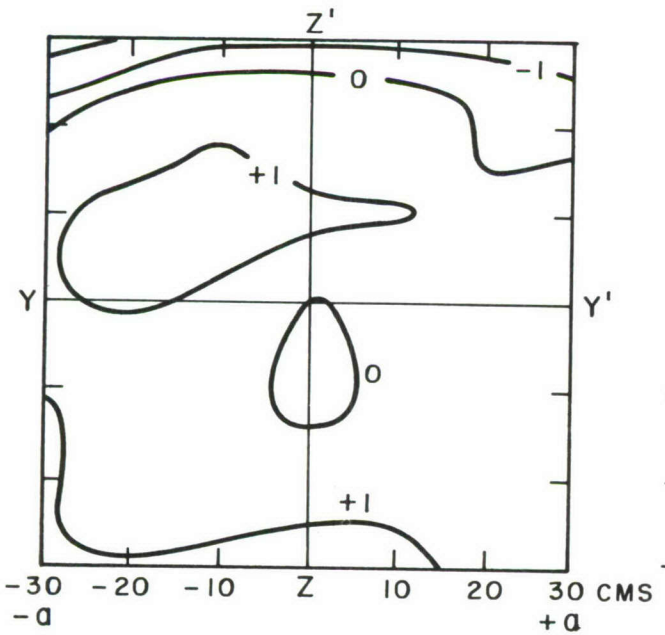
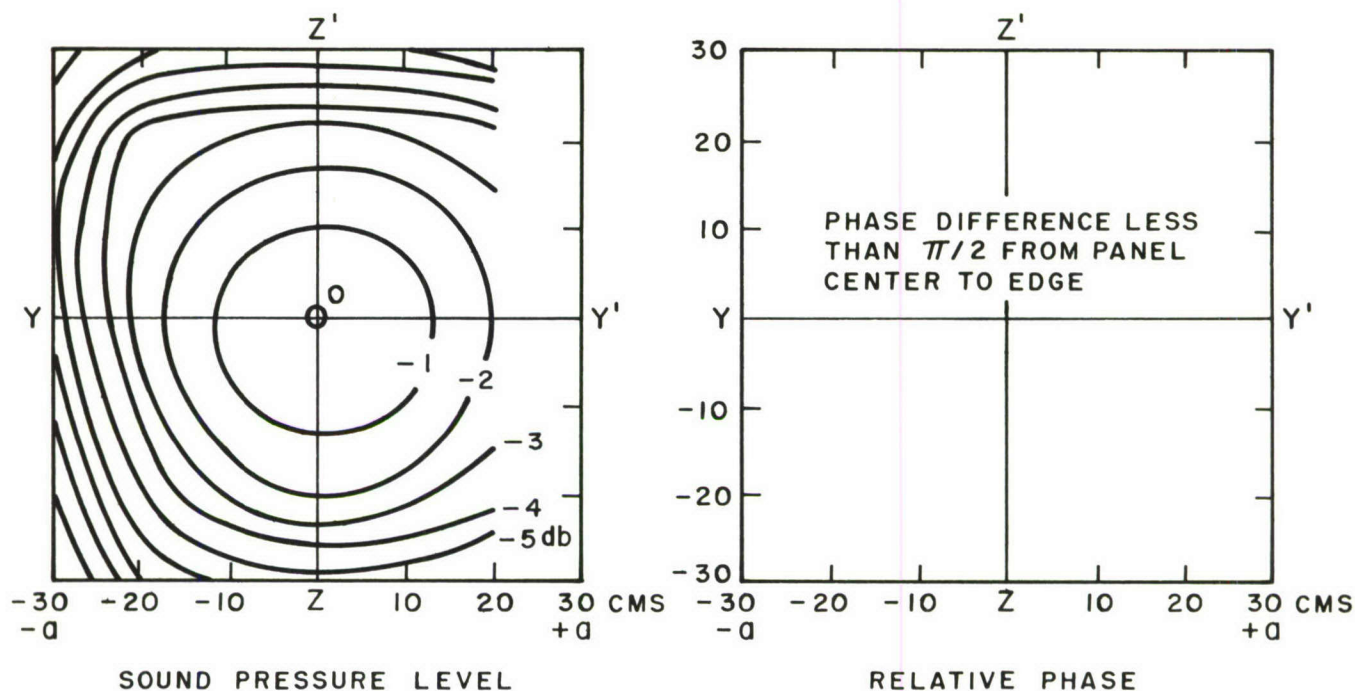


Figure 10. Pressure and Phase Distribution on Test Panel Under Anechoic Conditions, Tone Source 600 c/s, $\alpha = 30^\circ$, $\beta = 0^\circ$ and $\alpha = 0^\circ$, $\beta = 0^\circ$.

$\alpha = 90^\circ$, $\beta = 0^\circ$, $\Delta L = 9.5 \text{ db}$, 600 C/S, $Ka = 3.3$



$\alpha = 60^\circ$, $\beta = 0^\circ$, $\Delta L = 8.6 \text{ db}$, 600 C/S, $Ka = 3.3$

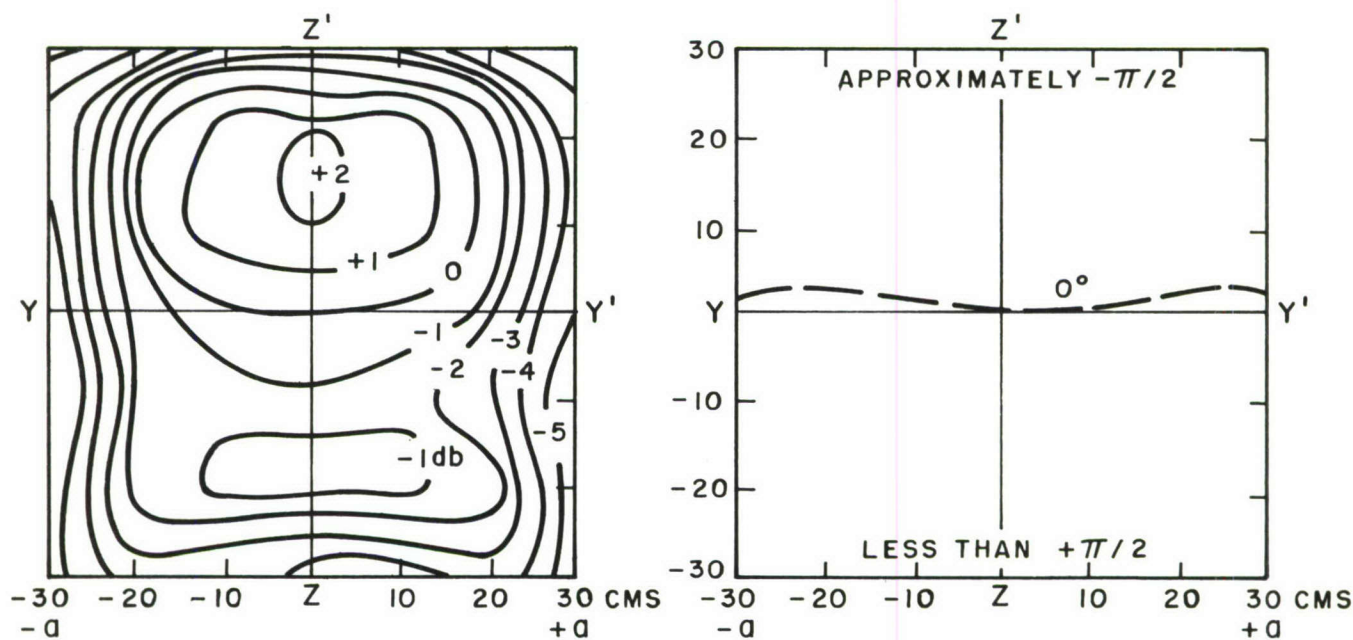
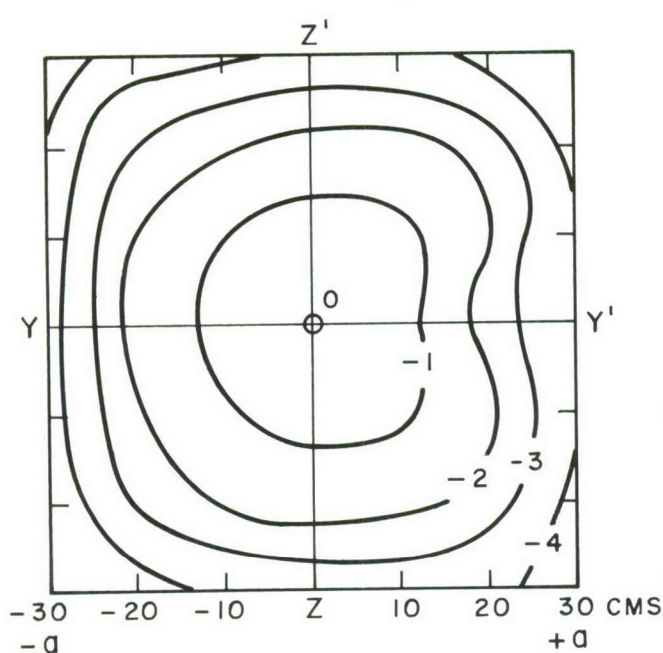
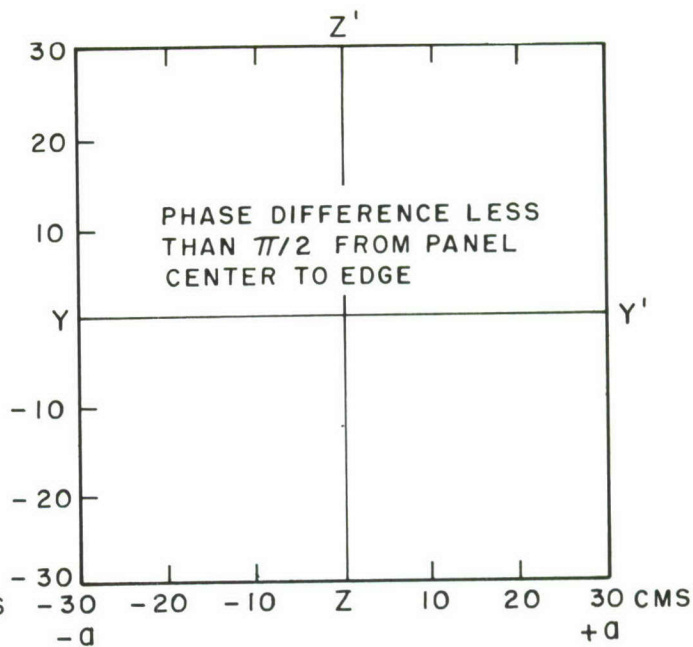


Figure 11. Pressure and Phase Distribution on Test Panel Under Anechoic Conditions, Tone Source 600 c/s, $\alpha = 90^\circ$, $\beta = 0^\circ$ and $\alpha = 60^\circ$, $\beta = 0^\circ$.

$\alpha = 90^\circ$, $\beta = 0^\circ$, $\Delta L = 4.9 \text{ db}$, 200 C/S, $Ka = 1.1$



SOUND PRESSURE LEVEL



RELATIVE PHASE

$\alpha = 60^\circ$, $\beta = 0^\circ$, $\Delta L = 4.1 \text{ db}$, 200 C/S, $Ka = 1.1$

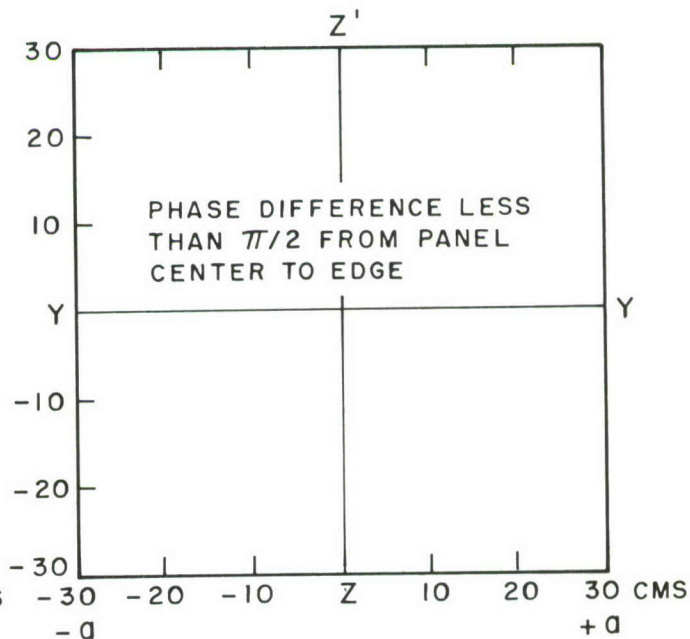
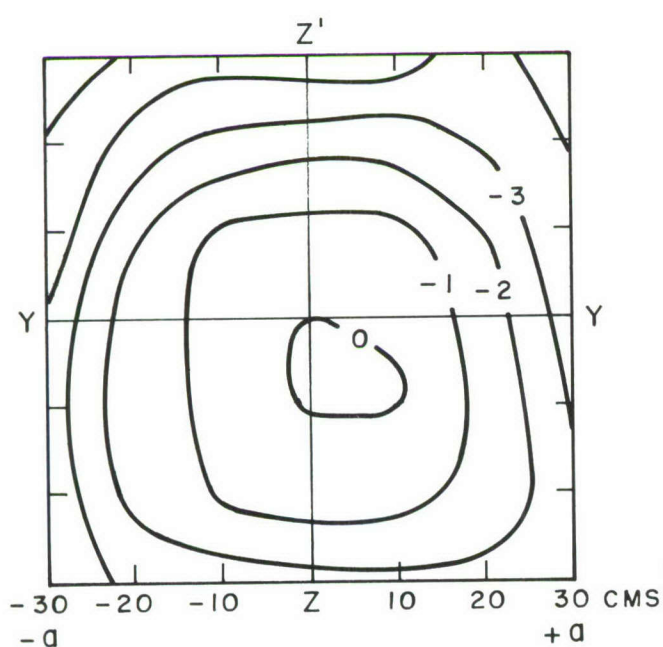


Figure 12. Pressure and Phase Distribution on Test Panel Under Anechoic Conditions, Tone Source 200 c/s, $\alpha = 90^\circ$, $\beta = 0^\circ$ and $\alpha = 60^\circ$, $\beta = 0^\circ$.

$\alpha = 30^\circ$, $\beta = 0^\circ$, $\Delta L = 1.6 \text{ db}$, 200 C/S, $Ka = 1.1$

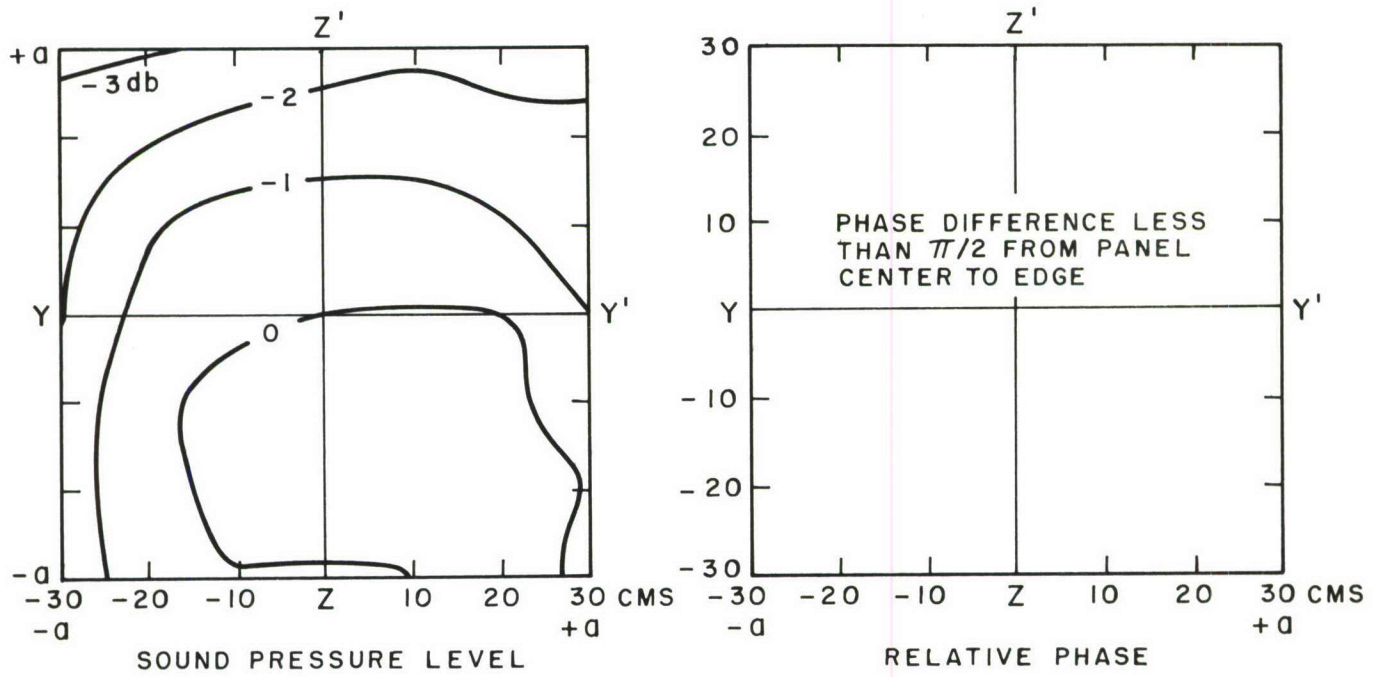


Figure 13. Pressure and Phase Distribution on Test Panel Under Anechoic Conditions, Tone Source 200 c/s, $\alpha = 30^\circ$, $\beta = 0^\circ$.

$\alpha = 30^\circ$, $\beta = 0^\circ$, $\Delta L = 4.3 \text{ db}$, 630 C/S , $K_a = 3.5$

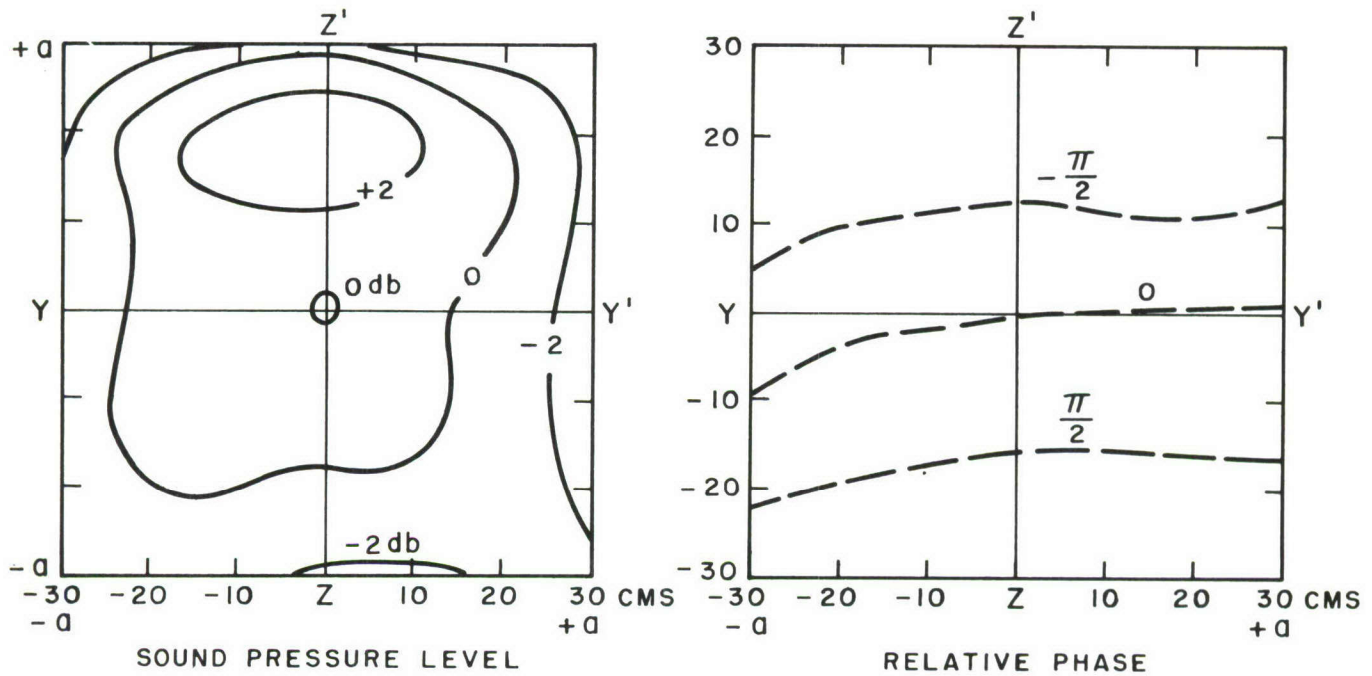
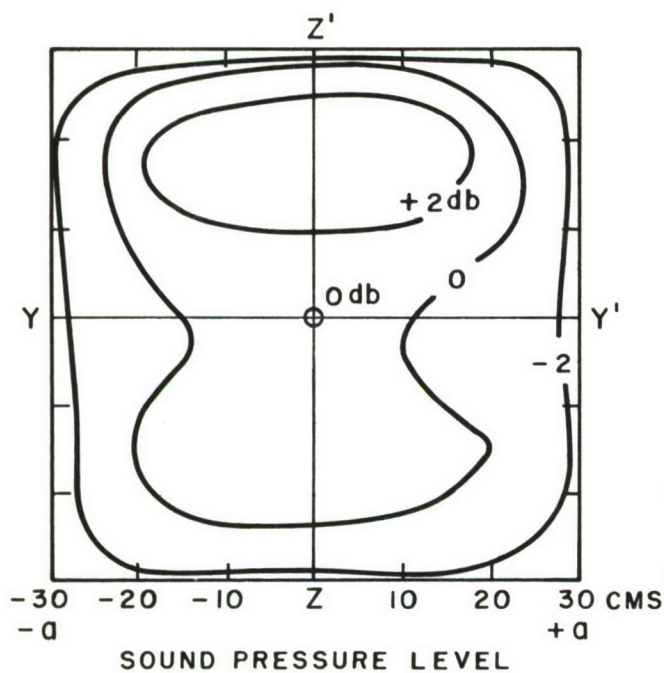


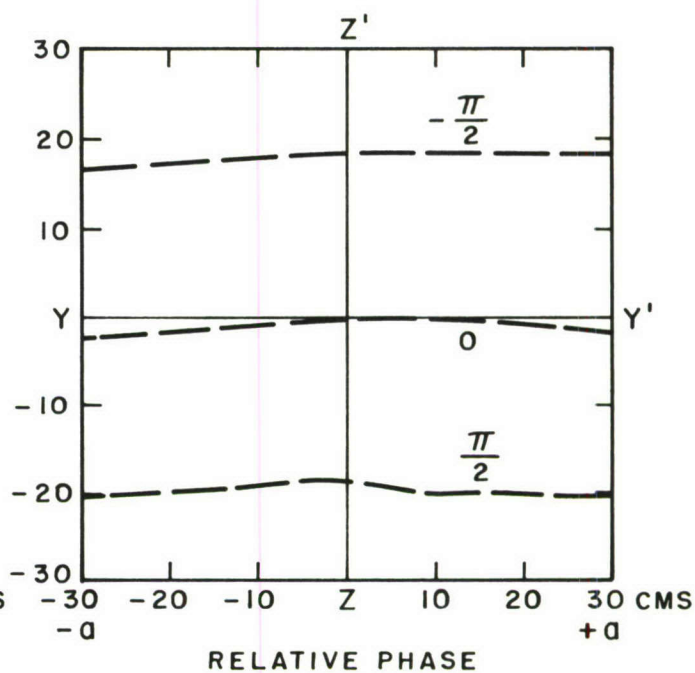
Figure 14. Pressure and Phase Distribution on Test Panel Under Anechoic Conditions, 1/3 Octave-Band Noise Source with Center Frequency 630 c/s, $\alpha = 30^\circ$, $\beta = 0^\circ$.

A 630 C/S, $Ka = 3.5$

$\alpha = 45^\circ$, $\beta = 0^\circ$, $\Delta L = 5.9$ db

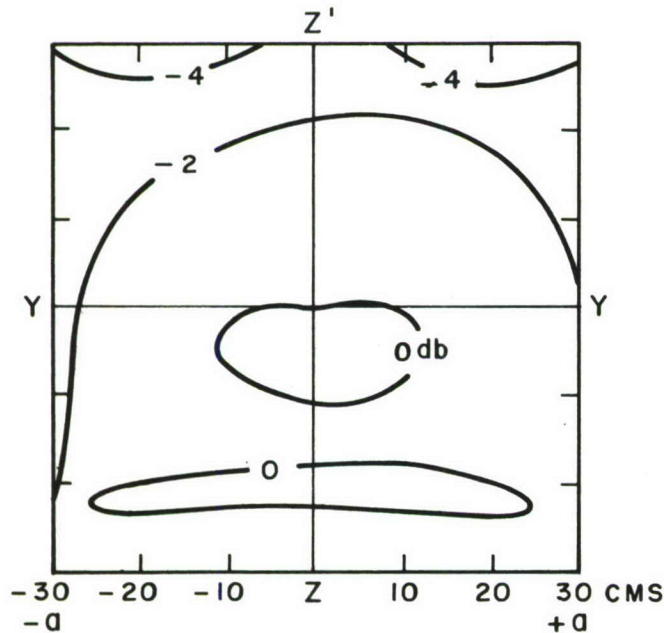


$\alpha = 45^\circ$, $\beta = 0^\circ$



B 200 C/S, $Ka = 1.1$

$\alpha = 45^\circ$, $\beta = 0^\circ$, $\Delta L = 3.0$ db



$\alpha = 45^\circ$, $\beta = 0^\circ$

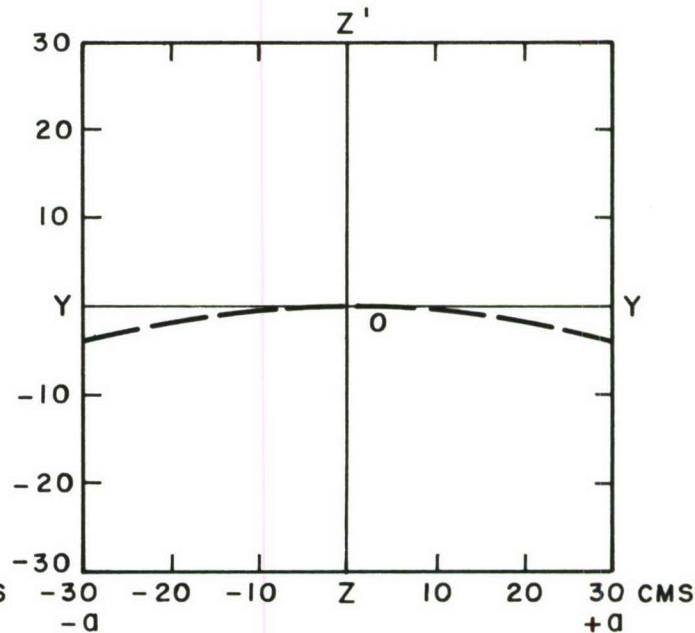


Figure 15. Pressure and Phase Distribution on Test Panel Under Anechoic Conditions, 1/3 Octave-Band Noise Source with Center Frequency 630 c/s and 200 c/s, $\alpha = 45^\circ$, $\beta = 0^\circ$.

$\alpha = 90^\circ$, $\beta = 0^\circ$, $\Delta L = 6.9 \text{ db}$, 630 C/S, $K_a = 7.0$, $K_b = 8.8$

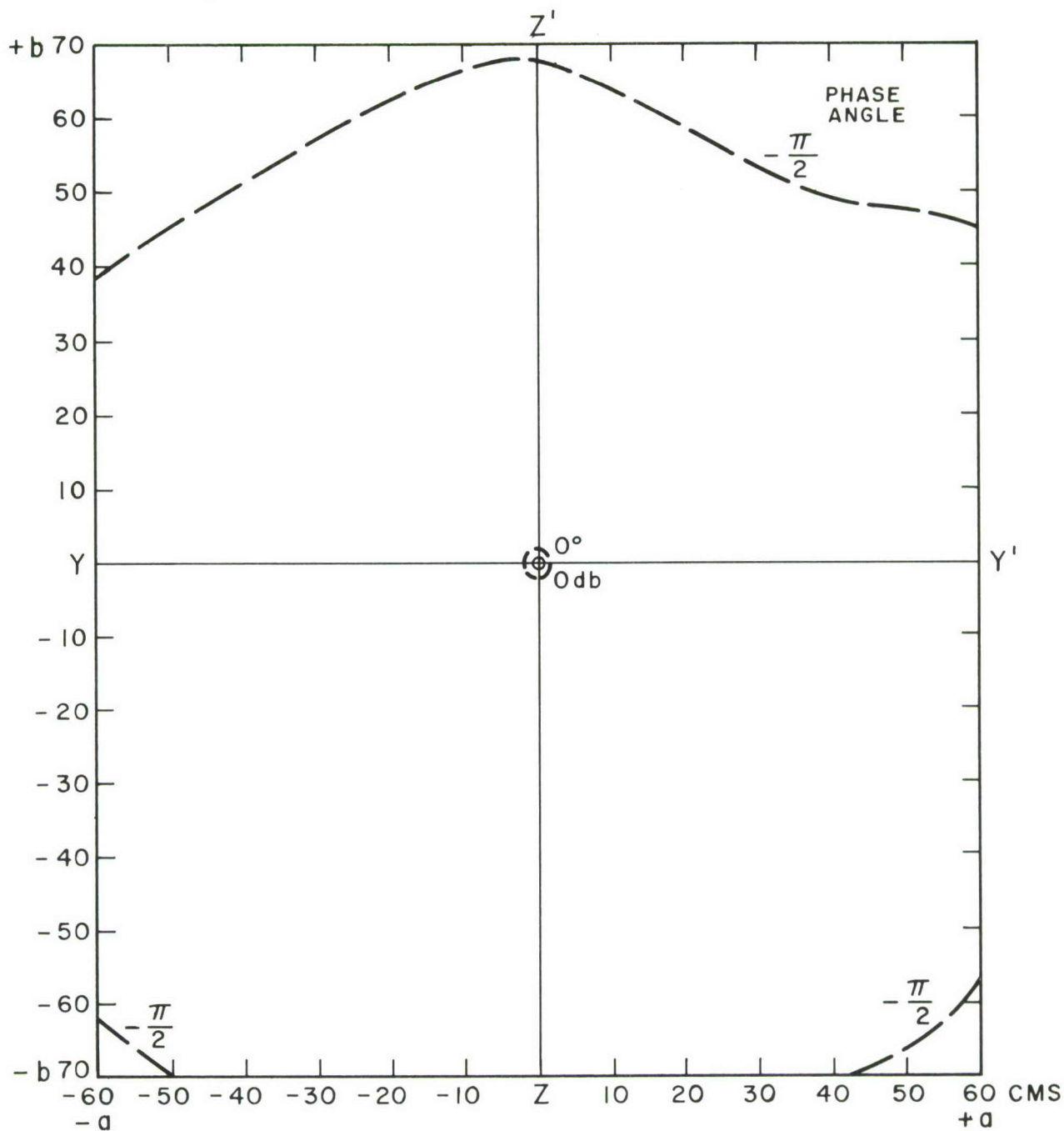


Figure 16. Pressure and Phase Distribution on Test Panel Under Anechoic Conditions, 1/3 Octave-Band Noise Source with Center Frequency 630 c/s, $\alpha = 90^\circ$, $\beta = 0^\circ$.

$\alpha = 90^\circ$, $\beta = 0^\circ$, $\Delta L = 6.2 \text{ db}$, 1600 C/S, $K_a = 18$, $K_b = 22$

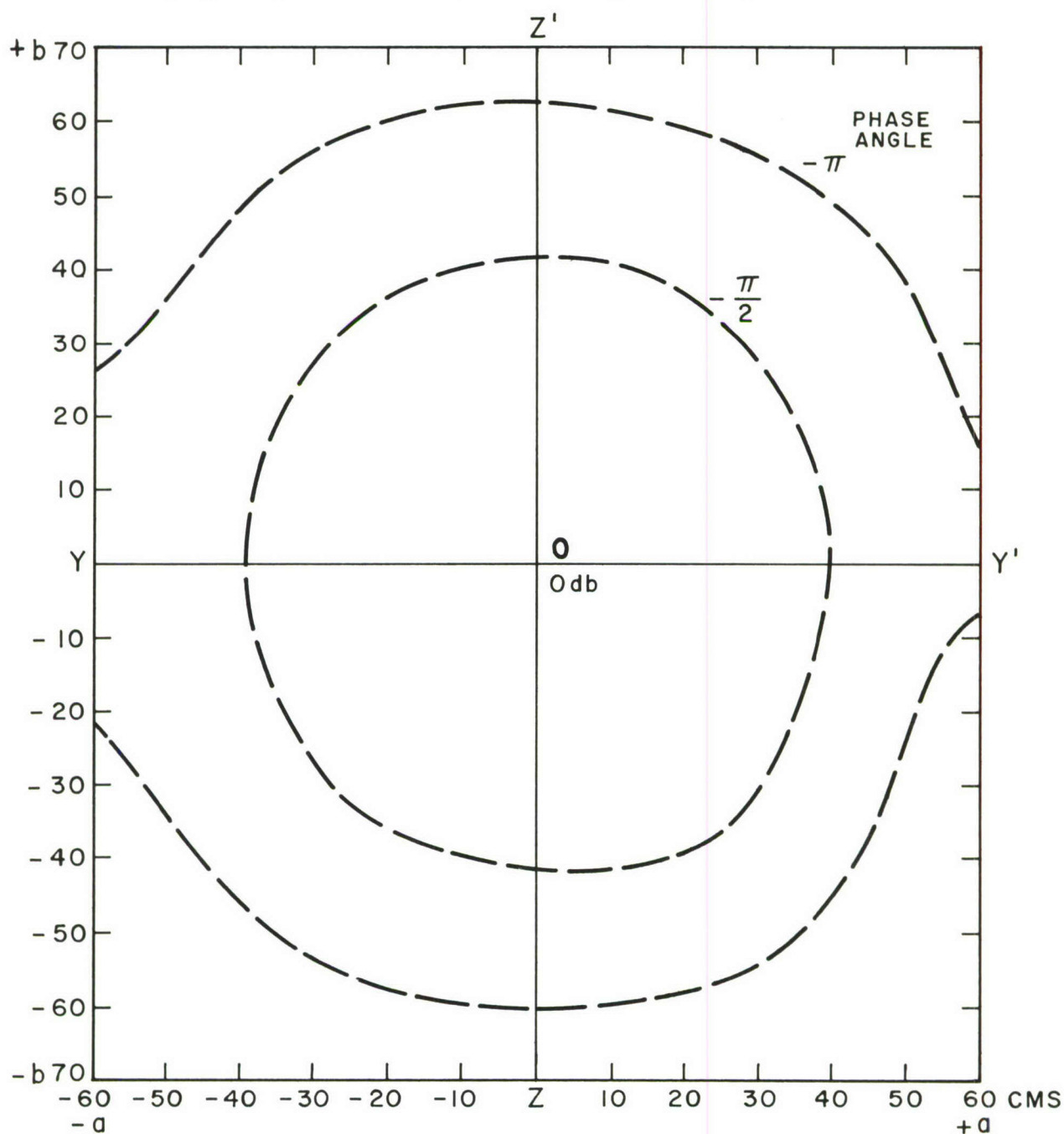


Figure 17. Pressure and Phase Distribution on Test Panel Under Anechoic Conditions, 1/3 Octave-Band Noise Source with Center Frequency 1600 c/s, $\alpha = 90^\circ$, $\beta = 0^\circ$.

$\alpha = 45^\circ$, $\beta = 0^\circ$, $\Delta L = 6.3 \text{ db}$, 630 C/S , $Ka = 7.0$, $Kb = 8.8$

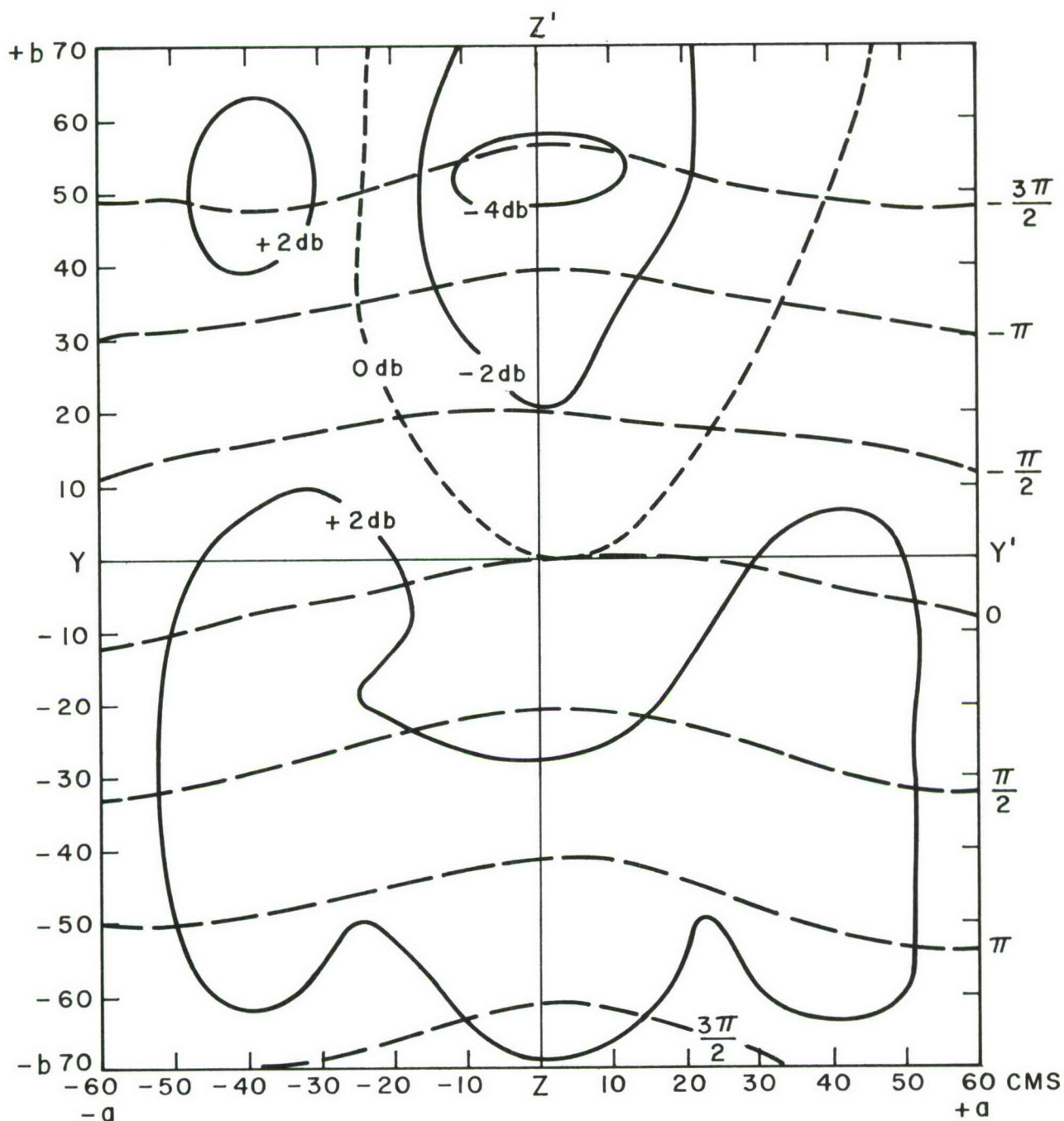


Figure 18. Pressure and Phase Distribution on Test Panel Under Anechoic Conditions, $1/3$ Octave-Band Noise Source with Center Frequency 630 c/s , $\alpha = 45^\circ$, $\beta = 0^\circ$.

$\alpha = 45^\circ$, $\beta = 0^\circ$, $\Delta L = 6 \text{ db}$, 1600 C/S , $K_a = 18$, $K_b = 22$

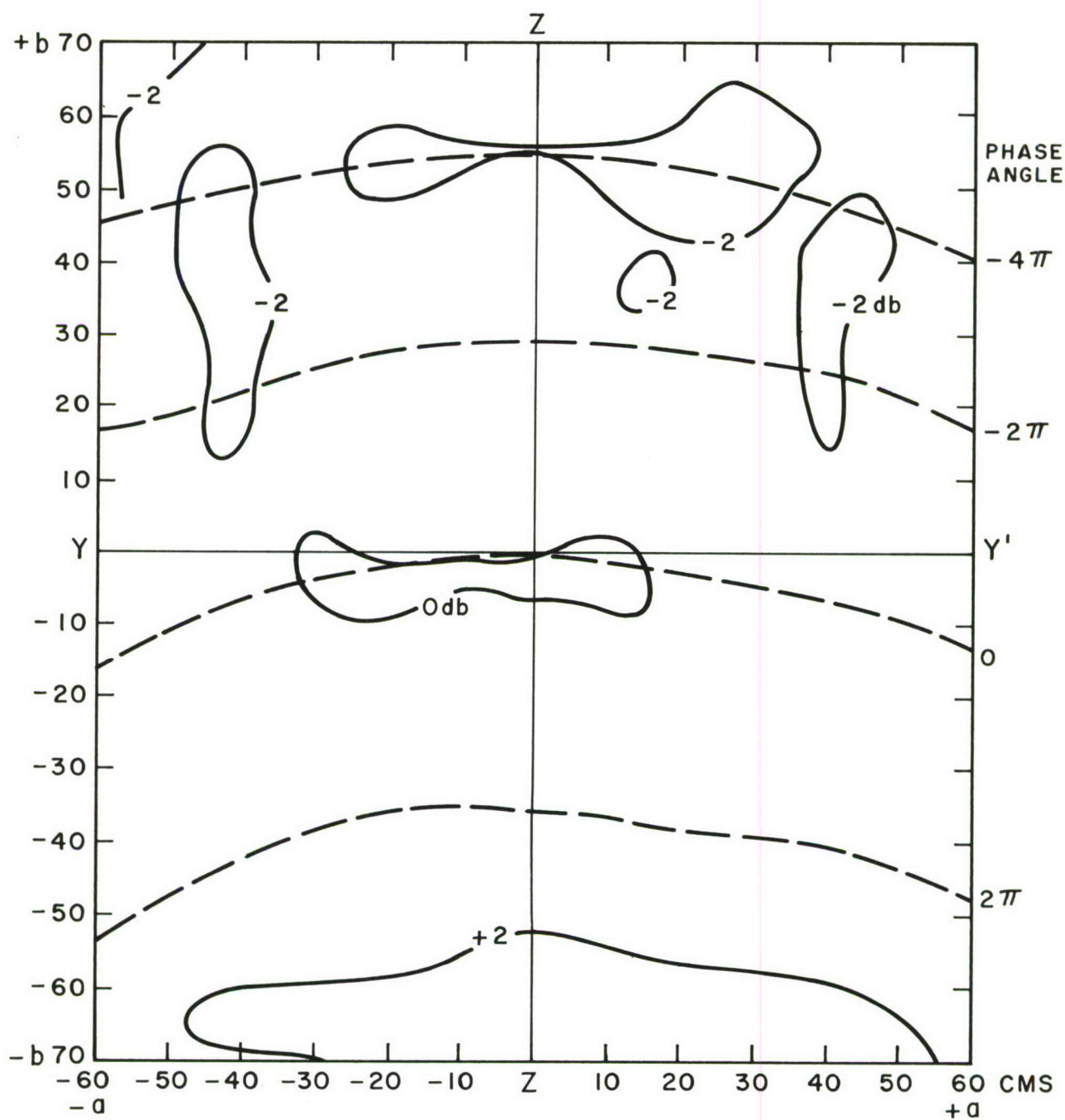


Figure 19. Pressure and Phase Distribution on Test Panel Under Anechoic Conditions, 1/3 Octave-Band Noise Source with Center Frequency 1600 c/s, $\alpha = 45^\circ$, $\beta = 0^\circ$.

$\alpha = 0^\circ$, $\beta = 0^\circ$, $\Delta L = -0.2 \text{ db}$, 630 C/S, $K_a = 7.0$, $K_b = 8.8$

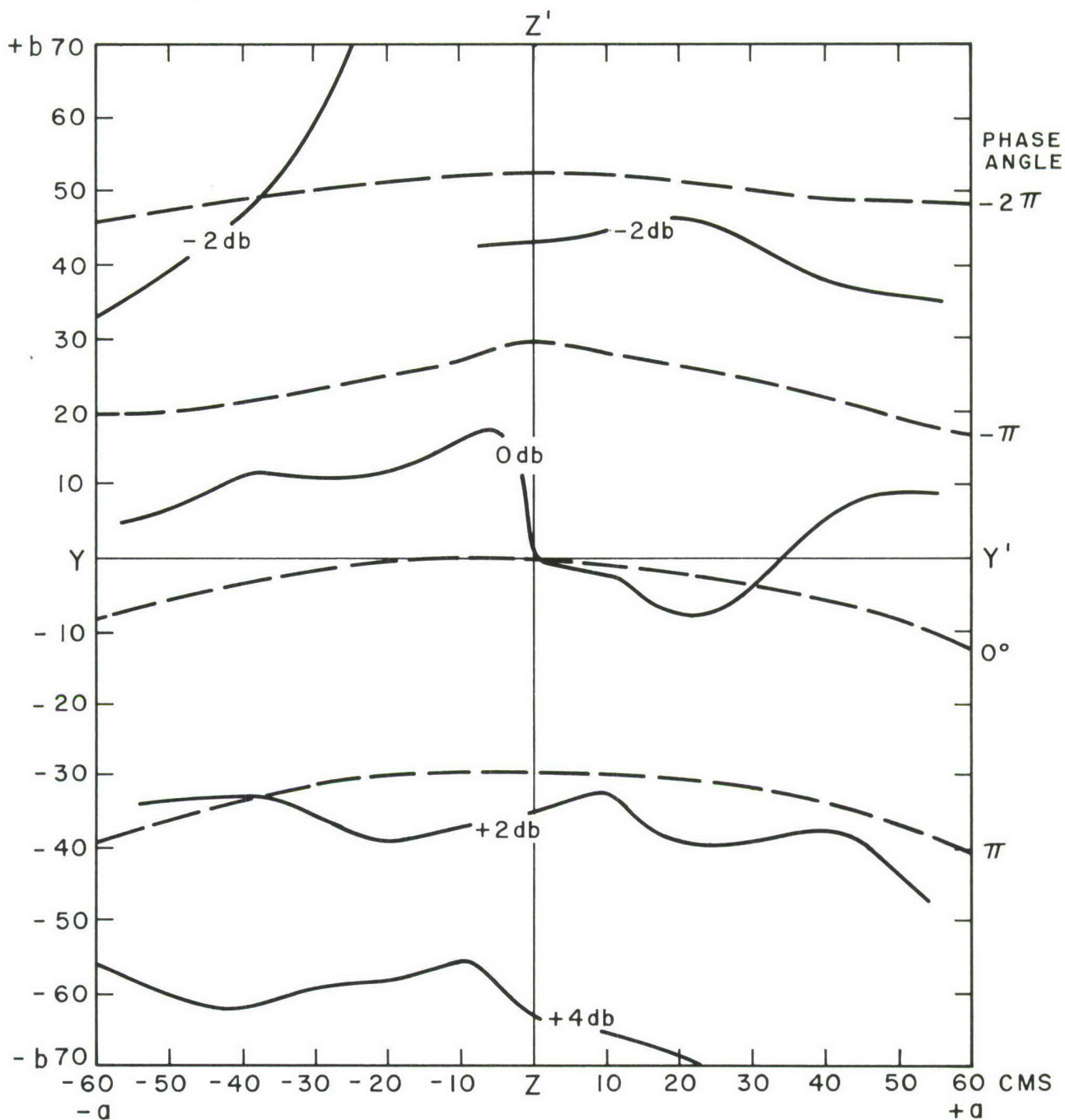


Figure 20. Pressure and Phase Distribution on Test Panel Under Anechoic Conditions, $1/3$ Octave-Band Noise Source with Center Frequency 630 c/s, $\alpha = 0^\circ$, $\beta = 0^\circ$.

$\alpha = 0^\circ$, $\beta = 0^\circ$, $\Delta L = -0.2 \text{ db}$, 1600 C/S, $Ka = 18$, $Kb = 22$

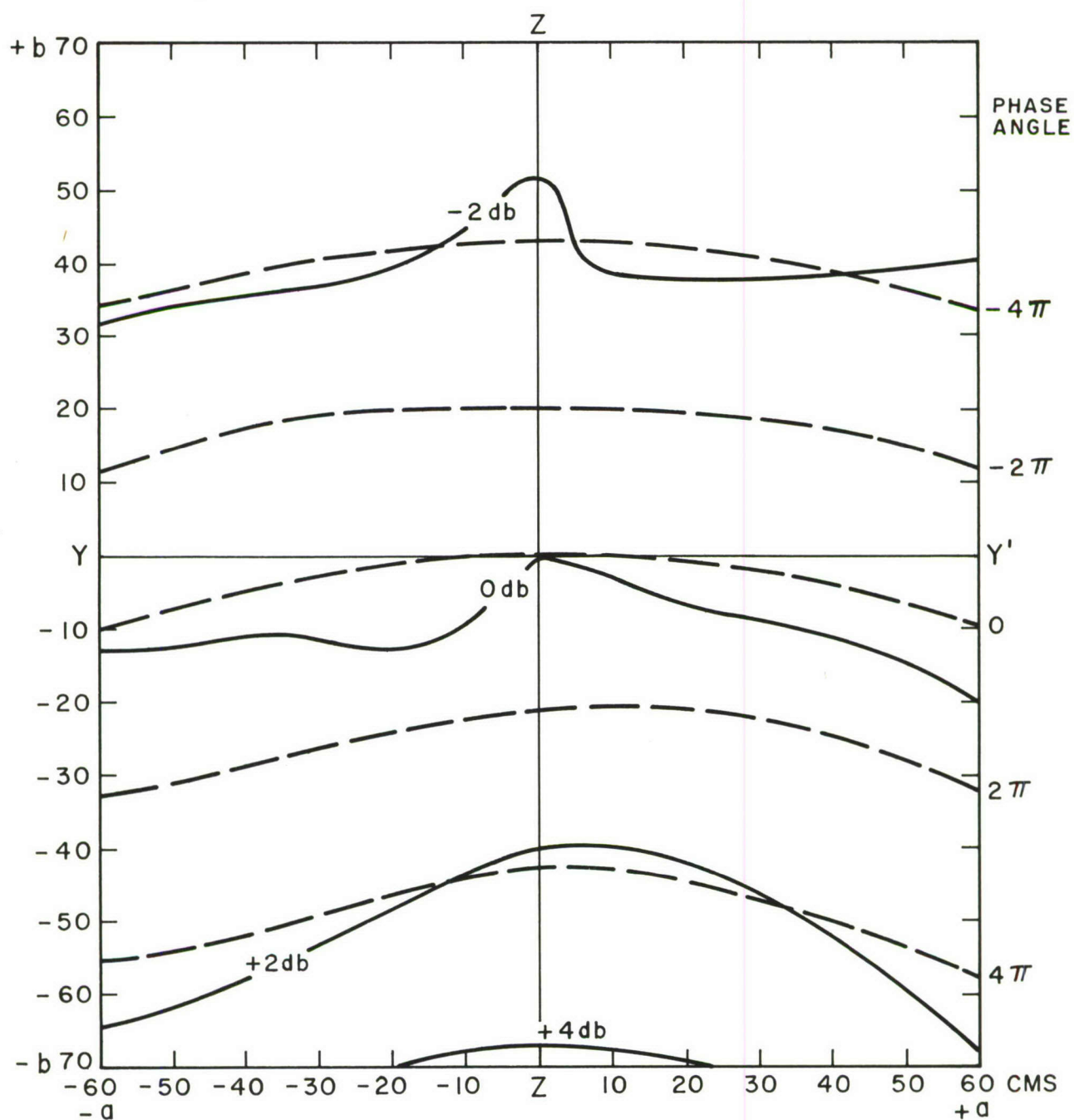


Figure 21. Pressure and Phase Distribution on Test Panel Under Anechoic Conditions, 1/3 Octave-Band Noise Source with Center Frequency 1600 c/s, $\alpha = 0^\circ$, $\beta = 0^\circ$.

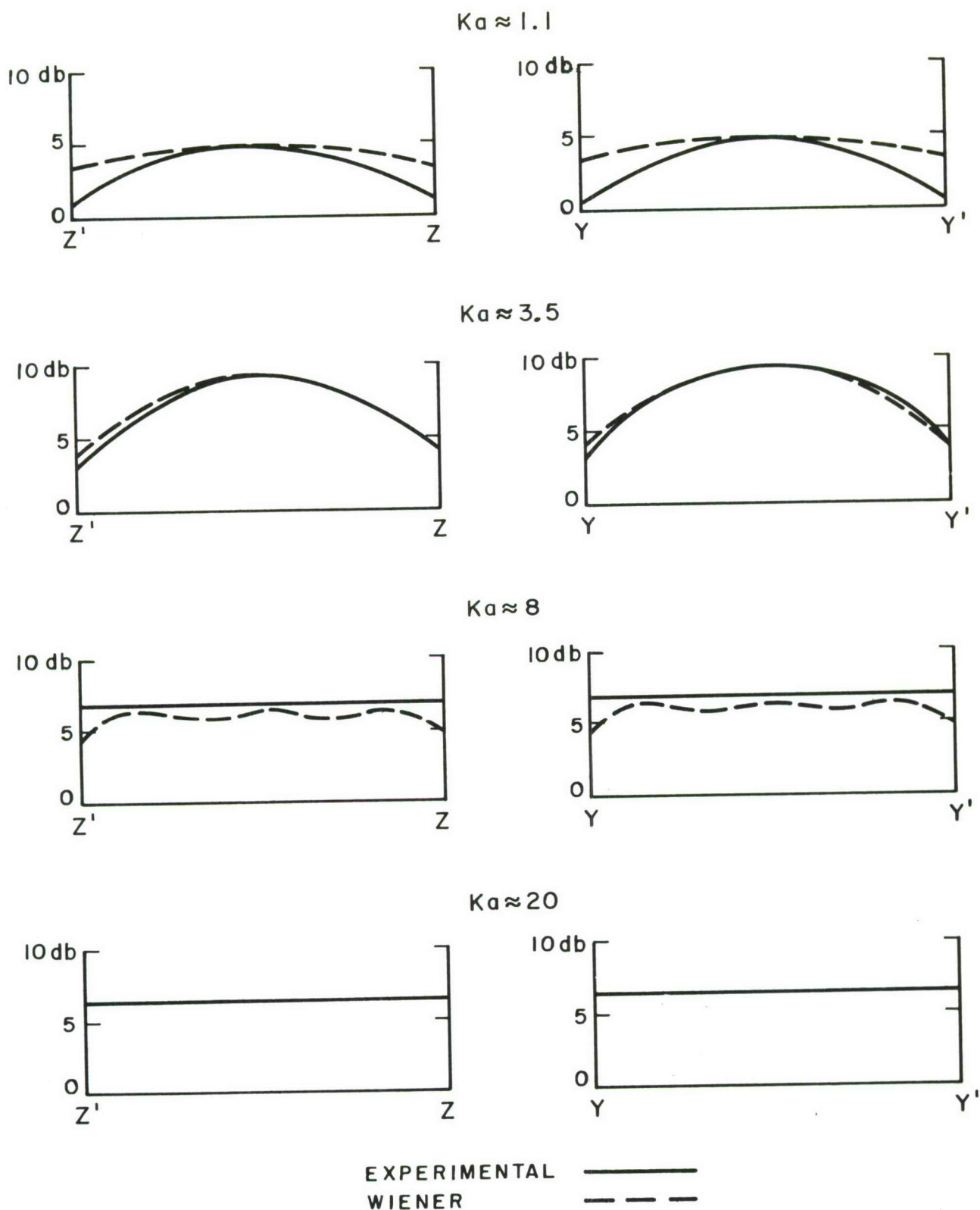


Figure 22. Absolute Pressure Increase Across ZZ' and YY' Axes of Panels, $\alpha = 90^\circ$, $\beta = 0^\circ$.

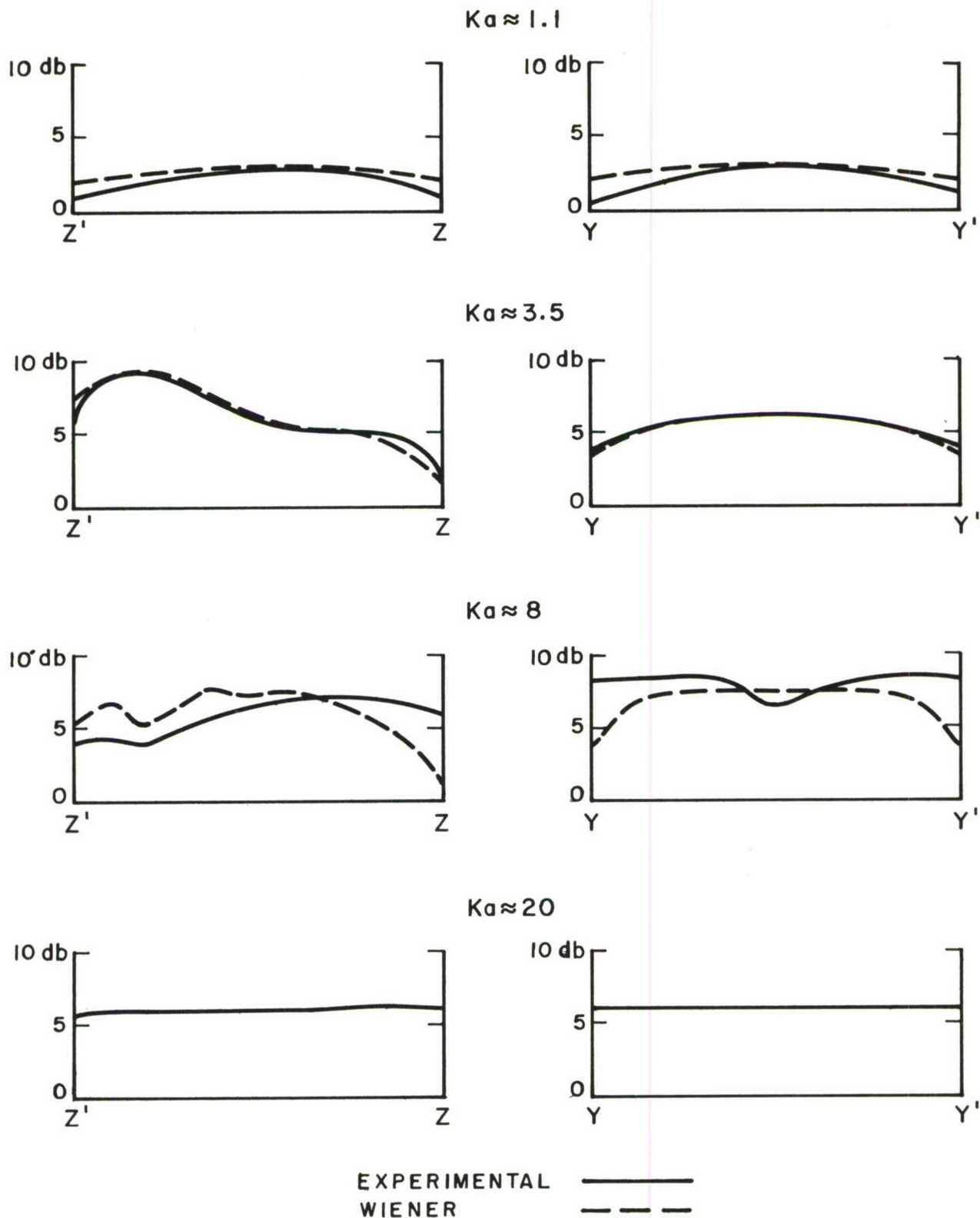


Figure 23. Absolute Pressure Increase Across ZZ' and YY' Axes of Panels, $\alpha = 45^\circ$, $\beta = 0^\circ$.

$\alpha = 90^\circ$, $\beta = 0^\circ$, $\Delta L = 12.1 \text{ db}$, $S_2 S_3 = 630 \text{ C S}$, $Ka = 7.0$, $Kb = 8.8$

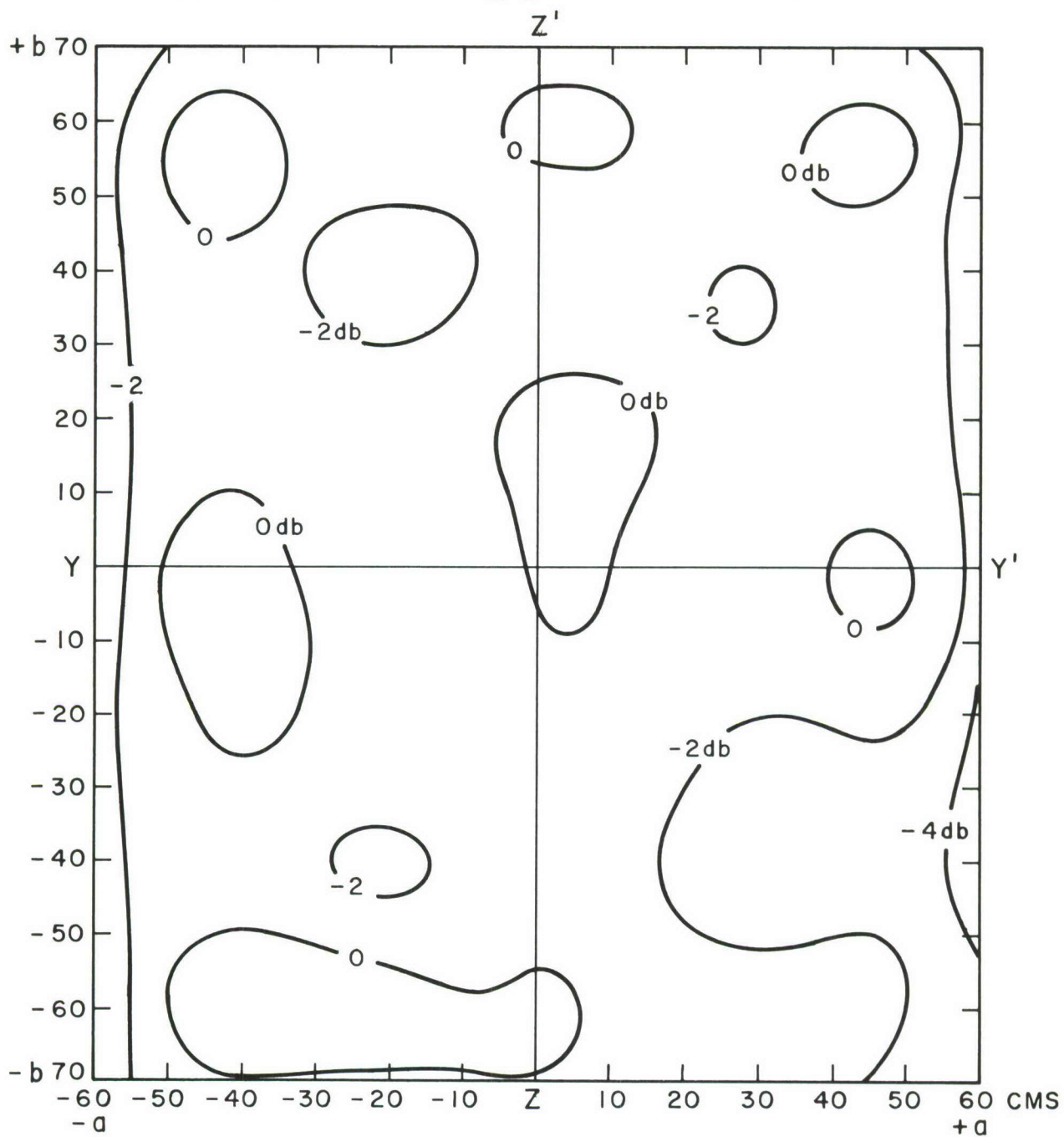


Figure 24. Pressure and Phase Distribution on Test Panel Under Anechoic Conditions, Coherent 1/3 Octave-Band Noise Sources S_2 , S_3 with Center Frequency 630 c/s, $\alpha = 90^\circ$, $\beta \approx 0^\circ$.

$\alpha = 45^\circ$, $\beta = 0^\circ$, $\Delta L = 10.5 \text{ db}$, $S_2 S_3 = 630 \text{ C/S}$, $Ka = 7.0$, $Kb = 8.8$

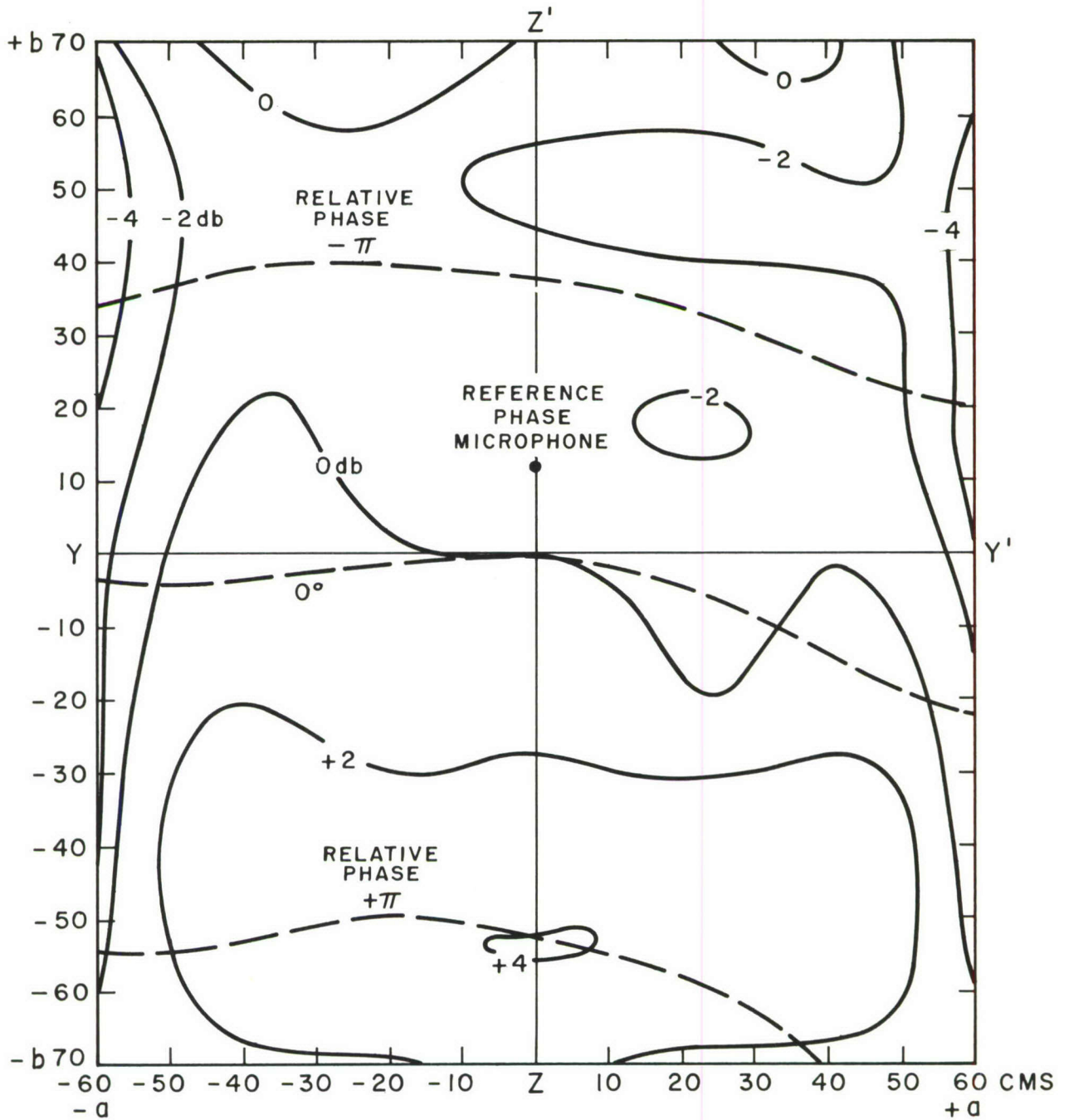


Figure 25. Pressure and Phase Distribution on Test Panel Under Anechoic Conditions, Coherent 1/3 Octave-Band Noise Sources S_2 , S_3 with Center Frequency 630 c/s, $\alpha = 45^\circ$, $\beta = 0^\circ$.

$\alpha = 45^\circ$, $\beta = 0^\circ$, $\Delta L = 5.7 \text{ db}$, $S_1 S_2 = 200 \text{ C/S}$, $K_a = 2.2$, $K_b = 2.8$

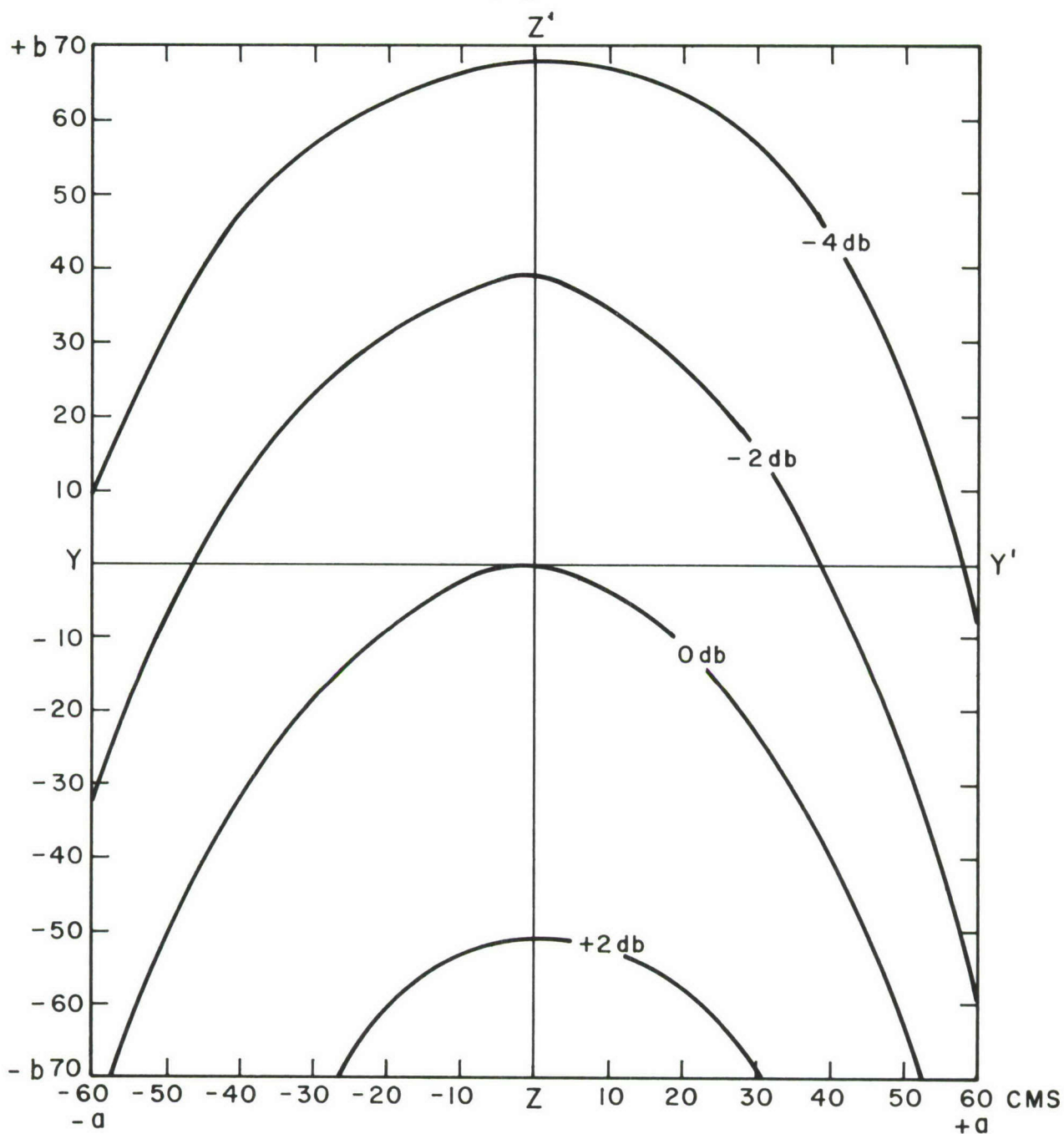


Figure 26.. Pressure and Phase Distribution on Test Panel Under Anechoic Conditions, Coherent 1/3 Octave-Band Noise Sources S_1 , S_2 with Center Frequency 200 c/s, $\alpha = 45^\circ$, $\beta = 0^\circ$.

$\alpha = 45^\circ$, $\beta = 0^\circ$, $\Delta L = 3.0 \text{ db}$, $S_1 S_2 = 630 \text{ C/S}$, $Ka = 7.0$, $Kb = 8.8$

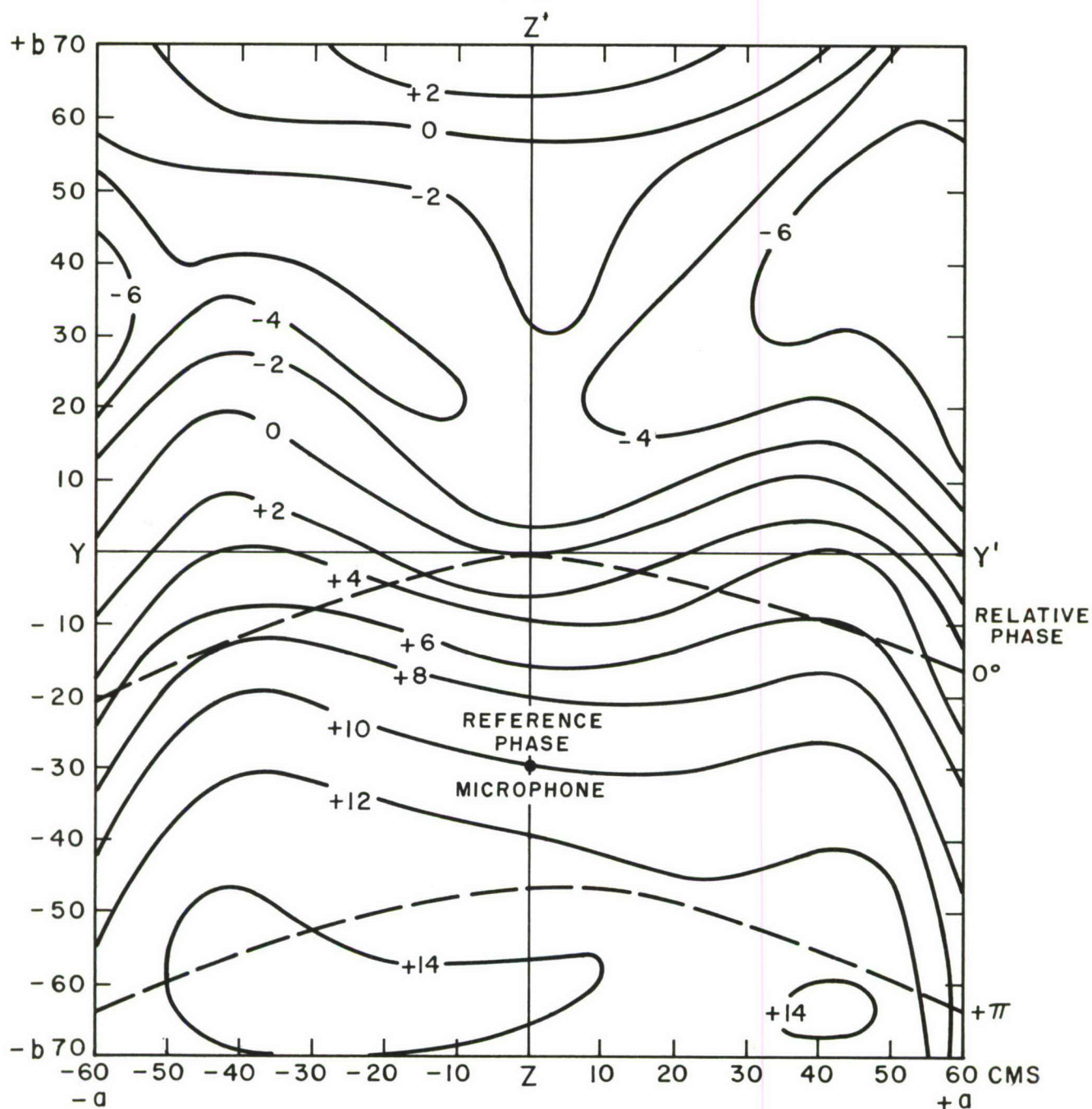


Figure 27. Pressure and Phase Distribution on Test Panel Under Anechoic Conditions, Coherent 1/3 Octave-Band Noise Sources S_1 , S_2 with Center Frequency 630 c/s, $\alpha = 45^\circ$, $\beta = 0^\circ$.

$\alpha = 45^\circ$, $\beta = 0^\circ$, $\Delta L = 6.6 \text{ db}$, $S_1 S_2 = 1600 \text{ C/S}$, $K_a = 17.8$, $K_b = 22.2$

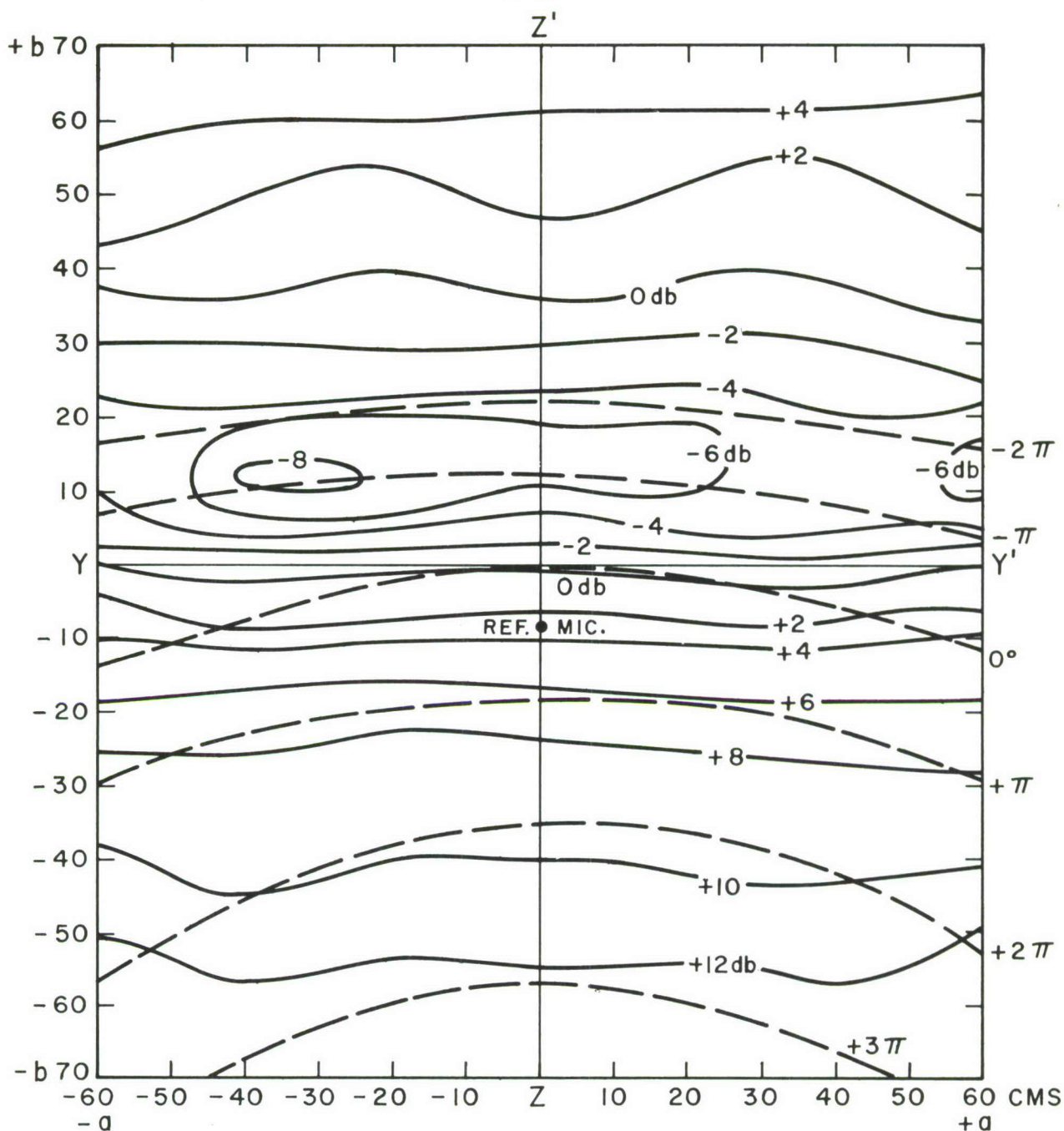


Figure 28. Pressure and Phase Distribution on Test Panel Under Anechoic Conditions, Coherent 1/3 Octave-Band Noise Sources S_1 , S_2 with Center Frequency 1600 c/s, $\alpha = 45^\circ$, $\beta = 0^\circ$.

$\alpha = 90^\circ$, $\beta \neq 0^\circ$, $\Delta L = 6.7 \text{ db}$, $S_1 S_2 S_3 = 630 \text{ C/S}$, $K_a = 7.0$, $K_b = 8.8$

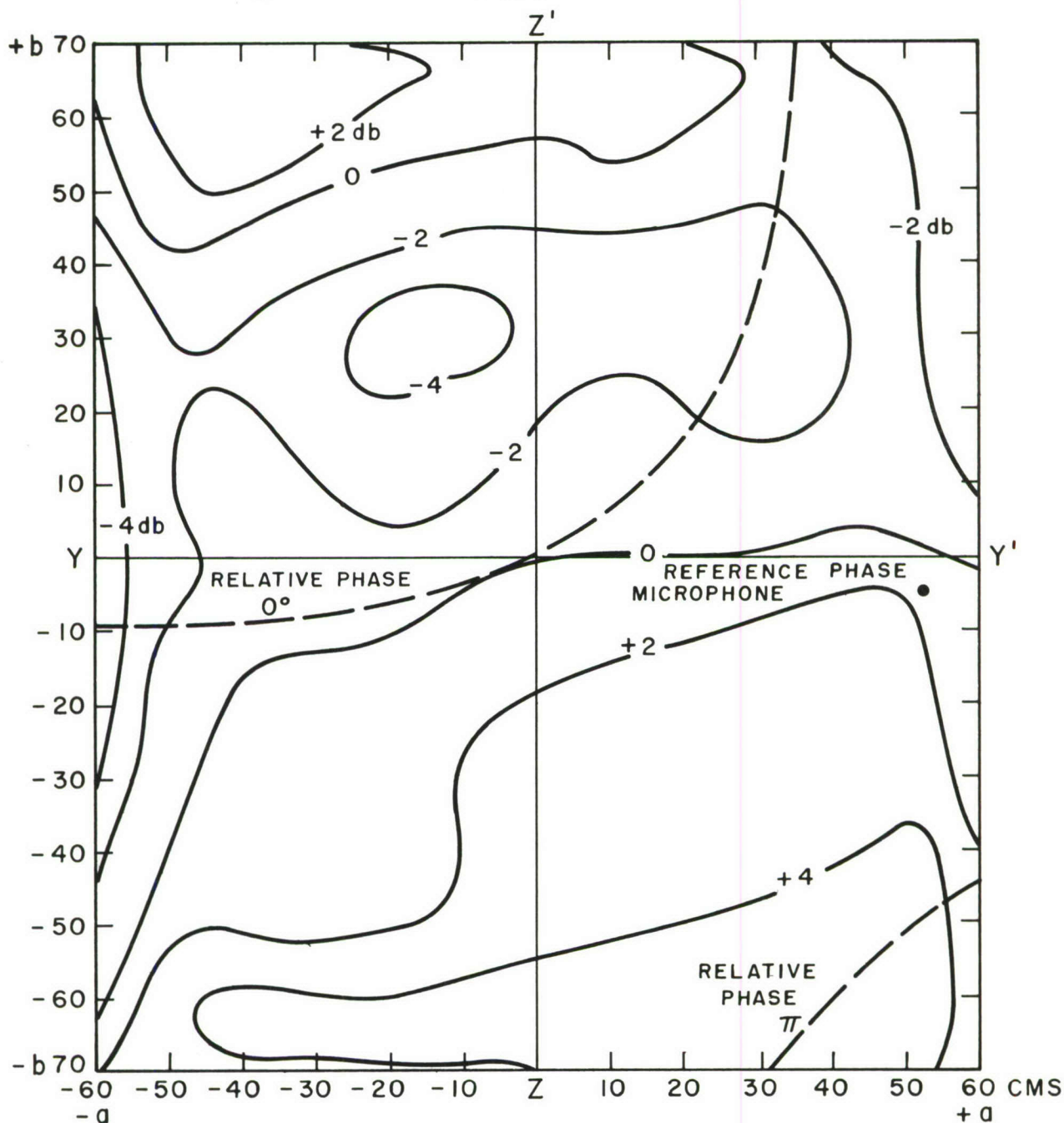


Figure 29. Pressure and Phase Distribution on Test Panel Under Anechoic Conditions, Coherent 1/3 Octave-Band Noise Sources S_1 , S_2 , S_3 with Center Frequency 630 c/s, $\alpha = 90^\circ$, $\beta = 0^\circ$.

$\alpha = 45^\circ$, $\beta = 0^\circ$, $\Delta L = 4.8 \text{ db}$, $S_1 S_2 S_3 = 630 \text{ C/S}$, $Ka = 7.0$ $Kb = 8.8$

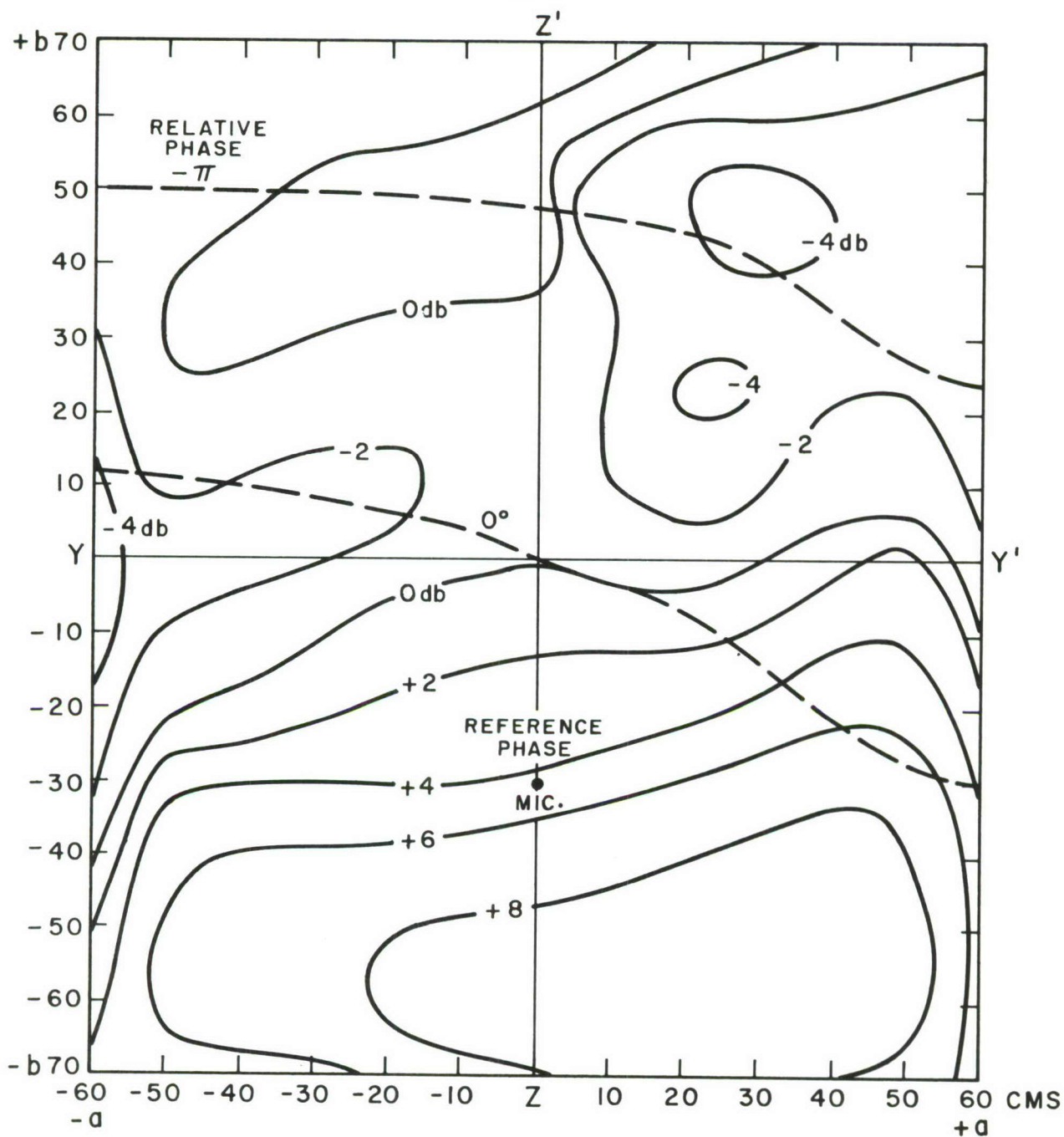


Figure 30. Pressure and Phase Distribution on Test Panel Under Anechoic Conditions, Coherent 1/3 Octave-Band Noise Sources S_1 , S_2 , S_3 with Center Frequency 630 c/s, $\alpha = 45^\circ$, $\beta = 0^\circ$.

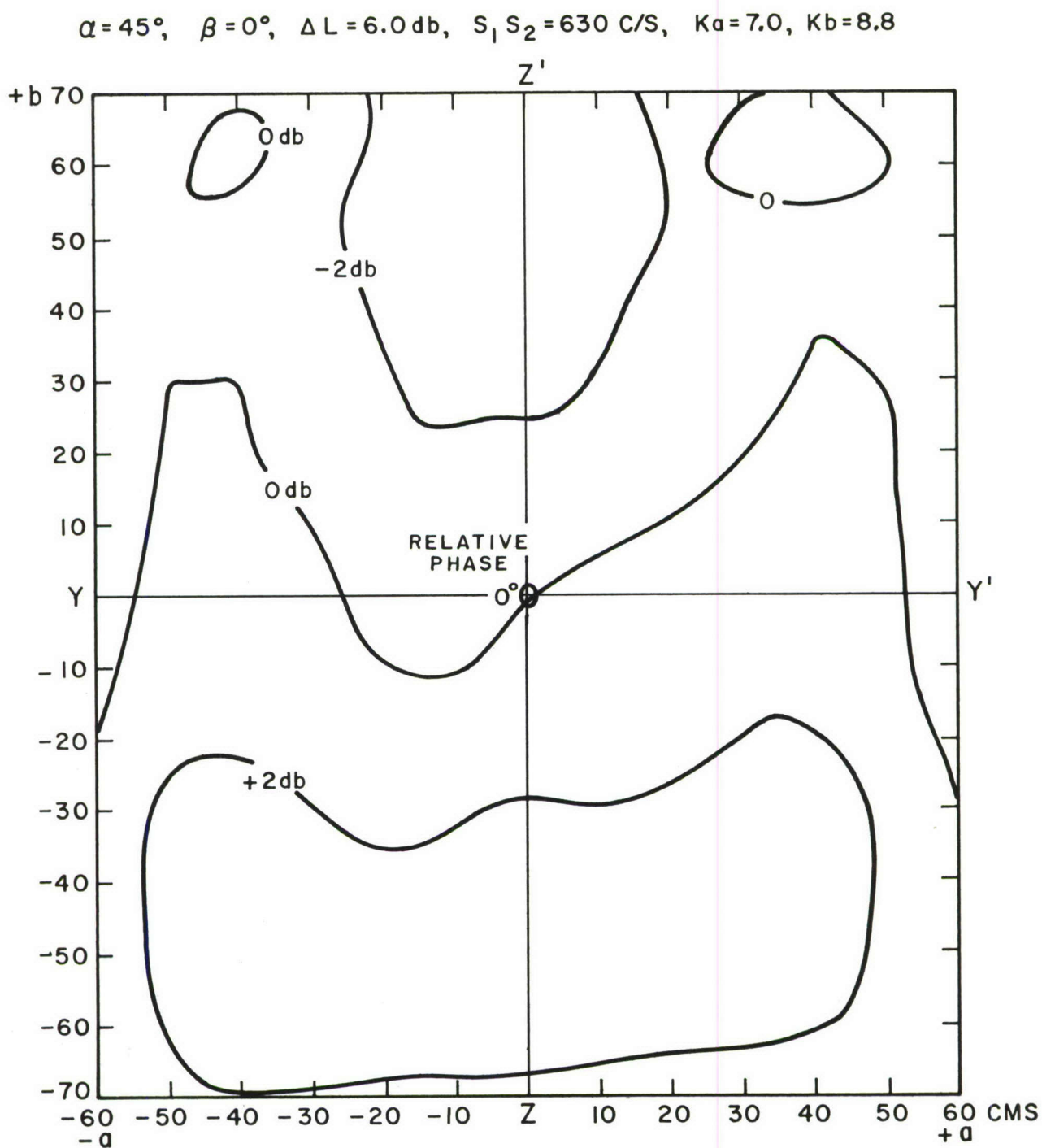


Figure 31, Pressure and Phase Distribution on Test Panel Under Anechoic Conditions, Incoherent 1/3 Octave-Band Noise Sources S_1, S_2 with Center Frequency 630 c/s, $\alpha = 45^\circ$, $\beta = 0^\circ$.

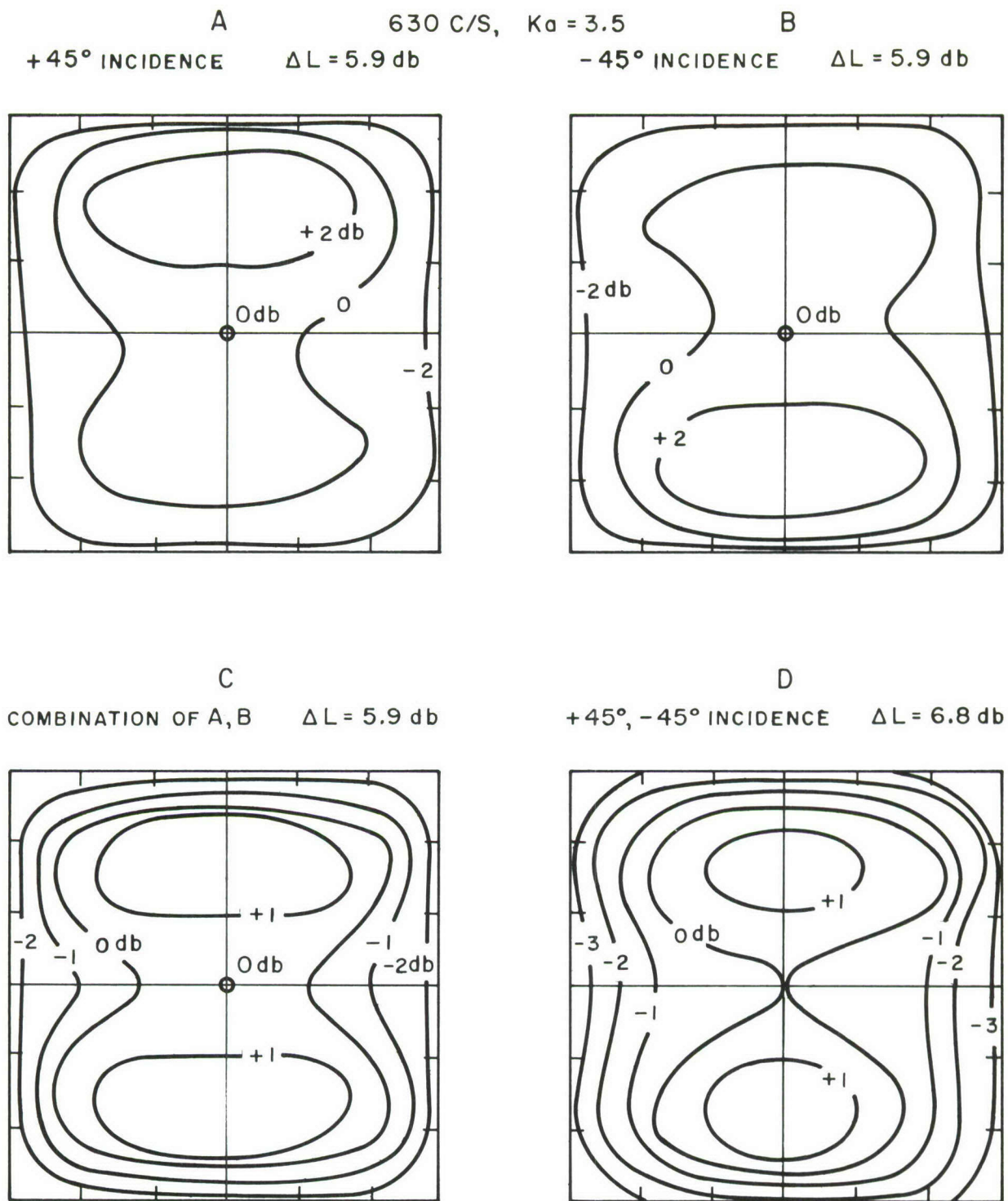


Figure 32. Pressure Distribution on Test Panel Under Anechoic Conditions. A Single 1/3 Octave-Band Noise Source, $\alpha = +45^\circ$. B Single 1/3 Octave-Band Noise Source, $\alpha = -45^\circ$. C Superimposed Combination of A and B. D Two Incoherent 1/3 Octave-Band Noise Sources, $\alpha = +45^\circ$ and -45° . Center Frequency = 630 cps.

$f = 630 \text{ C/S}, K\alpha = 3.5, D = 3 \text{ ft}$

$\alpha = 90^\circ, \beta = 0^\circ, \Delta L = 8.0 \text{ db}$

$\alpha = 0^\circ, \beta = 0^\circ, \Delta L = -0.6 \text{ db}$

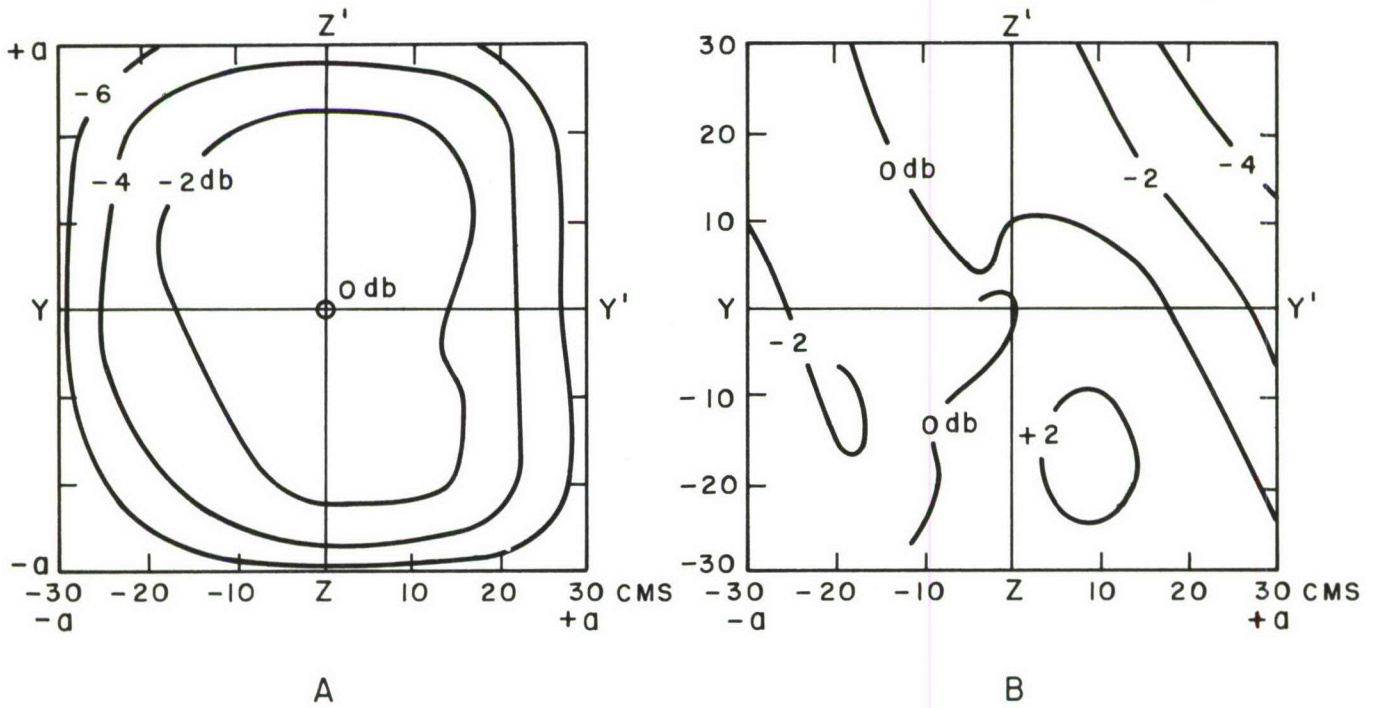
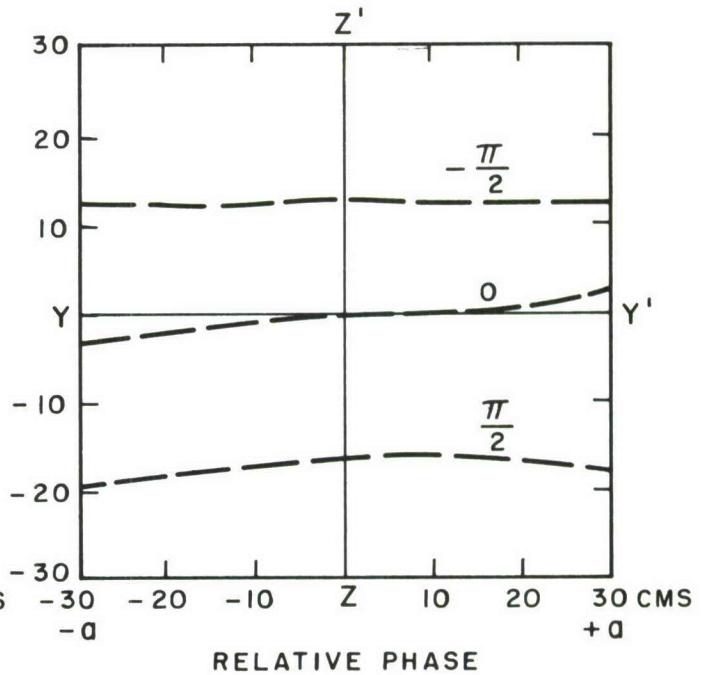
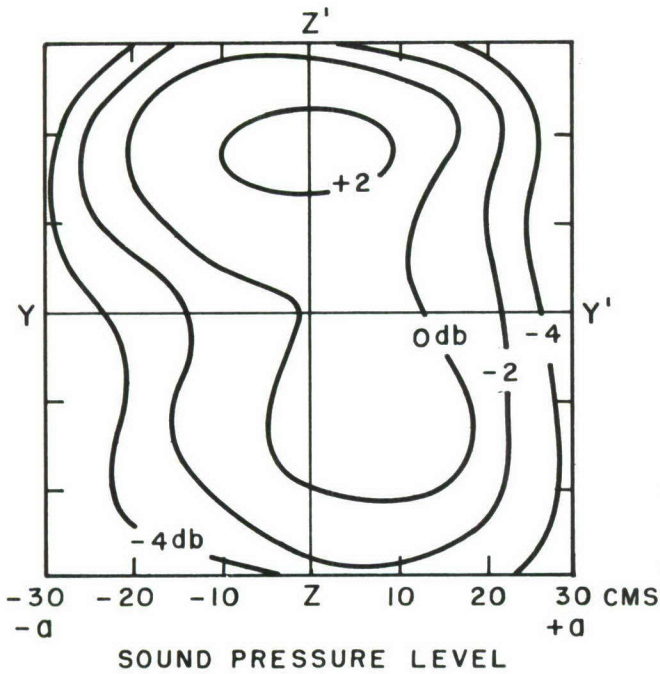


Figure 33. Pressure and Phase Distribution on Test Panel Under Semi-Anechoic Condition, 1/3 Octave-Band Noise Source with Center Frequency 630 c/s, $\alpha = 90^\circ, \beta = 0^\circ$, and $\alpha = 0^\circ, \beta = 0^\circ, D = 3 \text{ ft}$.

A 630 C/S, $Ka = 3.5$, $D = 3$ ft

$\alpha = 45^\circ$, $\beta = 0^\circ$, $\Delta L = 5.2$ db

$\alpha = 45^\circ$, $\beta = 0^\circ$



B 630 C/S, $Ka = 3.5$, $D = 3$ ft

$\alpha = 45^\circ$, $\beta = 45^\circ$, $\Delta L = 6.6$ db

$\alpha = 45^\circ$, $\beta = 45^\circ$

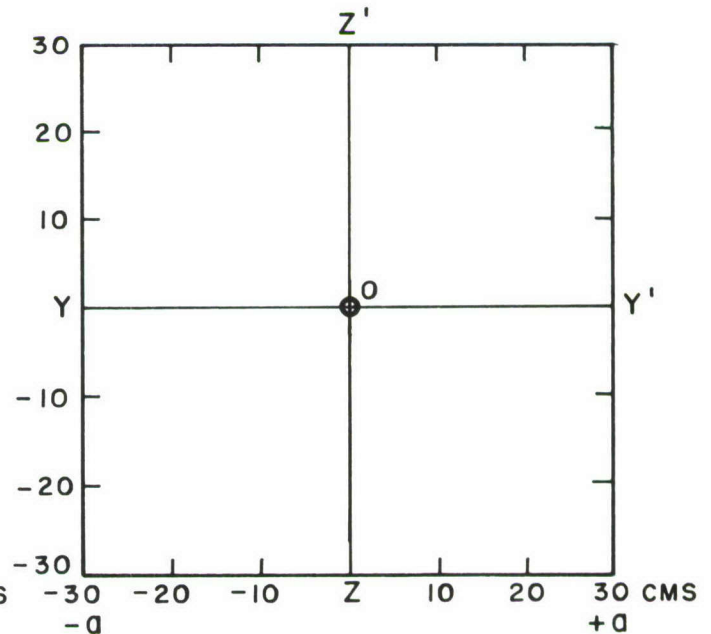
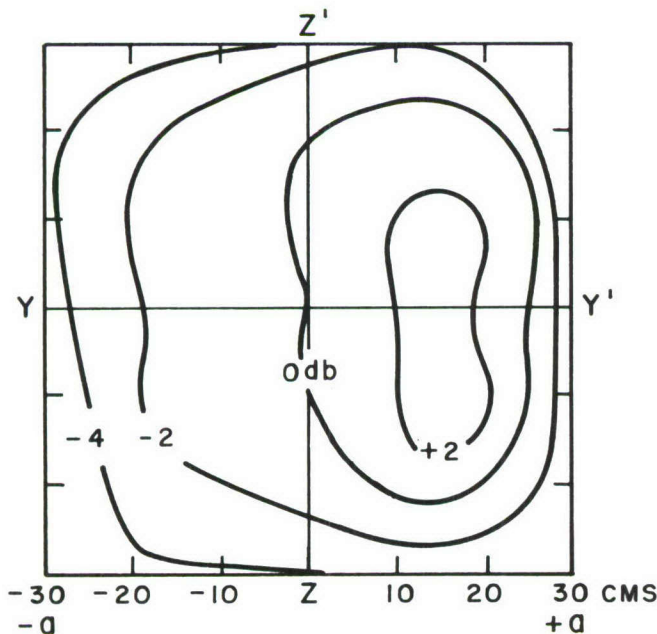


Figure 34. Pressure and Phase Distribution on Test Panel Under Semi-Anechoic Condition, 1/3 Octave-Band Noise Source with Center Frequency 630 c/s, $\alpha = 45^\circ$, $\beta = 0^\circ$, and $\alpha = 45^\circ$, $\beta = 45^\circ$, $D = 3$ ft.

$\alpha = 90^\circ$, $\beta = 0^\circ$, $\Delta L = 6.3 \text{ db}$, 630 C/S , $K_a = 7.0$, $K_b = 8.8$, $D = 3 \text{ ft.}$

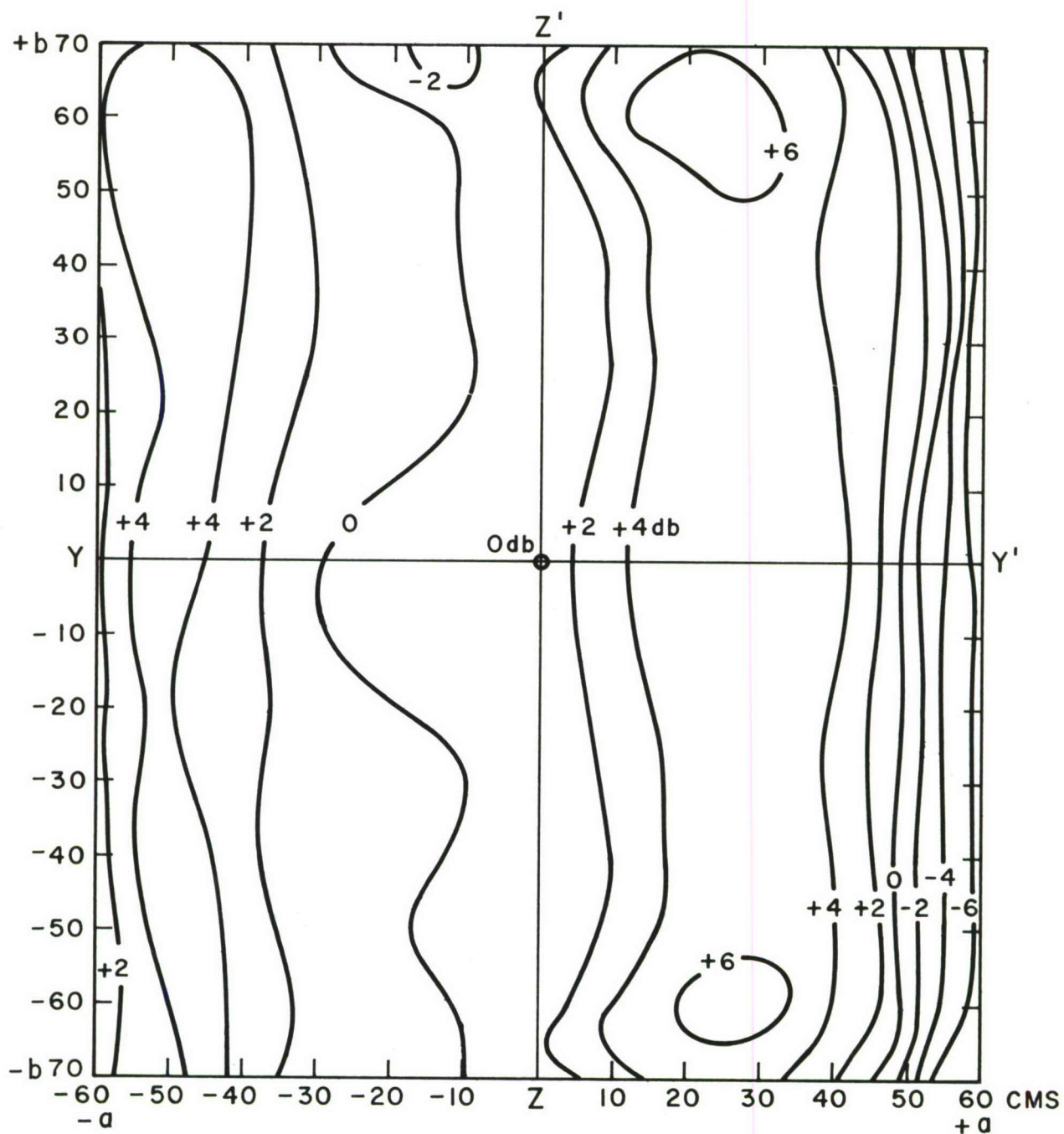


Figure 35. Pressure and Phase Distribution on Test Panel Under Semi-Anechoic Condition, 1/3 Octave-Band Noise Source with Center Frequency 630 c/s, $\alpha = 90^\circ$, $\beta = 0^\circ$, $D = 3 \text{ ft.}$

$\alpha = 45^\circ$, $\beta = 0^\circ$, $\Delta L = 5.5 \text{ db}$, 630 C/S , $K_a = 7.0$, $K_b = 8.8$, $D = 3 \text{ ft}$

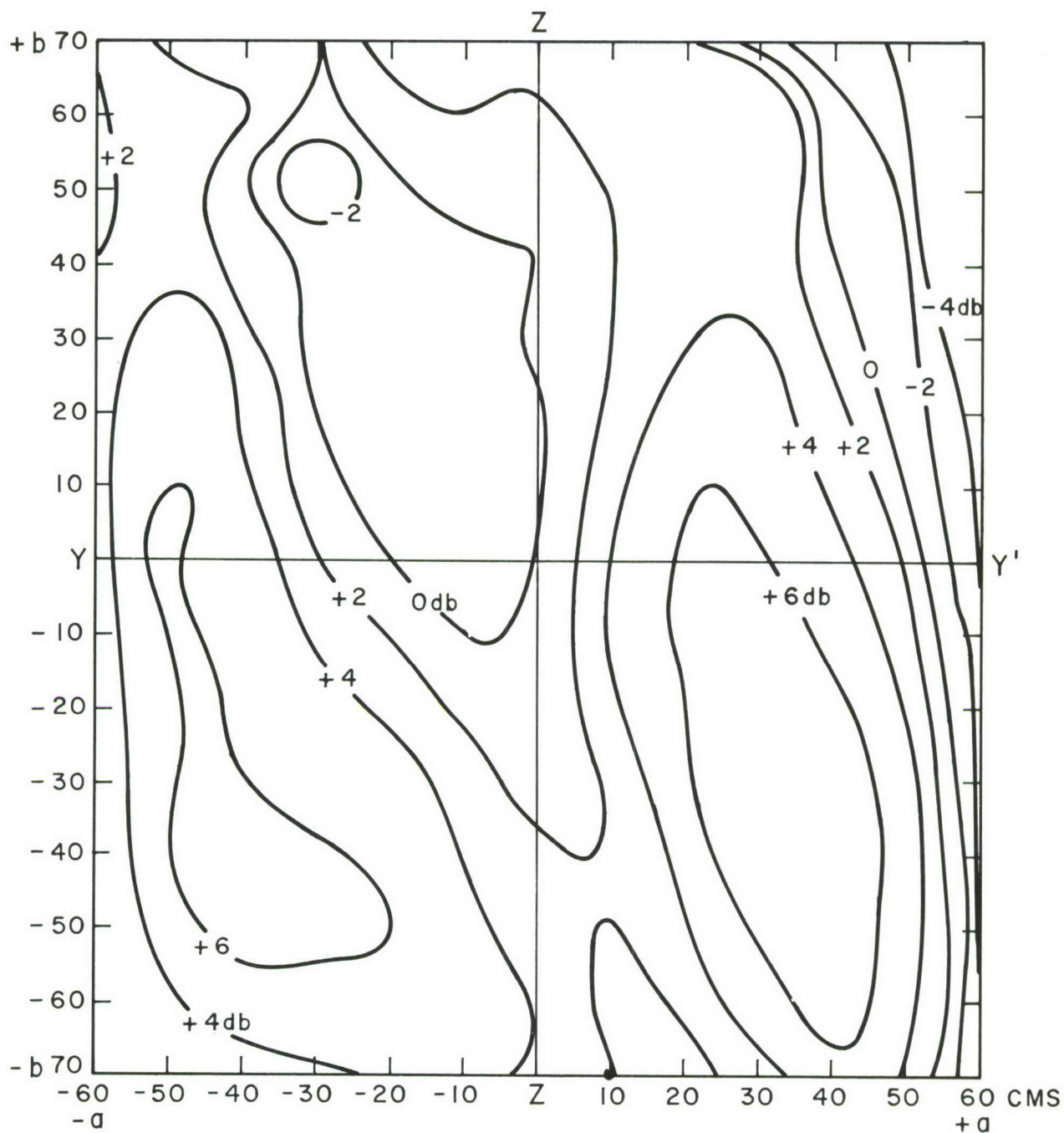


Figure 36. Pressure and Phase Distribution on Test Panel Under Semi-Anechoic Condition, 1/3 Octave-Band Noise Source with Center Frequency 630 c/s, $\alpha = 45^\circ$, $\beta = 0^\circ$, $D = 3 \text{ ft}$.

$\alpha = 0^\circ$, $\beta = 0^\circ$, $\Delta L = -1.2 \text{ db}$, 630 C/S, $K_a = 7.0$, $K_b = 8.8$, $D = 3 \text{ ft}$

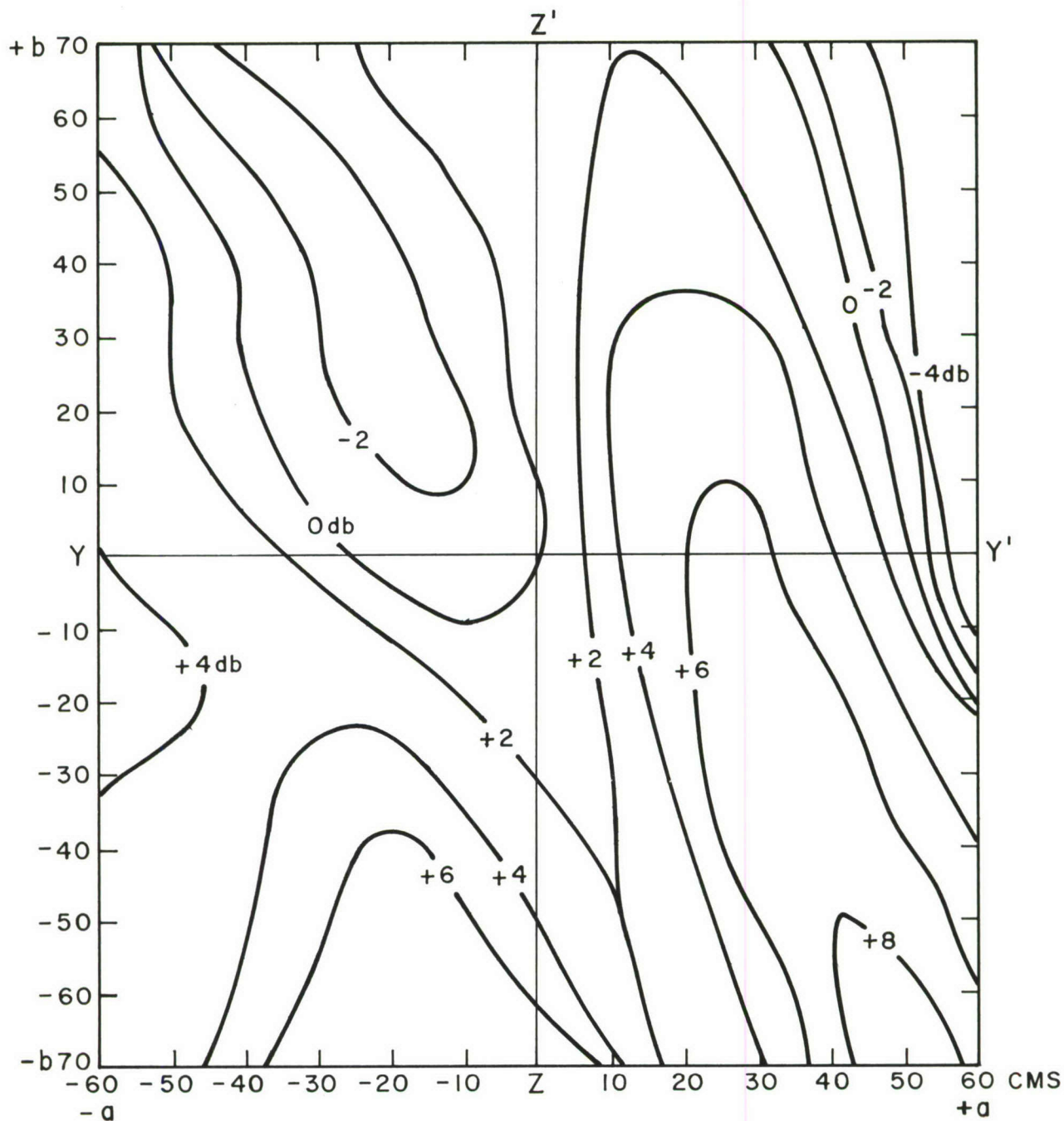


Figure 37. Pressure and Phase Distribution on Test Panel Under Semi-Anechoic Condition, 1/3 Octave-Band Noise Source with Center Frequency 630 c/s, $\alpha \approx 0^\circ$, $\beta \approx 0^\circ$, $D = 3 \text{ ft}$.

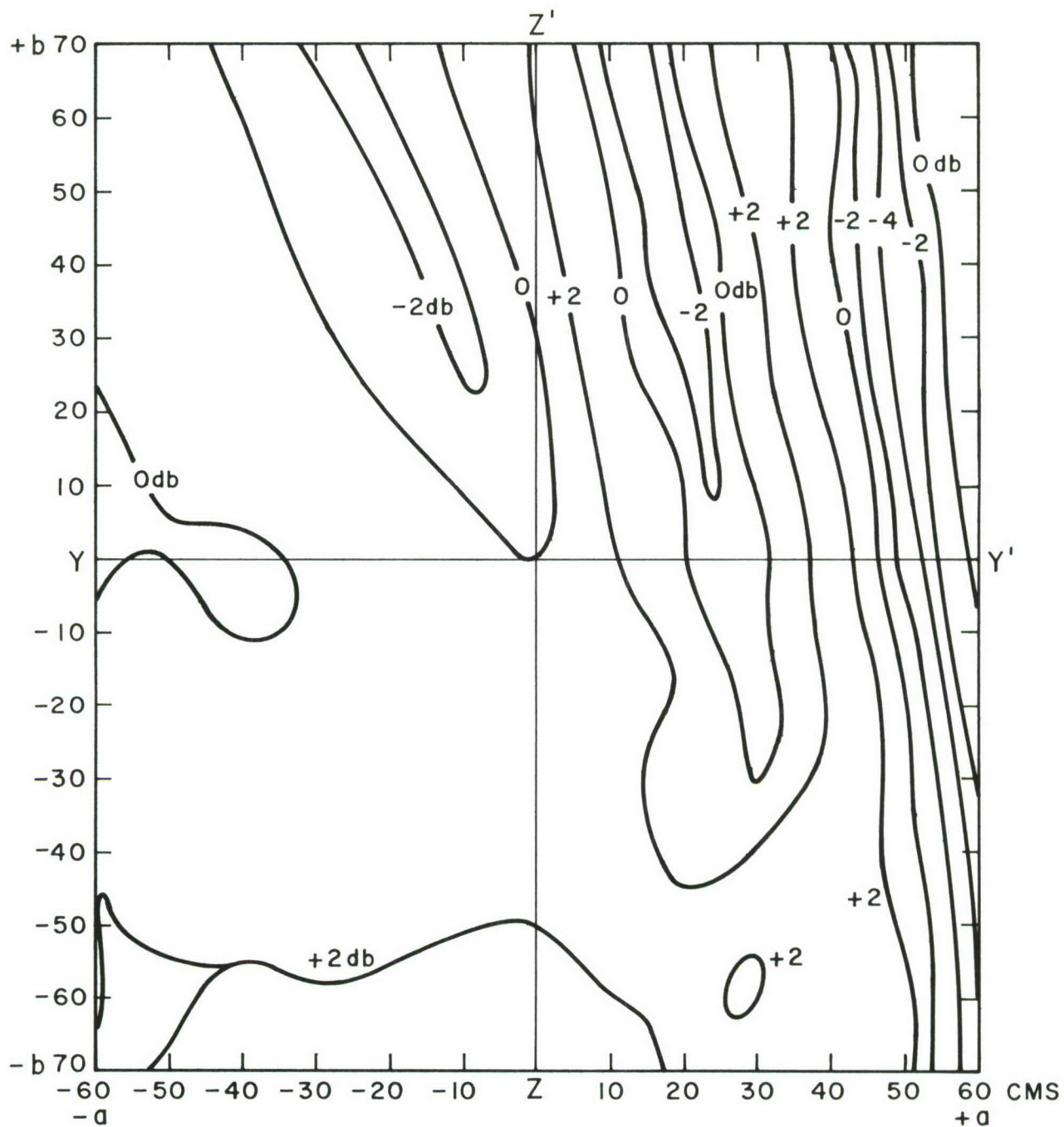
$$\alpha = 45^\circ, \beta = 0^\circ, \Delta L = 6.1 \text{ db}, 1600 \text{ C/S}, K_a = 17.8, K_b = 22.2, D = 3 \text{ ft}$$


Figure 38. Pressure and Phase Distribution on Test Panel Under Semi-Anechoic Condition, 1/3 Octave-Band Noise Source with Center Frequency 1600 c/s, $\alpha = 45^\circ$, $\beta = 0^\circ$, $D = 3$ ft.

$\alpha = 90^\circ$, $\beta = 0^\circ$, $\Delta L = 9.1 \text{ db}$, 630 C/S , $Ka = 3.5$, $D = 9 \text{ ins.}$

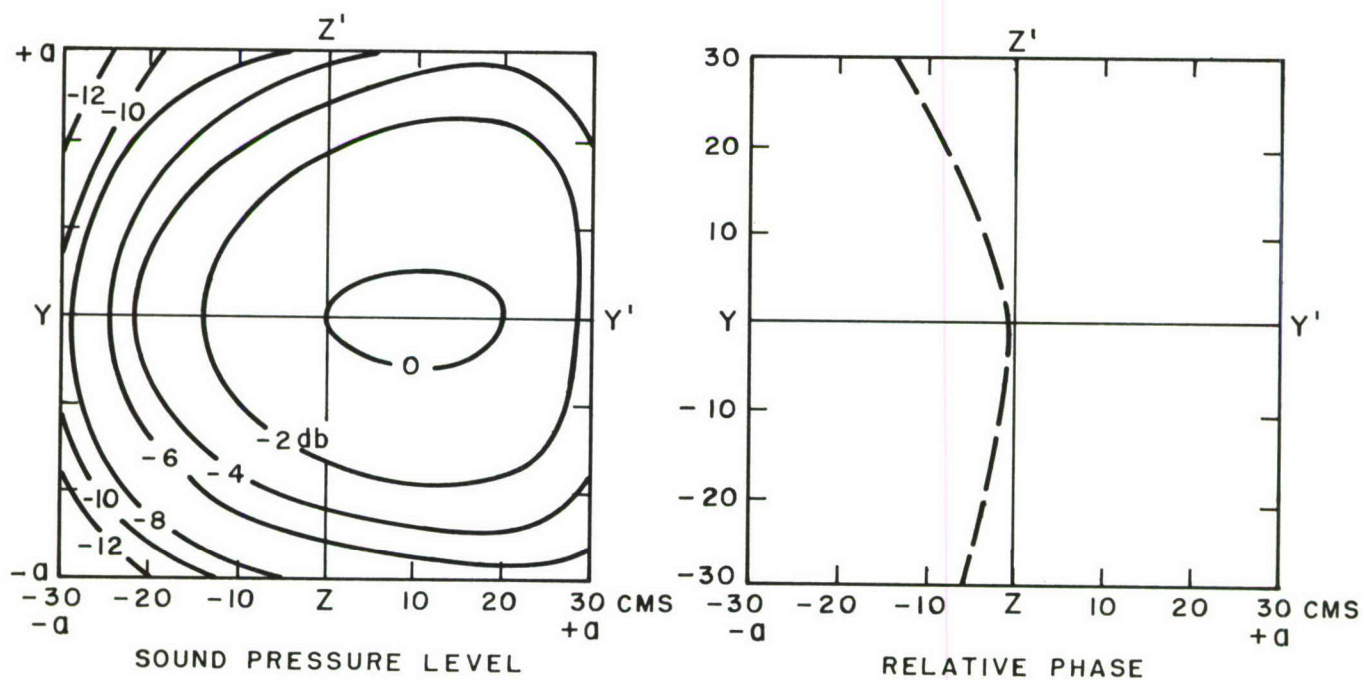


Figure 39. Pressure and Phase Distribution on Test Panel Under Semi-Anechoic Condition, 1/3 Octave-Band Noise Source with Center Frequency 630 c/s, $\alpha \approx 90^\circ$, $\beta = 0^\circ$, $D = 9 \text{ ins.}$

$\alpha = 90^\circ$, $\beta = 0^\circ$, $\Delta L = 6.8 \text{ db}$, 630 C/S, $Ka = 7.0$, $Kb = 8.8$, $D = 9 \text{ ins.}$

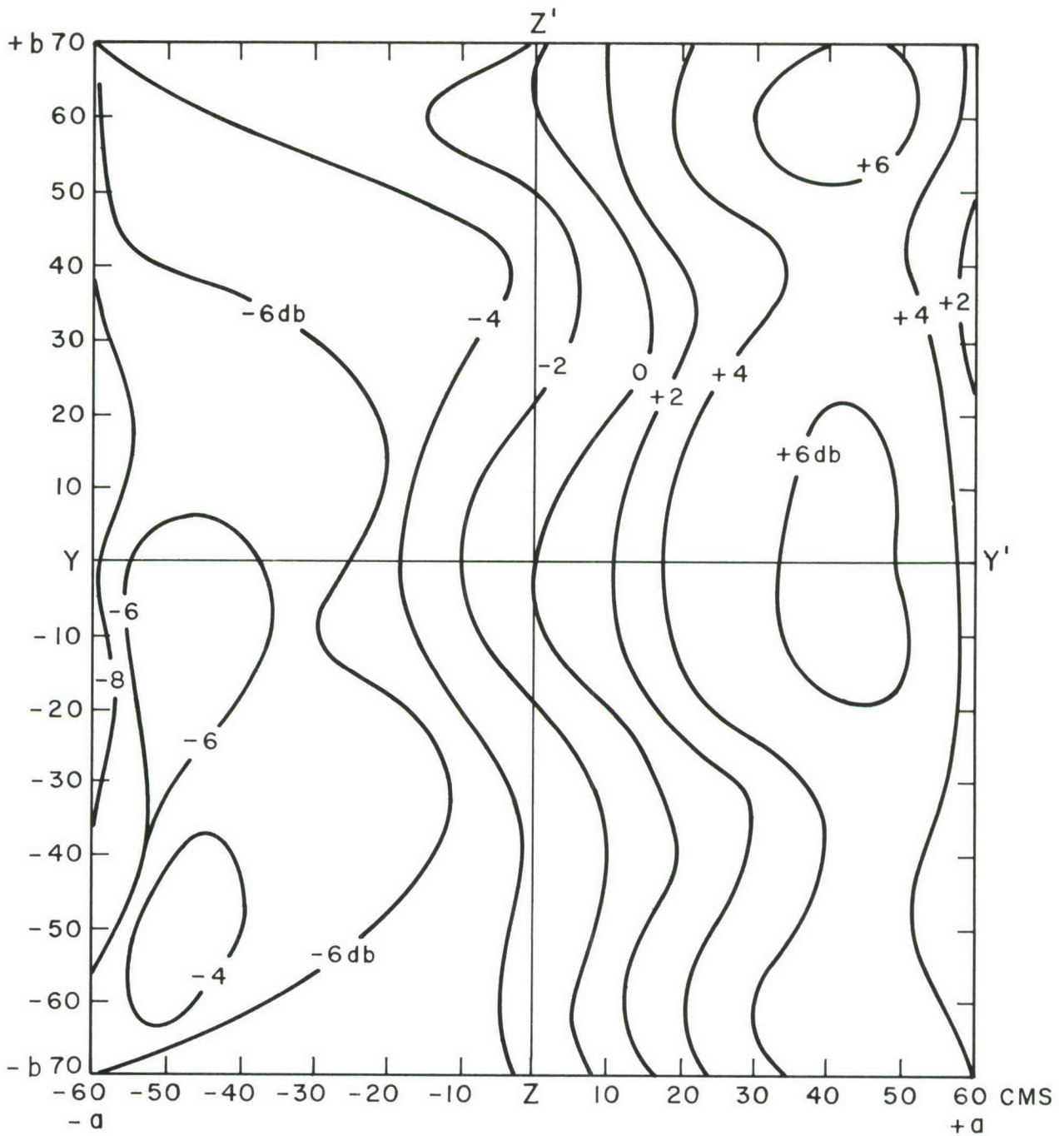


Figure 40. Pressure and Phase Distribution on Test Panel Under Semi-Anechoic Condition, 1/3 Octave-Band Noise Source with Center Frequency 630 c/s, $\alpha = 90^\circ$, $\beta = 0^\circ$, $D = 9 \text{ ins.}$

$\alpha = 45^\circ$, $\beta = 0^\circ$, $\Delta L = 7.2$ db, 630 C/S, $Ka = 7.0$, $Kb = 8.8$, $D = 9$ ins.

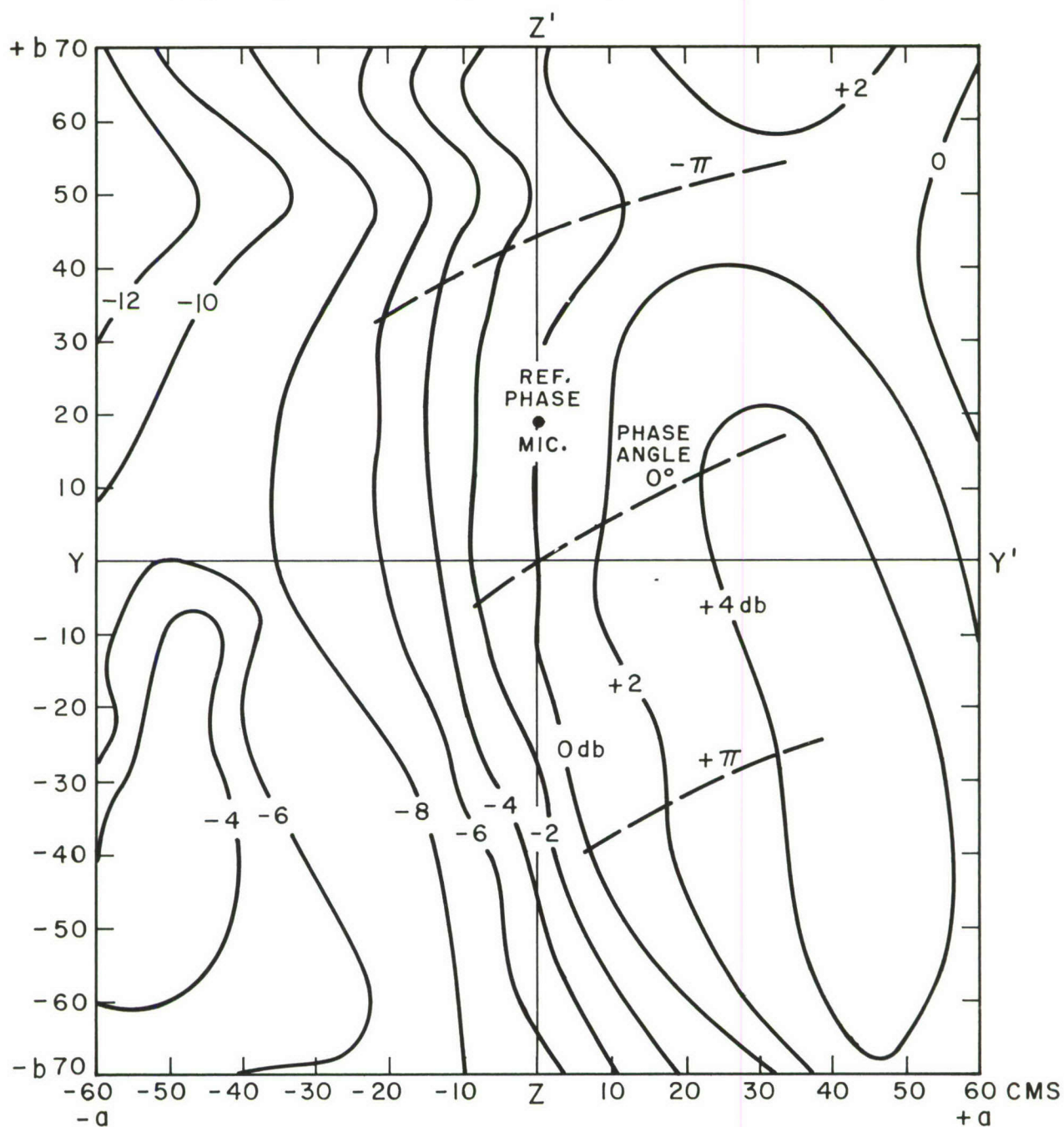


Figure 41. Pressure and Phase Distribution on Test Panel Under Semi-Anechoic Condition, 1/3 Octave-Band Noise Source with Center Frequency 630 c/s, $\alpha \approx 45^\circ$, $\beta = 0^\circ$, $D \approx 9$ ins.

$\alpha = 45^\circ$, $\beta = 0^\circ$, $\Delta L = 6.2 \text{ db}$, 1600 C/S, $K_a = 17.8$, $K_b = 22.2$, $D = 9 \text{ ins.}$

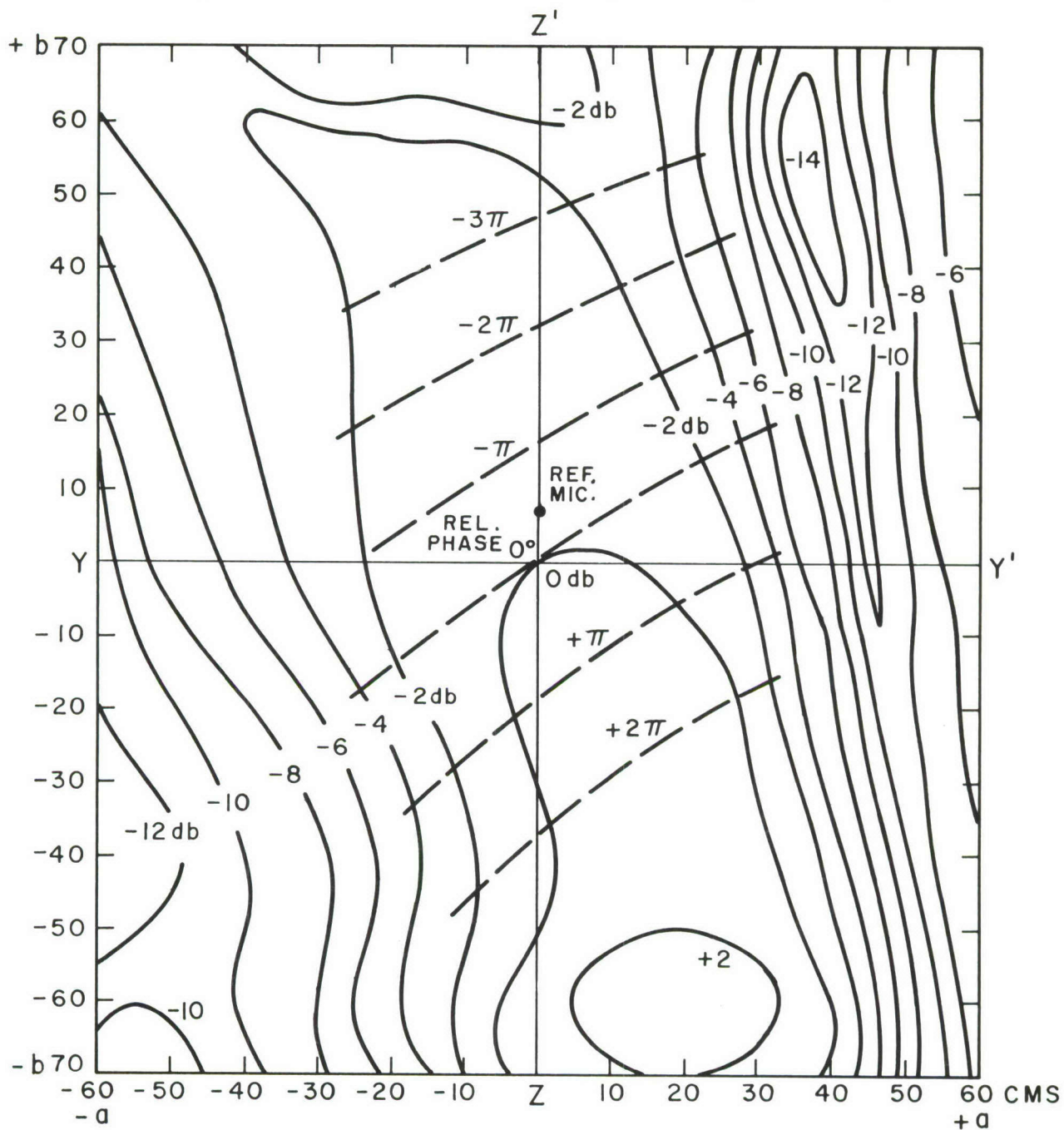


Figure 42. Pressure and Phase Distribution on Test Panel Under Semi-Anechoic Condition, 1/3 Octave-Band Noise Source with Center Frequency 1600 c/s, $\alpha = 45^\circ$, $\beta = 0^\circ$, $D = 9 \text{ ins.}$

$\alpha = 45^\circ$, $\beta = 0^\circ$, $\Delta L = 5.5 \text{ db}$, 630 C/S , $Ka = 7.0$, $Kb = 8.8$, $D = 3 \text{ ft.}$

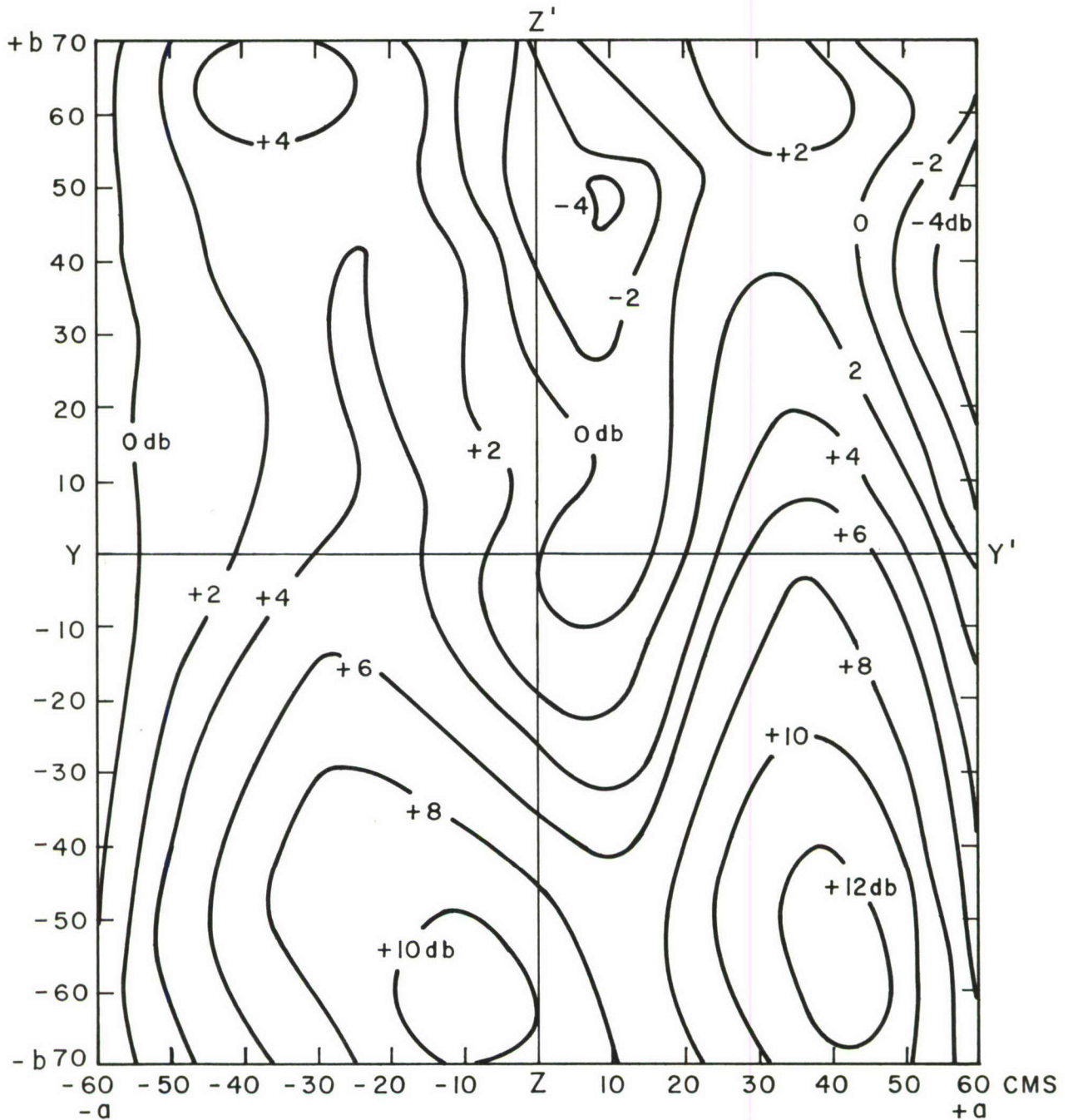


Figure 43. Pressure and Phase Distribution on Test Panel Under Semi-Anechoic Condition, Coherent 1/3 Octave-Band Noise Sources S_1 , S_2 , S_3 with Center Frequency 630 c/s, $\alpha = 45^\circ$, $\beta \approx 0^\circ$, $D \approx 3 \text{ ft.}$

$\alpha = 90^\circ$, $\beta = 0^\circ$, $\Delta L = 7.2 \text{ db}$, 630 C/S, $K_a = 7.0$, $K_b = 8.8$, $D = 9 \text{ ins.}$

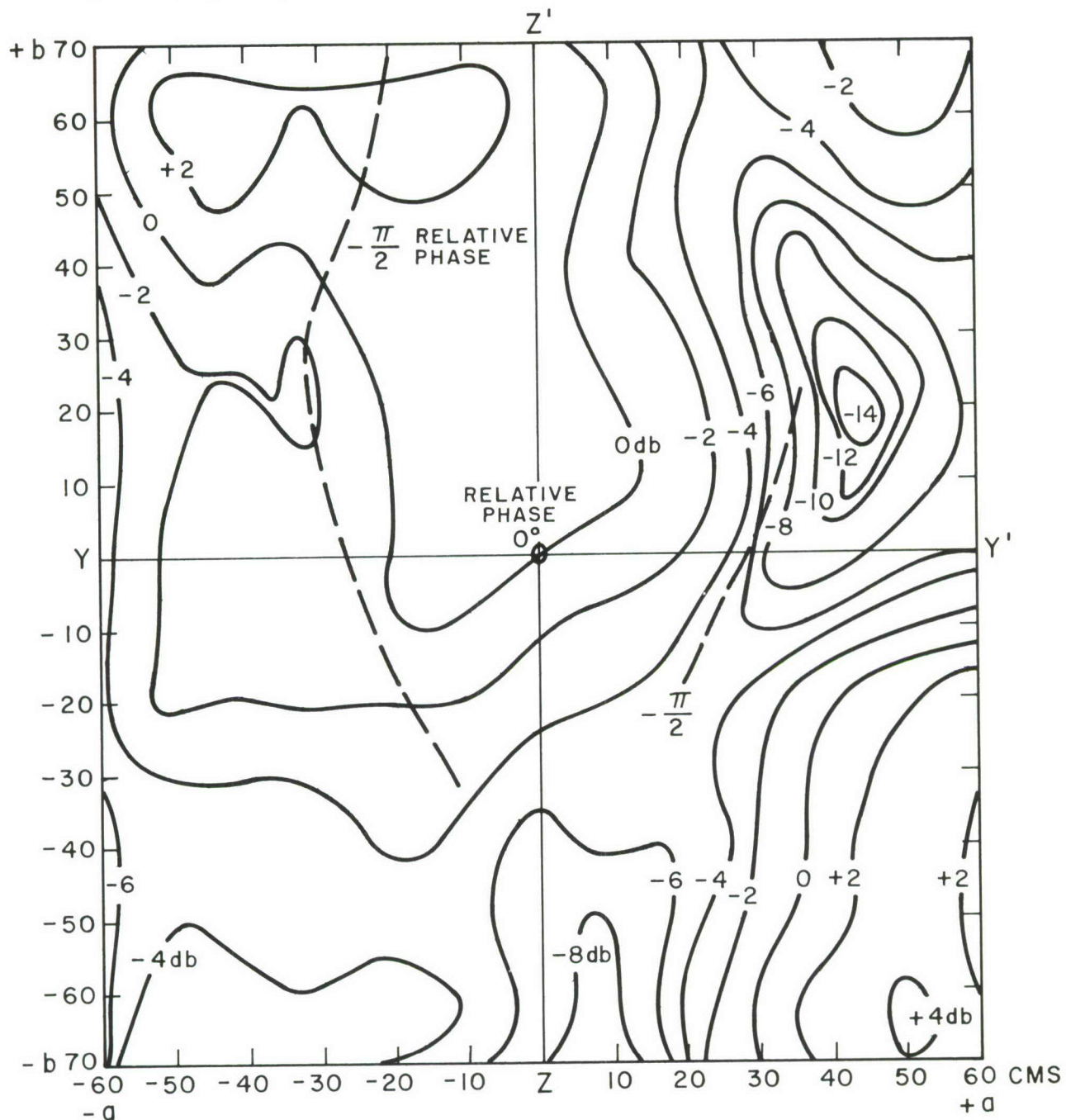


Figure 44. Pressure and Phase Distribution on Test Panel Under Semi-Anechoic Condition, Coherent $1/3$ Octave-Band Noise Sources S_1, S_2, S_3 with Center Frequency 630 c/s, $\alpha = 90^\circ$, $\beta = 0^\circ$, $D = 9 \text{ ins.}$

$\alpha=45^\circ$, $\beta=0^\circ$, $\Delta L=7.1\text{ db}$, 630 C/S, $K_a=7.0$, $K_b=8.8$, $D=9\text{ ins.}$

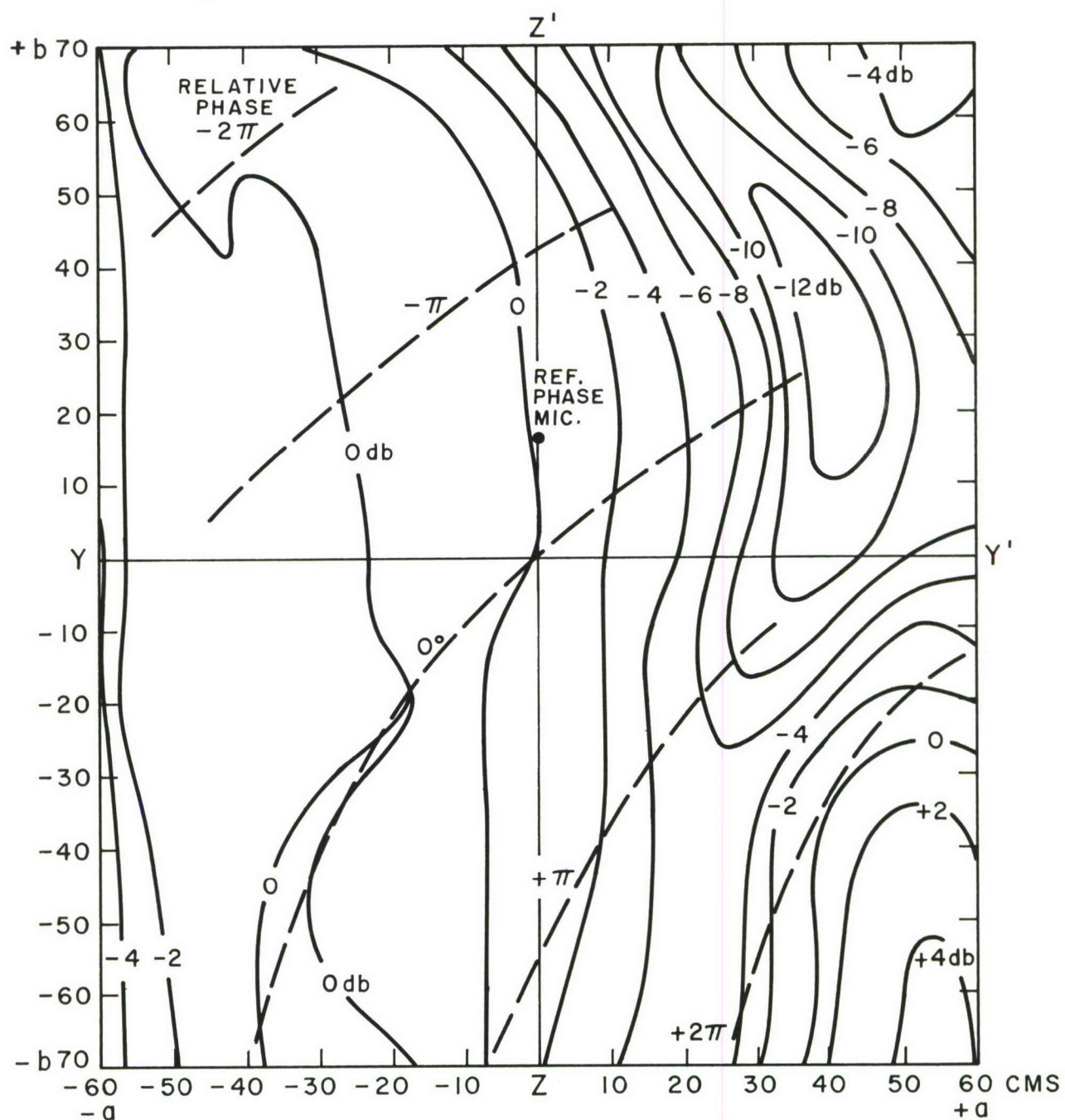
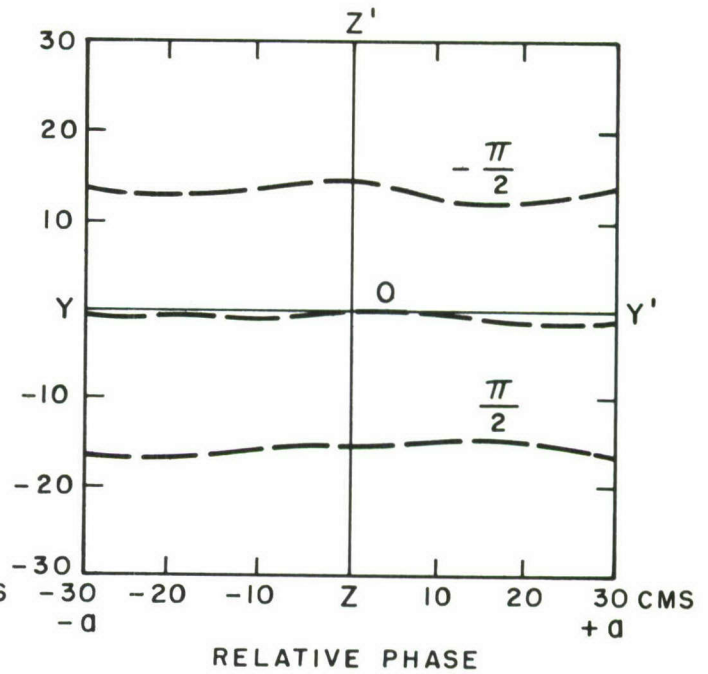
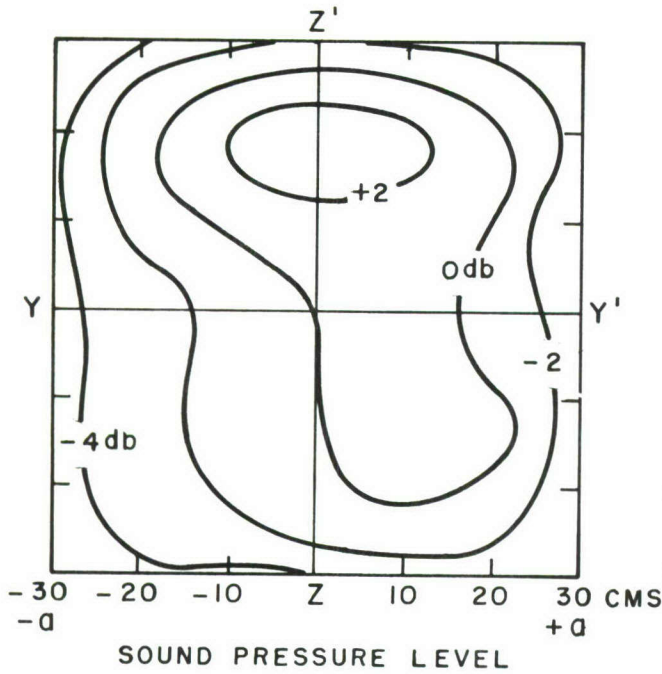


Figure 45. Pressure and Phase Distribution on Test Panel Under Semi-Anechoic Condition, Coherent 1/3 Octave-Band Noise Sources S_1 , S_2 , S_3 with Center Frequency 630 c/s, $\alpha = 45^\circ$, $\beta = 0^\circ$, $D = 9\text{ ins.}$

A 630 C/S, $Ka = 3.5$, $D = 3$ ft

$\alpha = 45^\circ$, $\beta = 0^\circ$, $\Delta L = 5.5$ db

$\alpha = 45^\circ$, $\beta = 0^\circ$



B 630 C/S, $Ka = 3.5$, $D = 3$ ft

$\alpha = 45^\circ$, $\beta = 0^\circ$, $\Delta L = 5.7$ db

$\alpha = 45^\circ$, $\beta = 0^\circ$

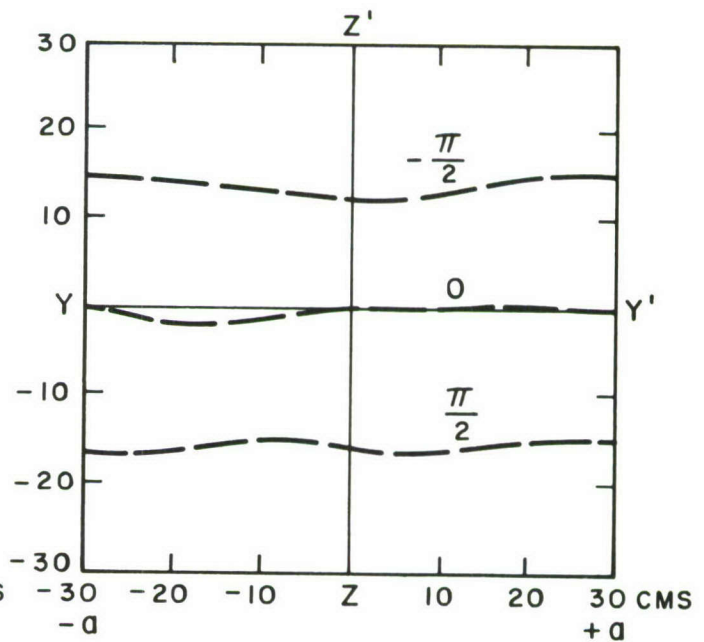
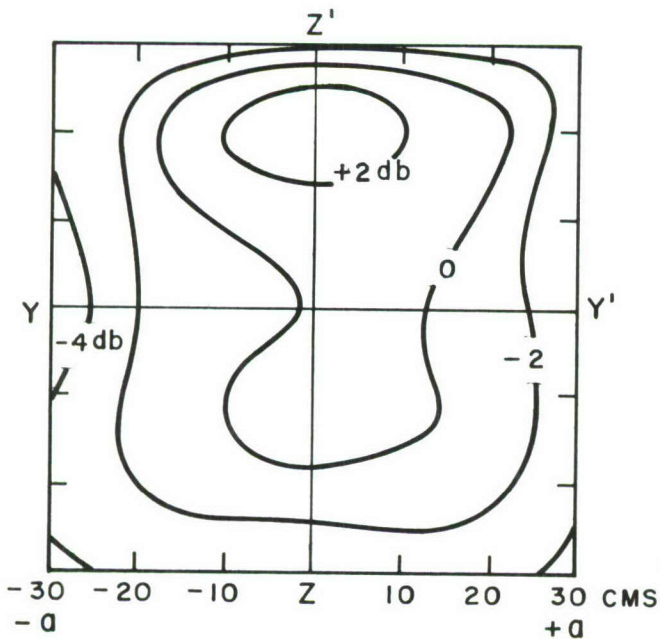


Figure 46. Pressure and Phase Distribution on Test Panel Under Semi-Anechoic Condition, 1/3 Octave-Band Noise Source with Center Frequency 630 c/s, $\alpha = 45^\circ$, $\beta = 0^\circ$, One and Two Layers Absorbent, $D = 3$ ft.

$\alpha = 45^\circ$, $\beta = 0^\circ$, $\Delta L = 6.0 \text{ db}$, 630 C/S, $K_a = 7.0$, $K_b = 8.8$, $D = 3 \text{ ft}$

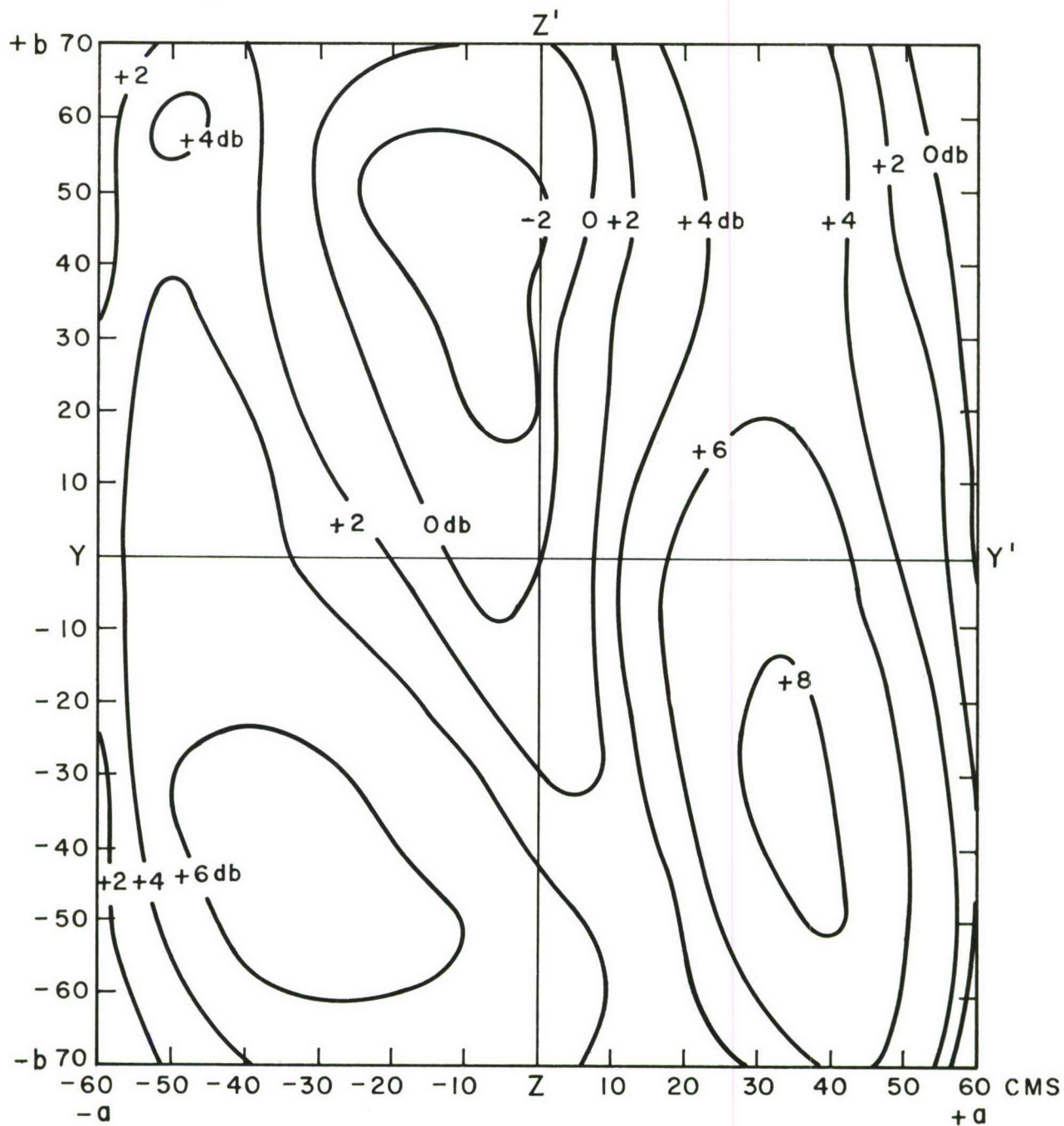


Figure 47. Pressure and Phase Distribution on Test Panel Under Semi-Anechoic Condition, 1/3 Octave-Band Noise Source with Center Frequency 630 c/s, $\alpha = 45^\circ$, $\beta = 0^\circ$, One Layer Absorbent, $D = 3 \text{ ft}$.

$\alpha = 45^\circ$, $\beta = 0^\circ$, $\Delta L = 5.3$ db, 630 C/S, $K_a = 7.0$, $K_b = 8.8$, $D = 3$ ft

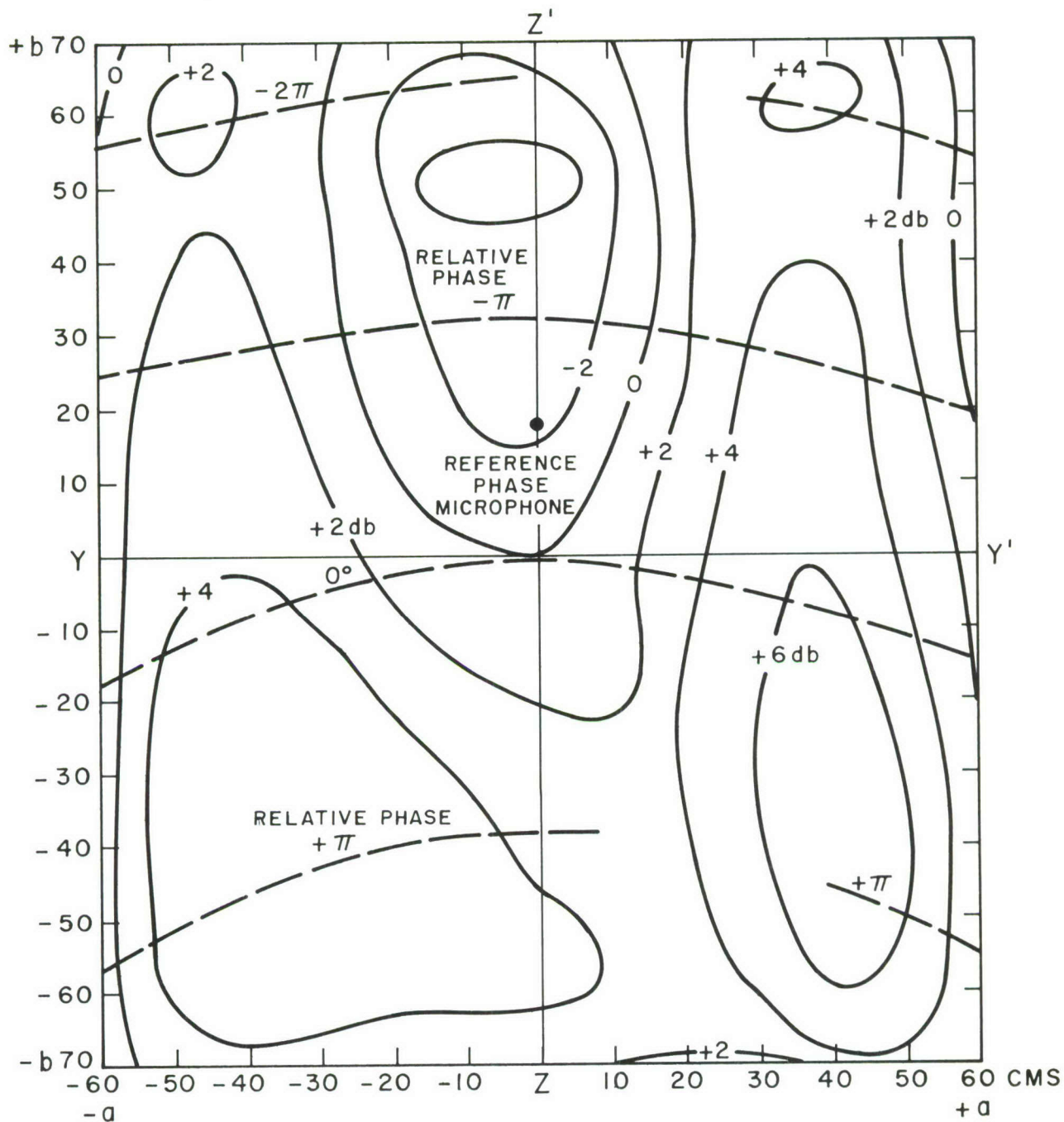


Figure 48. Pressure and Phase Distribution on Test Panel Under Semi-Anechoic Condition, 1/3 Octave-Band Noise Source with Center Frequency 630 c/s, $\alpha \approx 45^\circ$, $\beta \approx 0^\circ$, Two Layer Absorbent, $D \approx 3$ ft.

$\alpha = 45^\circ$, $\beta = 0^\circ$, $\Delta L = 5.5 \text{ db}$, 630 C/S, $K_a = 7.0$, $K_b = 8.8$, $D = 3 \text{ ft}$

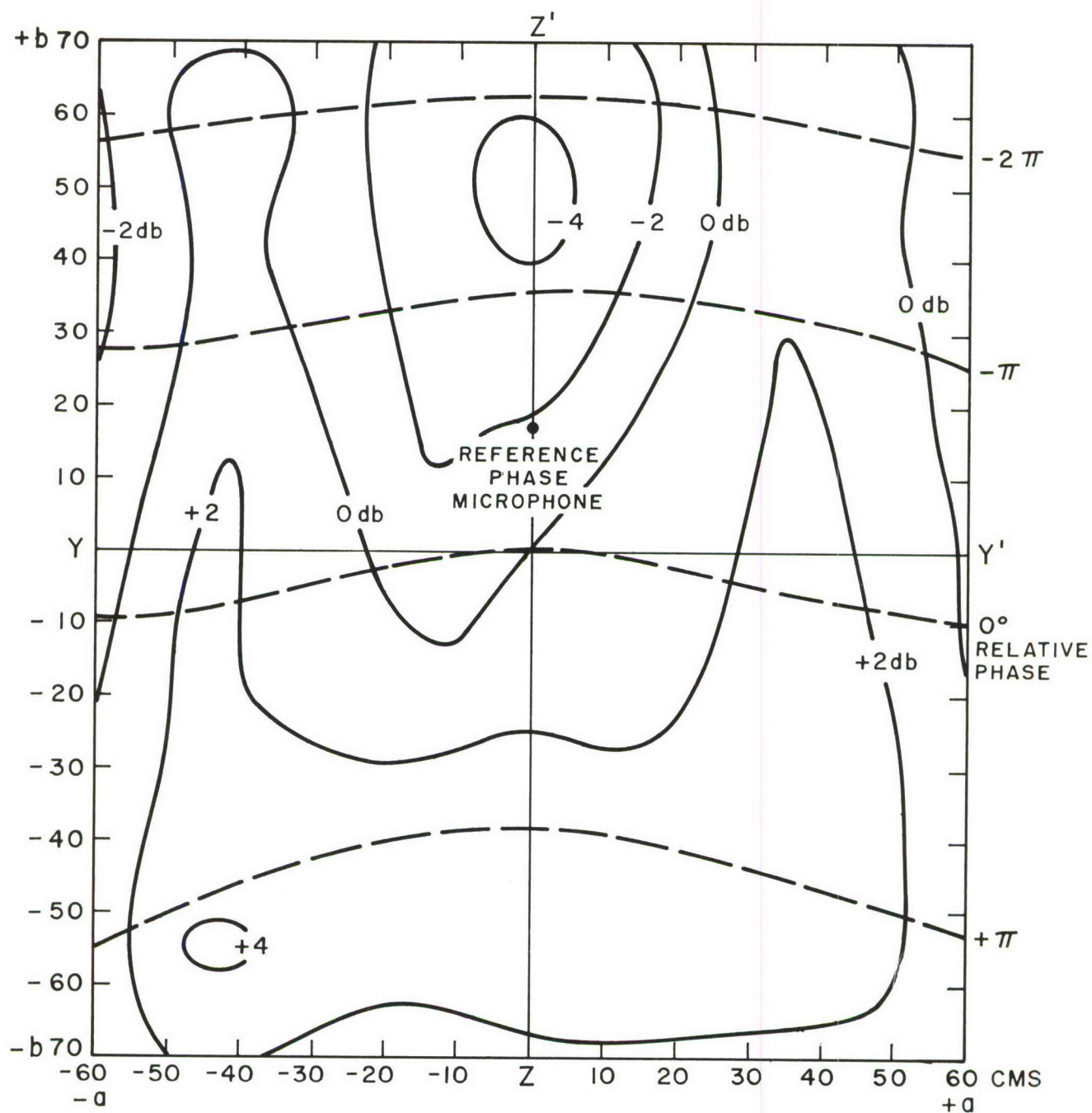


Figure 49. Pressure and Phase Distribution on Test Panel Under Semi-Anechoic Condition, 1/3 Octave-Band Noise Source with Center Frequency 630 c/s, $\alpha = 45^\circ$, $\beta = 0^\circ$, Three Layer Absorbent, $D = 3 \text{ ft}$.

APPENDIX A

SUMMATION OF COHERENT AND INCOHERENT SIGNALS

If we have two signals $G_1(t)$, $G_2(t)$ and they are independent of each other, they are said to be incoherent. If, however, information from one signal can be used to obtain some information about the other signal, the signals are said to be at least partially coherent.

Assuming that linearity holds, we may algebraically add these signals to obtain the quadratic content which will be proportional to the energy

$$\int [G_1(t) + G_2(t)]^2 dt = \int ([G_1(t)]^2 + [G_2(t)]^2) dt + \int 2 G_1(t) G_2(t) dt \quad (A1)$$

of the combined signal. It may be shown (Ref. 19) that if the signals are indeed incoherent, the latter term reduces to zero, i.e.

$$\int [G_1(t) + G_2(t)]^2 dt = \int ([G_1(t)]^2 + [G_2(t)]^2) dt \quad (A2)$$

If we operate two sound sources, A and B, at the same frequency, f , then at some point P in space, the resultant pressure will be

$$p = p_A e^{-j(kr + ct + \Phi)} + p_B e^{-j(kr + ct)} \quad (A3)$$

assuming that $PA = PB = r$, Φ is the phase difference between the two signals at P and p_A , p_B are the pressure amplitudes of the signals at P produced by sources A and B respectively.

The RMS pressure at P given by

$$p_r = \left[\frac{1}{T} \int_0^T p^2 dt \right]^{1/2} = \left[\frac{1}{T} \int_0^T (p_A e^{-j(kr + ct + \Phi)} + p_B e^{-j(kr + ct)})^2 dt \right]^{1/2} \quad (A4)$$

$$\begin{aligned}
p_r = & \left[\frac{1}{T} \int_0^T \left(\left[p_A e^{-j(kr + ct + \Phi)} \right]^2 + \left[p_B e^{-j(kr + ct)} \right]^2 \right) dt \right. \\
& \left. + \frac{1}{T} \int \left[2 p_A p_B e^{-j(kr + ct + \Phi)} e^{-j(kr + ct)} \right] dt \right]^{1/2}
\end{aligned} \tag{A5}$$

Since we have stated conditions for coherence, it follows that

$$p_r = \left(\frac{p_A^2}{2} + \frac{p_B^2}{2} + p_A p_B \cos \Phi \right)^{1/2} \tag{A6}$$

Now the RMS values of the signals at P are $p_A/\sqrt{2}$ and $p_B/\sqrt{2}$ which we call P_A, P_B . So

$$p_r = (P_A^2 + P_B^2 + 2 P_A P_B \cos \Phi)^{1/2} \tag{A7}$$

If these signals were completely incoherent, for example, two incoherent narrow band noise signals, the following would hold,

$$p_r = (P_A^2 + P_B^2)^{1/2} \tag{A8}$$

since in this case the long-time average of $2 P_A P_B \cos \Phi$ is zero.

"ACOUSTIC ENVIRONMENTS IN THE ASD SONIC FATIGUE FACILITY"

by

David F. Pernet and Franklin G. Tyzzer
IIT Research Institute

Paper presented at Institute of Environmental Sciences Technical Meeting;
Philadelphia, 13-15 April 1964

ABSTRACT

The problems encountered in meeting the acoustical requirements desired in the ASD sonic fatigue test facility are presented along with a discussion of the properties of the removable anechoic treatment. The extreme versatility of this facility enables an infinity of acoustic environments to be produced, but simultaneously creates problems in analysis and control of these environments. Acoustic environments have been analyzed, as a result of both theoretical and model studies, with regard to spatial distribution and correlation of sound pressure in terms of the significant parameters. These parameters involve source operating conditions (e.g. number, distribution, and coherence between sources in particular frequency bands), the acoustic environment in the facility (e.g. reverberant or semi-anechoic), as well as the presence or absence of test structures. In addition methods of modifying the environment in localized areas by means of introducing acoustic field shaping devices into the facility are reviewed.

(Supported by Sonics Branch, Aeronautical Systems Division)

ACOUSTIC ENVIRONMENTS IN THE ASD SONIC FATIGUE FACILITY

By: David F. Pernet and Franklin G. Tyzzer, IIT Research Institute



D. F. Pernet



F. G. Tyzzer

David F. Pernet received his B.Sc. in physics in 1959 and his Ph.D. in 1963 from the University of Southampton, England. His thesis subject was acoustic filter performance under high speed flow conditions. Since joining IITRI his interests have included jet noise and acoustic modeling studies.

Franklin G. Tyzzer has spent over 30 years in physics research since receiving his B.S. in electrical engineering from Massachusetts Institute of Technology specializing in acoustic and vibration problems. He has authored many papers in wide areas of his field and his current interests include architectural acoustics, noise and vibration control, and studies of intense sound.

INTRODUCTION

The ASD Sonic Fatigue Facility will serve a dual purpose. Firstly it will provide information on the fragility levels of structures, and secondly it will make possible the proof-testing of final design structures. The facility which has been described in detail by Kolb and Rogers (Ref. 1) was designed as a tool for investigating the effects of acoustic excitation on structures of flight vehicles and of electronic and power equipment. It consists of a test chamber 70 by 56 by 42 ft in size with a volume of approximately 165,000 ft³. Acoustic power is provided by a bank of fixed sirens with a maximum acoustic power output of 10⁶ watts, and movable sirens with a maximum acoustic power output of 90,000 watts. By means of an acoustical lining with removable and collapsible elements to be described later, the facility is capable of being operated under either progressive wave or diffuse field conditions. These two extreme methods of operation are particularly significant with respect to service environments. Fields of interest which are classified under the progressive type would include the fields on the exterior surfaces of planes, missiles, or other flight vehicles. These fields result from combinations of the following sources which produce pressure fluctuations; jet or rocket engines sources, and aerodynamic noise sources in all their various forms. Diffuse-type fields would include those encountered in the interior spaces of flight vehicles or in missile silos. The pressure fluctuations which result from either jet or rocket engine noise and several of the various aerodynamic noise sources are very similar. Characteristically both

types possess broad-band spectral distribution and may be of very intense level. However, there are other parameters of sound fields whose values are characteristic of the type of source producing the sound field. This raises the question as to which are the most important parameters which must be reproduced in any service field simulation. Ideally any fatigue facility should reproduce all of the characteristic parameters of a service field. To attain such a goal is beyond the present state of the art and consequently it is not expected that the facility can reproduce all the parameters of a service field but only that it will simulate the most important of these. The most significant parameters would certainly appear to include the spatial power spectral distribution as well as the temporal and spatial correlation of the field. Thus, if a service field can be specified in terms of its most important parameters, such as those mentioned above, the objective in the service field simulation would be that of producing a field possessing as good a reproduction of those parameters as possible. This still might appear a formidable problem but one must recognize that it is not necessary to simulate a service field over a complete volume in space so long as the simulation occurs adjacent to the surface of the test structure. It is, of course, necessary to know whether the sound field parameters are to be simulated in the presence or absence of the test structure. In most cases, a service field will be specified at the surface of a test structure but there may be other instances in which the characteristics of the field are known in the absence of the test structure, for example the predicted or measured environment in a space vehicle in which a structure is to be located.

Assuming that a service field has been specified in terms of its important parameters it is necessary to simulate this field in the ASD facility and in order to achieve this with the minimum of operational effort and in the most economical manner it was necessary to make an analysis of the acoustical environments which could be produced in the facility. This study is currently being carried out at IIT Research Institute and it is the purpose of this paper to outline this study and its results. The solutions to the problems encountered in meeting the requirement of a removable anechoic treatment for the facility are also discussed.

ACOUSTICAL TREATMENT OF THE ASD FACILITY

Since the facility is to be operated in either a reverberant or progressive wave condition, a sound absorbing lining was designed by the IIT Research Institute to cover the walls and ceiling (Ref. 2). Sound absorption on the floor was considered impractical except in local areas. The design of the anechoic wall and ceiling treatment for the facility not only involved rather severe acoustical requirements but also necessitated the choice of materials and supporting structures to satisfy non-acoustical requirements, such as low cost, collapsibility, and durability under extremes of

temperature, humidity, and sound pressure level. The desired acoustical characteristic was a normal incidence absorption greater than 96 per cent for a frequency range between 20 and 10,000 c/s at sound pressure levels as high as 160 db. The low frequency limit for 96 per cent absorption was approximately 50 cps since the maximum thickness of the treatment was 6 ft. The materials and supporting structures to be used had to be able to tolerate relative humidity close to 100 per cent and temperatures up to 250°F; they had to have a total surface density less than 10 lbs/ft²; they had to be collapsible and able to be stored when the facility is used as a reverberant space; and they had to be sufficiently durable to withstand normal handling and the effects of the intense sound. The cost of the treatment was also an important factor and required the use of commercially available materials of fairly low cost.

Absorbing treatments for anechoic rooms for low intensity sound have generally consisted of wedges of absorbing material. Because the acoustical properties of absorbing materials vary with sound level in the range of above 130 to 140 db it was necessary to test the absorbing treatment at high levels. However, wedges do not lend themselves readily to testing at high intensities over wide frequency ranges. This is because when a wedge is inserted into an impedance tube for the normal incidence absorption measurements the width of the tube which must accommodate the wedge imposes an upper limit on the frequency range over which the test can be made as well as creating a difficulty in producing sufficiently high levels in the tube. In addition, difficulties were anticipated in designing and constructing collapsible wedges. Therefore, it was decided to develop a treatment using spaced layers of absorbing material. The normal incidence absorption coefficients can be measured over wide ranges of frequencies at higher intensity because narrower impedance tubes may be employed for this type of treatment, the absorption coefficient being independent of area. In addition, by using irregular layer spacings, the absorption at non-normal incidence can be made more satisfactory. This will overcome the phenomena that occurs for a single layer, or a regularly spaced layer treatment that the absorption is considerably reduced at certain frequencies and angles of incidence where the layer spacing divided by the cosine of the angle of incidence (with respect to normal incidence) is equal to $n\lambda/2$.

In order to test the layer treatments a high intensity test facility was developed which consisted of three impedance tubes covering the frequency ranges 50 c/s to 7,000 c/s and producing levels of 160 db. Some 25 different layer systems were designed and tested. In addition, limited life tests at 160 db levels eliminated many materials for this high intensity application. Etched polyurethane foam (skeletal polyurethane) and fine wire mesh were not damaged in such life tests. As a result of these tests a treatment was recommended which consisted of six layers of polyurethane foam supported by open mesh wire screen with spacings between layers ranging from 7 to 17 inches. Figure 1 shows the normal incidence absorption of the recommended treatment and a diagram showing the layer spacings and DC resistance values. The

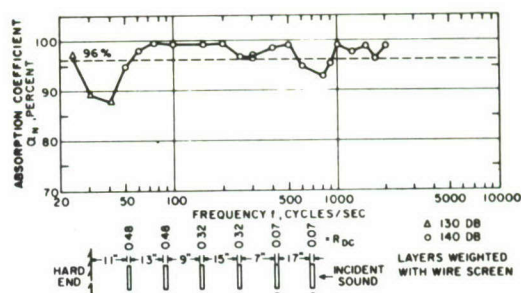


Fig. 1 Normal Incidence Absorption Coefficient for the Recommended Spaced Layer Treatment, the Spacings and DC Resistance Values of the Polyurethane Layers. Thickness of layers 1 and 2 is 1 1/2 ins, 3 and 4 is 1 in, and 5 and 6 is 1/2 ins.

resistance of layers close to the hard end (room surface) was made greater than that of layers distant from the hard end by using thicker and more dense material. The measurements for Fig. 1 were made at a sound pressure level of 140 db in most of the frequency ranges. Tests at higher sound pressure levels (up to 160 db) showed that the absorption was nearly the same at this level. Motion of layer material, caused by acoustic excitation at low frequency, was prevented by mounting the low surface density material between wire screens. This allowed the layers of the ceiling treatment to be suspended by cables, so that they could be lowered to the floor and removed enabling the room to be used under diffuse field conditions. The layers for the wall treatment are supported as flexible curtains by means of a weighted nylon net. For diffuse field conditions, the curtains are raised in a looped condition and are stored in the upper portion of the walls. The wall and ceiling treatments are now being fabricated and installed.

APPROACH TO ANALYSIS OF ACOUSTICAL ENVIRONMENT OBTAINABLE IN THE ASD FACILITY

Our approach to this analysis was the following. In order that the siren assembly can produce a broad-band noise such as is desired in most service fields it will be necessary for the assembly to be frequency distributed. Either one or a small number of sirens would contribute energy to a narrow segment of a band operating as either a discrete frequency source or a source modulated over a narrow band. Several such groupings could be used, covering different segments of a band and in this manner a broad-band source would be obtained. Thus, the aim of our analysis was to consider what acoustic fields could be produced when a small number of sirens was operated at a given frequency. This analysis was carried out at a number of frequencies in order to obtain representative results for the frequency range of interest. Our choice of a maximum of three siren sources operating at a single frequency would provide eight sources at different frequencies which might be spread over an octave band and their output could be considered a fair simulation of a band of noise. The analytical treatment was that of determining the spatial distribution of pressure in an anechoic room for configurations of one, two, and three sources operating in phase at the same frequency, for various

frequency values. Under the reverberant room conditions the distribution in the near and far field was established. These analyses then enabled the fields possible in the facility in the absence of any test structure to be established. The experimental study has considered what types of field exist on the surface of test structures exposed to fields in both an anechoic and a semi-anechoic condition. No experimental study under reverberant conditions has been made.

ACOUSTICAL ENVIRONMENT IN THE REVERBERANT CONDITION

The facility has an untreated area of approximately 16,600 sq ft. If we assume a typical average random incidence absorption coefficient of 2 per cent for concrete, the absorption in sabins is 332. The reverberation time for the facility in an untreated condition is approximately 20.7 sec as determined from the conventional formula

$$T = \frac{0.049V}{A} \quad (1)$$

Preliminary reverberation time measurement at low frequencies (250 - 450 c/s) indicates values between 20 and 22 secs. At higher frequencies the reverberation time is considerably lowered due to air absorption effects being 15 sec at 1 kc/s and 6 secs at 4 kc/s.

The absorption of the collapsed wall treatment will lower the reverberation times. Using an estimated absorption of about 3,200 sabins for the room with collapsed treatment, the reverberation time was calculated as about 2.2 sec. For this estimation of absorption the direct level of sound from a nondirectional source is at least 9 db below the total sound level at source distances greater than 20 ft. Diffuse field conditions will thus be obtained over most of the volume of the room.

The design goal for the reverberation sound field was 160 db re 0.0002 dynes/cm². More information on the absorption of the collapsed wall lining and the output of the sirens is required before a reliable estimate of the sound pressure can be made.

ANALYSIS OF THE FIELD UNDER ANECHOIC CONDITIONS PRODUCED BY SMALL NUMBERS OF SOURCES OPERATING AT IDENTICAL FREQUENCIES AND IN PHASE

In calculating the sound field we consider only three different source arrays; those of a single source; those of two adjacent sources; and those of three adjacent sources arranged on three corners of a square. We compute only the far-field distribution of these source arrays because, (1) the far-field exists to within only a very short distance from the array in the facility, and (2) the computation is relatively simple to evaluate. Accepted criteria (Ref. 3) which must be fulfilled are that if r is the limiting distance of the far-field to the source array then

$$r > \frac{\lambda}{6} \quad \text{and} \quad r > \frac{2b^2}{\lambda} \quad (2)$$

where b is the extent of the array. For the above mentioned arrays in the facility, b will be 2.5 ft. For the frequency range of interest, i.e. 50 to 1000 c/s, λ ranges from 20 to 1 ft. These criteria imply that, in the worst condition of operating the facility at 1000 c/s, the far-field will extend to within twelve feet of the source array. At lower frequencies the far-field will extend even closer to the source array. Thus, for all practical purposes one can assume that the far-field extends over the whole volume of the facility. Using the symbols shown in Fig. 2 and neglecting phase, the

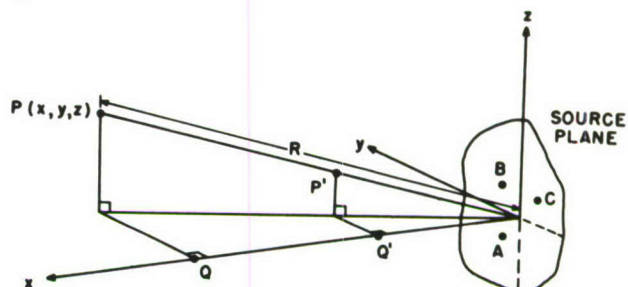


Fig. 2 Geometry for the Far-Field Distribution in a Plane Parallel to the Source Plane and Containing Point $P(x, y, z)$, Distance ' R ' from the Source System. A, B, and C represent three sources with spacing s arranged on three corners of a square.

following three expressions represent the pressure amplitude at a point $P(x, y, z)$ for cases of a single source A, a double source AB, and a triple source ABC.

$$p_A = \frac{p_0}{R} \quad (3)$$

$$p_{AB} = \frac{p_0}{R} \left[2 + 2 \cos \frac{ksz}{R} \right]^{1/2} \quad (4)$$

$$p_{ABC} = \frac{p_0}{R} \left[3 + 2 \left(\cos \frac{ksz}{R} + \cos \frac{kxy}{R} + \cos \frac{ks(z+y)}{R} \right) \right]^{1/2} \quad (5)$$

where p_0 represents the pressure amplitude at unit distance from a single source.

To obtain an idea of how these values vary over space, we have calculated these pressure distributions at frequencies of approximately 100, 200, and 400 c/s, over a plane, situated in the far-field at a distance of approximately 50 ft from the source system, parallel to the source plane. Because of the orientation of the fixed bank of sirens, this plane approximately represents a diagonal plane of the facility. Equal pressure contours plotted in Fig. 3 are plotted relative to the maximum pressure on the plane which occurs at a point on the plane perpendicular to the center of the array. These contours are obtained assuming that the individual sources are non-directional. However, if

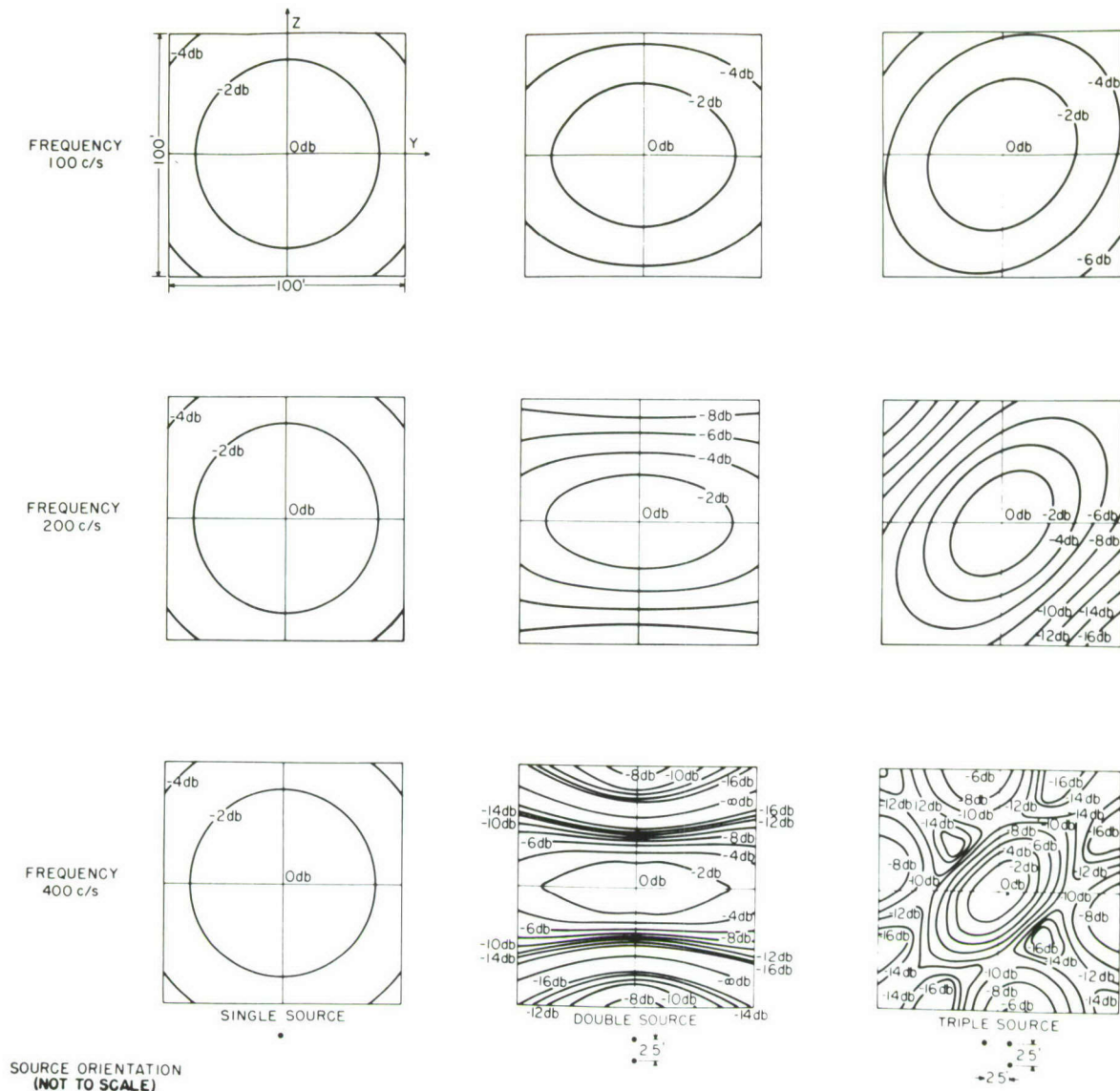


Fig. 3 Pressure Distribution on a 100 ft Square Plane, Parallel to the Source Plane and Located 50 ft from it, for Three Different Source Systems at Three Different Frequencies.

the directivity of the sources is known, it is a simple matter to adjust these contours. From the distribution in this plane it is possible to establish the pressure at any other point, P' , in the facility. With reference to Fig. 2 the pressure at P' relative to Q' will be the same as the pressure at P relative to Q from geometrical reasoning and the pressure at Q' relative to Q can be obtained from the inverse square law.

The value of knowing these distributions in the far-field is twofold. Firstly, it enables those regions to be defined in which the spatial distribution is (a) only changing gradually or not at all, and (b) changing rapidly. When a test object is placed in a region where there is an even distribution of pressure, the distribution existing on the surface of a structure can be predicted approximately by a method outlined later, the assumption being made that the source system can be considered as acting

as a single source with regard to the particular region of interest in the far-field. In regions where the rapid changes in spatial distribution occur in the field without the test panel, it may be anticipated that this will produce more complexity in distribution on a panel placed in this field. These complex distributions, however, can certainly be expected to be of interest in producing service field simulation.

EXPERIMENTAL MODEL STUDY OF THE ANECHOIC AND SEMI-ANECHOIC OPERATION OF THE FACILITY

A. Test Conditions for Model Study

The aim of this experimental study was to obtain generalized information on the types of sound fields which may exist at the surface of simulated test structures exposed to progressive waves.

The fields were to be studied as functions of the size of the structure, its location and orientation with respect to the sound source or sources as well as the number, distribution, and operating frequency of the sources and the degree of coherence existing between them. For this purpose the IITRI anechoic chamber was used as a model of the ASD facility in the progressive wave condition. Because of the difference in size between the IITRI and the ASD facility, a modelling technique was adopted and a scaling factor of $1/4$ was chosen for the study. Thus, all dimensions of the source system, test structure, and distances in the ASD facility were scaled down by this factor in the IITRI anechoic chamber. To preserve scaling similarity all frequencies of interest were scaled up by a factor of 4.

Because large test structures may be used in the ASD facility, it may not be possible to operate the room in a completely anechoic condition, which would involve lining the floor of the facility with absorbent treatment. Consequently our experimental study has also incorporated a semi-anechoic investigation. For this purpose one wall of the IITRI anechoic chamber was faced with a thick plywood surface which simulated the exposed concrete floor of the ASD facility. The reason for covering a wall rather than a floor was simply that of experimental convenience. The diagram of Fig. 4

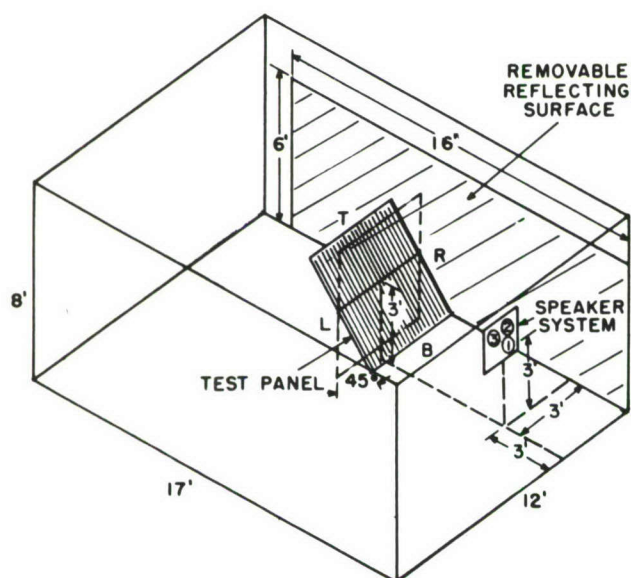


Fig. 4 Anechoic Chamber Used in Model Study. 4 x 5 ft test panel arranged at 45° to speaker system. (Dashed test panel outline corresponds to normal incidence orientation). Speaker system composed of 8 ins speakers with 10 ins center spacings.

shows the arrangement for measurements in the model study. For anechoic conditions, the wall, floor, and ceiling surfaces were covered with absorbing wedges and, for the semi-anechoic condition, a portion of one wall was covered with plywood panels to simulate the reflecting floor of the ASD room.

The model sources consisted of four 8-inch cone loudspeakers mounted in individual enclosures and arranged in a square array. This represented a good approximation to four adjacent sirens arranged in a square array in the ASD facility. The investigation was carried out at three frequencies; 200, 600, and 1800 c/s. These scaled frequencies are representative of an operating range in the ASD facility of approximately 50 - 450 c/s. The simulated test structures were two plywood panels of dimensions 4 by 5 ft and 2 by 2 ft, representing ASD test structures of 16 by 20 ft and 8 by 8 ft. These panels were mounted in frames which enabled the panels to be placed in any orientation to the source system. The center of the panels was always 6 ft from this source system representing a 24 ft distance in the ASD facility. The pressure distribution at the surface of a panel was explored in terms of the difference between the pressure measured at any point on the surface of the panel and the pressure at the same point when the panel was removed. In this manner the reflecting (strictly the diffracting) effect of the panel was determined. The exploration of the pressure distribution was conducted using a hand-held scanning microphone.

Relative phase distributions over the surface of the panel were obtained by comparing the output of the microphone to that of a fixed reference microphone by forming a Lissajou figure of the two outputs on an oscilloscope. If the sound source is sinusoidal in nature, it is expected that the phase determination can be made even with very large separation of the microphones, but using a $1/3$ octave band noise source, the determination cannot be expected to be made when the separations are excessive since the two microphones signals would be uncorrelated. This method of phase determination gives a qualitative indication of correlation between signals. Tests conducted by placing 2 microphones in a progressive wave field indicated that no phase determinations were possible when the separation of the microphone, in the direction of propagation, was greater than a distance of the order of the wavelength corresponding to the center frequency of the $1/3$ octave band. At three center frequencies, 200, 630, and 1600 c/s, these distances were of the order of $\lambda/2$, λ , and $3\lambda/2$ respectively.

In general, only three major orientations of panel were considered. These corresponded to normal incidence, grazing incidence, and 45° incidence of the sound. Initially the sound source, source 1 as shown in Fig. 4, was operated sinusoidally. But, because of interference effects caused by the presence of the operator, the true pressure distribution was difficult to obtain especially at the higher frequencies. Consequently, the sinusoidal signals were replaced by $1/3$ octave bands of noise with center frequencies 200, 630, and 1600 c/s. It was then found that the presence of the operator did not significantly disturb the pressure distributions on the panel. Good agreement was found between distributions obtained using $1/3$ octave band noise and pure tone sources when the latter's distribution was obtained with great care, as is shown in Fig. 5. These patterns were measured on a 2 ft by 2 ft panel at 60° incidence and are typical of comparisons between patterns for sinusoidal and $1/3$ octave band signals. The ΔP referred to in Fig. 5 represents the pressure change at the panel center. All

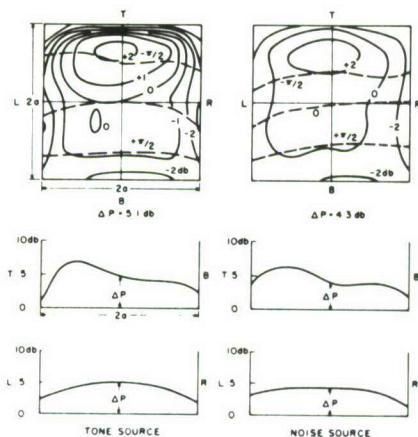


Fig. 5 Comparison of Pressure and Phase Distribution on a Test Panel of Dimensions '2a' Obtained Using a Tone Source and a 1/3 Octave Band Noise Source (Center Frequency = 630 c/s; $ka = 3.3$) Sound Incident at 60° ; ΔP Represents the Pressure Difference With and Without the Panel at the Position of the Panel Center.

other pressure distributions are relative to this value. The panel orientation in terms of L, T, R and B is illustrated in Fig. 4.

B. Single Source Under Anechoic Conditions

Distribution patterns of sound pressure level and relative phase obtained experimentally were of the type shown in Fig. 5. Their presentation is simplified in some cases by illustrating distributions along only the two principal axes of the panel as shown in the lower half of Fig. 5. Figure 6 shows such distributions of sound pressure level for various values of ka in the case of sound at normal incidence, and Fig. 7 shows distributions at 45° incidence. In order to illustrate diffraction effects, the sound pressure levels at each point are relative to the level in free space (without the panel). Thus the values shown in Figs. 6 and 7

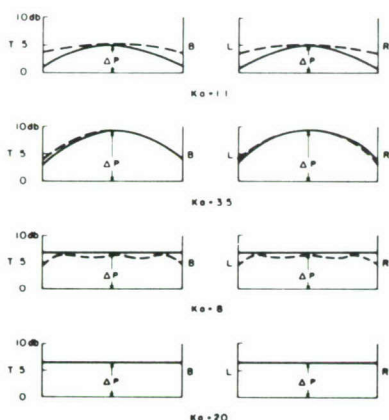


Fig. 6 Pressure Distribution on Test-Panels Normal to the Source, as Functions of ka , Compared to Calculated Values (Dashed Line) for Square Panels after Wiener.

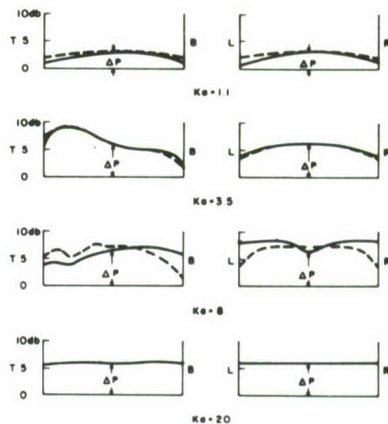


Fig. 7 Pressure Distribution on Test-Panels at 45° to the Source System, as Functions of ka , Compared to Calculated Values (Dashed Line) for Circular Disc Panels after Wiener.

differ from the measured values of the pressure level contours over the whole panel as illustrated in Fig. 5 since they have been "corrected" for spherical spreading effects. These "corrections" are small for normal incidence but are appreciable at 45° and grazing incidence.

It is noted that the distributions are not at all complicated. The pressure increase for large values of " ka " is uniform over the panel and tends to the 'pressure doubling' value of 6 db. The distributions for 1/3 octave band signals are compared in Figs. 6 and 7 with those predicted for plane wave incidence of pure tone signals by Wiener (Ref. 4) by an approximate calculation method for having the same angle of incidence and approximately the same values of ka . The predicted and observed distribution patterns are quite similar, although the observed increases in sound pressure level caused by the panel are for spherical propagation and the predicted increases are for plane wave propagation.

It is again noticed that for large ka values these corrected distributions are uniform across the panel. In addition it may be noted that, at intermediate ka values, pressure increases are observed which are well in excess of the pressure doubling value of 6 db. Phase determinations produced expected results, as shown in Fig. 5, and only the following brief comments need be made. In the cases of panels at normal incidence, concentric circular phase contours were obtained extending over the whole area of the panels. In the cases of 45° and grazing incidence, approximate circular arcs extending across the full area of the panel were found, similar to those shown in Fig. 5. The spatial separation of the contours agreed with calculated values.

In conclusion it may be said that the above described experimental model enables the distribution in pressure and phase to be determined on structures exposed to a single, 1/3 octave band source and the experimental results show good agreement with distributions calculated for a single source field having a discrete frequency equal to the center frequency of the 1/3 octave band.

C. Double and Treble Sources Under Anechoic Conditions

The aim of this part of the study was to repeat certain of the experimental determinations of pressure distributions on panels, replacing the previous single source with either a double or a treble source system. For the purpose of this paper, only representative experimental results are presented as illustrations of observed trends. A representative inclination of the test panels of 45° to the plane of the sources was chosen, since the previous single source study at this inclination showed that this produced the most varied pressure distributions. The distribution for a single source operation at $ka = 8$ is shown in Fig. 8a for comparison

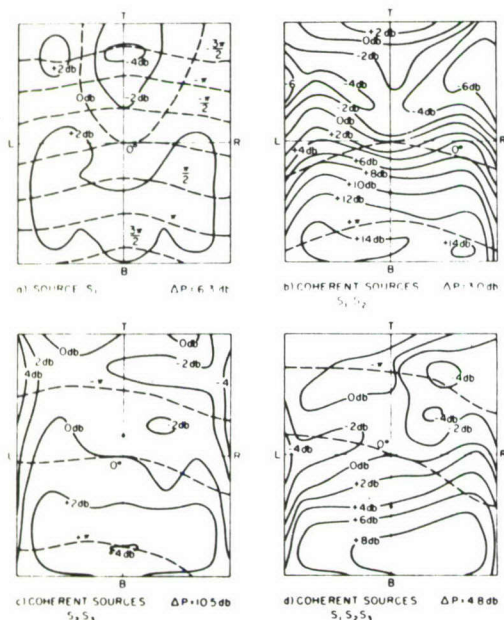


Fig. 8 Pressure and Phase Distributions on Test Panels, at 45° to the Source System, for Cases of (a) a Single Source S_1 (b) Double Source S_1, S_2 (c) Double Source S_2, S_3 , and (d) a Triple Source S_1, S_2, S_3 (as Designated in Fig. 4). All sources operated coherently, $ka = 8$. * marks the position of the phase reference microphone.

with operation for double and treble sources. In the case of the double source the pressure distribution on this inclined panel is dependent on the orientation of the lines of centers of the two sources with respect to the panel. The orientation of sources and test panel is shown in Fig. 4, with the sources designated as S_1, S_2 and S_2, S_3 . In each of these cases the loudspeakers are driven from the same $1/3$ octave noise generating system and consequently are considered as coherent sources. The differences between the two distributions (Figs. 8b and 8c) are quite marked. In the first case the orientation of the sources is such as to allow interference effects between the two sources to predominate, producing very rapid variation in pressure along the length of the panel. Figure 8d shows the distribution when three sources S_1, S_2, S_3 are operated coherently.

At present there appears no simple means by which the distribution on a panel, produced by a small number of coherent sources, can be predicted from knowledge of the distribution produced by a single source. The approximate calculation method of Wiener (Ref. 4) might be extended to a number of sources, but evaluation for all possible numbers and configurations of sources would be a formidable task. As previously mentioned it may be necessary in the ASD facility to operate several sirens in the same frequency range to obtain sufficiently intense levels. Thus it may be necessary to be able to predict the distribution for numbers of sources. To this end, we repeated the experiment with two sources in which the apparent interference effects predominated. However, this time, sources S_1 and S_2 were operated from two independent noise generating systems operating at the same $1/3$ octave band frequency. Thus S_1, S_2 represent two incoherent sources and the distribution on the panel illustrated in Fig. 9a is noted to be

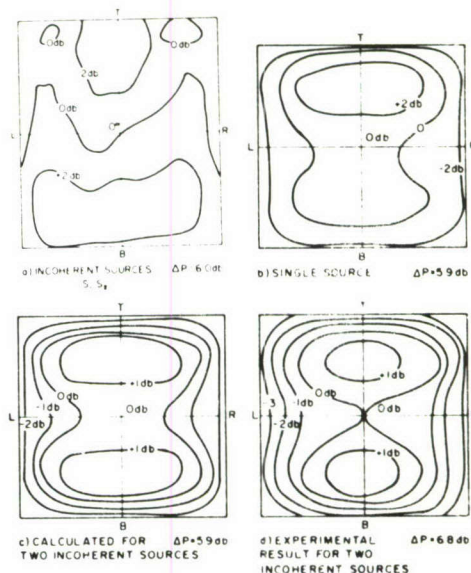


Fig. 9 Pressure and Phase Distribution on a Test Panel, at 45° to the Source System, for the Case of (a) Two Incoherent Sources S_1, S_2 ; $ka = 8$. Also (b) pressure distribution on test panel, at 45° to a single source; (c) the calculated distribution for two incoherent sources having 45° and 135° incidence; and (d) the experimentally determined distribution, $ka = 3.5$. * marks the position of the phase reference microphone.

remarkably similar to that obtained using a single source in Fig. 8a. However, no continuous phase contours were determinable. We may interpret the resemblance to the single source case as being a result of the fact that when two sources, A and B, are operated coherently, the RMS pressure p_x at a point X is given by

$$p_x = (p_A^2 + p_B^2 + 2p_A p_B \cos \theta)^{1/2} \quad (6)$$

where p_A and p_B are the individual RMS pressures at the point produced by each source, and θ represents the phase difference at X between the signals. When the sources are incoherent, such as two independent noise sources, the RMS pressure reduces to

$$p_x = (p_A^2 + p_B^2)^{1/2} \quad (7)$$

because in this case the long term average of $\cos \theta$ is zero.

Thus when incoherent sources are used to produce a pressure distribution on a panel, this distribution will simply be equal to the result of superimposing the distribution from one source onto that obtained from the other source by use of Eq. 7. For the double source described, the two individual distributions are almost identical because the angle of incidence is approximately 45° for both sources and consequently the distribution resulting from their both operating incoherently will be identical to that resulting from either source operating alone. This hypothesis was further verified in the case of two incoherent sources having widely separated angles of incidence upon the panel of 45° and 135° . The anticipated pressure distribution would be equal to that of the superposition of the distribution from one source (at 45° incidence) on the distribution from the other source (at 135°) obtained by rotating the first distribution pattern through an angle of 180° . Figure 9b shows the 45° incidence distribution and Fig. 9c shows the computed distribution obtained from this result for incoherent sources at 45° and 135° incidence. A comparison between the computed distribution and the experimentally determined distribution in the case of two incoherent sources having 45° and 135° incidence is very favorable (Fig. 9d).

The conclusions which may be drawn from these limited experiments are:

1. Using small numbers of coherent sources, the distributions on panels may be expected to be more complicated and possess wider pressure variations than those obtained for single sources, due to possible interference effects between sources.
2. The distributions will revert to those obtained using a single source if the sources are closely situated, producing equal angles of incidence, and are operated incoherently.
3. When widely separated sources are operated incoherently so that the angles of incidence and also the directions vary from source to source, the distribution can be computed by simple RMS addition of sound pressures.
4. In the cases of incoherent sources, continuous phase contours are not produced.

D. Sources Under Semi-Anechoic Conditions

As explained previously, semi-anechoic conditions in the model study were obtained by covering

the greater part of one wall of the IITRI anechoic room with plywood panels as shown in Fig. 4. As a result of this reflecting surface there will be formed an image of any source system operating in the room. The distance of the source from the reflecting surface can certainly be expected to influence the sound field produced by the source system and its image. For this study we chose only two values for the distance separating the source and the simulated reflecting floor. These values were 9 in and 3 ft representing scaled distances of about 3 and 12 ft, the minimum and maximum separation of the sirens from the floor in the ASD facility. Again we chose the 45° orientation of the test panel for a representative test study. Figures 10a and 10b show the distributions for a single source with

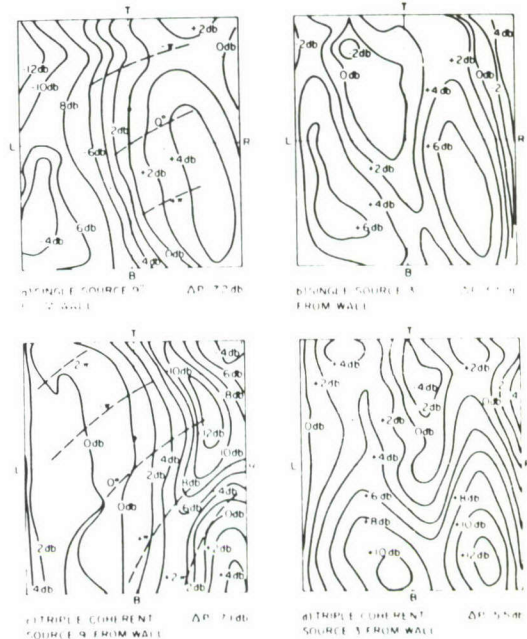


Fig. 10 Pressure and Phase Distribution on Test Panels, at 45° to Source System, Under Semi-Anechoic Conditions for Single Source and Triple Coherent Source. Source separations from reflecting surface 9 in and 3 ft. * marks the position of the phase reference microphone.

these source-to-"floor" separations. An overall similarity in the distributions is noted, but the pressure contours exhibit significantly more maximum and minimum values across the width of the panel in the case of the 3 ft separation. This may be attributed to the fact that a sound source and its image produce more rapid changes in their interference pattern with distance along a line parallel to their line of centers as their separation increases. This is observed in the directivity pattern of two in-phase sources as the ratio of their separation to the wavelength increases (Ref. 5). In addition, it is noted that continuous phase contours only exist in the case of the smaller separation and they do not occur over the full extent of the panel, but only in an elongated region. The direction of elongation is such as to approximately contain the point on the reflecting surface midway between the source and its image.

When the single source is replaced by three coherent sources the distributions for the 9-inch and 3-foot separations shown in Fig. 10c and 10d appear similar to those obtained with a single source for the respective separations and this is especially noticeable in the case of the larger separation. This lends support to the hypothesis that, in cases where a reflecting surface is present, a single source may be replaced by a number of sources operated coherently without much change in pressure level distribution on a test panel, especially where the separation between the source and image is large. In such cases the addition of further sources adjacent to the original does not then significantly alter the separation of the source system and its image. This implies that the source system and its image are more important in producing the interference type of distribution effects than the composition of sources forming the source group.

The conclusion that may be drawn from this semi-anechoic study is similar to that for the double source study in the anechoic condition. That is, the distributions are more complex and unpredictable than those of a single source under anechoic conditions and the variations in pressure across the panel are very marked because of the interference effect between sources or sources and their images. This situation cannot be simplified in the manner suggested with double sources (incoherent operation) because an image source cannot be operated in any other manner than coherently with its true source.

The fact that continuous phase contours exist only over a narrow elongated region when the separation of sources (or source and image) is large compared to a wavelength may be important in simulation of boundary-layer type fields. With this type of field, phase correlation areas are narrow and elongated in the direction of propagation.

SUGGESTED METHODS OF MODIFYING THE SOUND FIELD

Although it is anticipated that the facility can be operated to produce many varied types of field, it will still be necessary to modify the field further though probably only in small areas adjacent to a test structure. These localized modifications will require the use of portable, robust devices that can be placed in the facility to modify the fields. The purpose of this section is to outline the various types of devices which exhibit a potential of modifying fields in predictable manners. Modifications which may be desirable would include devices which increase the sound pressure levels at some portion of a test structure or which alter the spatial distribution of sound pressure or relative phase distribution. It is, of course, possible to use the portable sirens for local modifications of the sound field at frequencies above 500 c/s. The devices discussed below would supplement these sirens at high frequencies and be effective at lower frequencies. A simple device such as a flat or curved panel reflector offers possibilities as a field shaper. Using such a reflector the pressure distribution on a panel may be reinforced or decreased in certain areas, depending on whether this secondary pressure fluctuation is in or out of phase with the primary pressure fluctuation on the panel. These

devices raise the question of how they would behave as a function of frequency. Reflector devices are only effective when their dimensions are considerably in excess of the wavelength of interest. In addition, the device placed in such a location as to produce the required modification in field at one frequency may adversely effect the field at another frequency. Alternatively, it may effect the field in a distant region of interest by acting as an obstacle to the primary field on the test panel. This leads to another type of device which would modify fields on panels by a simple shielding effect, in other words, by producing shadow zones on the test panel. Absorbing panels can be used to reduce or eliminate reflections from the reflecting floor if this is desirable. The dimensions of such panels with respect to wavelength must also be considered.

Another device which might be used is an acoustic lens. Again the criterion is that the lens should possess an aperture considerably in excess of a few wavelengths. It may be possible to construct a lens formed from two curved plates or membranes with the space between them filled with a gas or liquid other than air. A major problem would be to produce a lens having a sufficiently low transmission loss. Acoustic lenses, which do not rely on the refraction effect, are also a possibility. These employ a lens-shaped construction which is not solid but consists of rows of shutters with suitable inclinations so as to produce a lens effect by reflection rather than refraction. In addition, true diffraction devices such as zone plates or diffraction gratings offer some possibility of use.

The above devices are mentioned because of their direct relationship with devices used in optics to modify light fields. Devices which might be considered purely on acoustic grounds might include horns and resonant devices. If very large modifications are required it may be practical to consider using horn devices to couple either a single or a number of sirens directly to areas on a panel, or even to incorporate the panel into a side-wall of the horn. Resonant devices such as quarter-wave tubes or Helmholtz resonators also offer means by which fields in localized areas may be modified. These devices when placed in a field will absorb energy at their resonant frequency and re-radiate it. They, therefore, act as secondary sources producing spherical radiation fields which can be used to modify the primary field.

The application considered for these devices has primarily been one of modifying fields in the anechoic operation. Their application to the diffuse field operation is somewhat less meaningful. However, in the case where a directional source operation in the reverberant condition produces a true diffuse field only at large distances from the source, reflector type devices could be used close to the source to modify the beam and reduce the directionality of the system, consequently increasing the extent of the diffuse field in the facility. Such a modification would enable larger test objects to be placed in a diffuse field in the facility.

Model studies of devices to modify the sound field have an advantage in that the cost of constructing small elements is much less than the cost for full-scale devices and tests leading to optimum design are much less expensive.

REFERENCES

1. Kolb, A.W., Rogers, O.R., "The ASD Sonic Fatigue Facility," 30th Symposium on Shock and Vibration, Detroit, 10-12 October 1961.
2. Tyzzer, F.G., "Development of a Suitable Anechoic Treatment for the ASD Sonic Fatigue Facility," Technical Documentary Report ASD-TDR-62-985, November 1962, Contract No. AF 33(657)-7434.
3. Beranek, L.L., Acoustics, McGraw-Hill Book Company, Inc., New York, pp. 100, 1960.
4. Wiener, F.M., "The Diffraction of Sound by Rigid Disks and Rigid Square Plates," J. Acoust. Soc. Am., Vol. 21, No. 4, p. 334, July 1949.
5. Olson, H.F., Acoustical Engineering, Van Nostrand and Company, New York, Fig. 2.3, p. 35, 1957.